Generalized Time Series Models and Spectral Density Based Parameters Estimation

A thesis submitted
in partial fulfillment of the requirements
for the degree of

DOCTOR OF PHILOSOPHY

by

Niharika Bhootna
(2018MAZ0010)

DEPARTMENT OF MATHEMATICS
INDIAN INSTITUTE OF TECHNOLOGY ROPAR

April, 2024

Niharika Bhootna: *Generalized Time Series Models and Spectral Density Based Parameters Estimation*

In memory of my beloved mother.

"Your love is the symphony of my soul, the harmony that resonates through every note of my journey."

Declaration of Originality

I hereby declare that the work being presented in the thesis entitled **Generalized Time Series Models and Spectral Density Based Parameters Estimation** has been solely authored by me. It presents the result of my independent investigation/research conducted during the period from January 2019 to January 2024 under the supervision of Dr. Arun Kumar, Associate Professor, Department of Mathematics, Indian Institute of Technology Ropar.

To the best of my knowledge, it is an original work, both in terms of research content and narrative, and has not been submitted or accepted elsewhere, in part or in full, for the award of any degree, diploma, fellowship, associateship, or similar title of any university or institution. Further, due credit has been attributed to the relevant state-of-the-art and collaborations with appropriate citations and acknowledgments, in line with established ethical norms and practices. I also declare that any idea/data/fact/source stated in my thesis has not been fabricated/ falsified/misrepresented. All the principles of academic honesty and integrity have been followed. I fully understand that if the thesis is found to be unoriginal, fabricated, or plagiarized, the institute reserves the right to withdraw the thesis from its archive and revoke the associated degree conferred. Additionally, the institute also reserves the right to appraise all concerned sections of society of the matter for their information and necessary action. If accepted, I hereby consent for my thesis to be available online in the institute's open access repository, inter-library loan, and the title and abstract to be made available to outside organizations.

Signature

Name: Niharika Bhootna
Entry Number: 2018MAZ0010
Program: Ph. D.
Department of Mathematics
Indian Institute of Technology Ropar
Rupnagar, Punjab 140001

Date: 02/04/24

Acknowledgement

I am deeply grateful to everyone who has played a unique role in the successful completion of this thesis. Foremost, my heartfelt appreciation goes to my Ph.D. mentor, Dr. Arun Kumar, for his indispensable guidance, unwavering patience, and constant encouragement. His expertise and support have been instrumental in molding the direction of my research journey. I am also thankful to the members of my doctoral committee, Dr. Arvind Kumar Gupta, Dr. Manju Khan, Dr. Manoranjan Mishra, and Dr. Mukesh Saini for their constructive feedback, suggestions, and continuous evaluation of my research progress. I am also grateful to my collaborator, Prof. Nikolai Leonenko, whose collaboration and insights have significantly enriched the scope and depth of my research. I would like to express my sincere gratitude to Prof. Neeraj Misra and Prof. Agnieszka Wyłomańska for their invaluable time, expertise, and meticulous review of my thesis.

I extend my gratitude to the Indian Institute of Technology Ropar for their generous financial support, which has been instrumental in facilitating this research endeavor and also for providing essential facilities and fostering a conducive research environment. Furthermore, I wish to express my appreciation to Mr. Neeraj Sharma, our dedicated office assistant, for his invaluable assistance with technical requirements. I am also grateful for the support rendered by Ms. Jaspreet Kaur in handling various official tasks. Additionally, I extend my heartfelt thanks to my esteemed colleagues in the research group - Neha Di, Monika, Naman, Priti, Pawan, and Meenu - for engaging in fruitful discussions and enjoyable dinner outings.

Throughout my PhD journey, Sonam and Aditi stand as my camaraderie connoisseurs, weaving memories, and moments with their unparalleled bond. Their encouragement, understanding, and laughter have been the pillars of strength that have sustained me through the challenges and triumphs of this endeavor. I express deep gratitude for the close-knit bond within our circle, where Sonam, Aditi, Monika, Vikas, Sahil, and I are as thick as thieves, navigating academic journey together with unwavering support and boundless laughter. I am appreciative of the friendship extended to me by Surya, Suman, Kusum, Ayantika, Ankita, Arzoo, Swati, Nikhil and Priyanshu. Additionally, I humbly recognize the invaluable guidance provided by my esteemed seniors: Amrendra Bhaiya, Gopika Di, Neha Di, and Taran Di. I gratefully acknowledge the presence of my friends beyond the confines of my department: Sakshi and Aaditya. My heartfelt appreciation extends to Bisma, a dear friend whose presence holds a treasured spot in my heart. I owe a special acknowledgment to Vikas, with whom I shared countless memorable moments and whose unwavering support has been a cornerstone of my journey.

In the mosaic of my existence, I pay homage to the constellation of souls who have

graced my journey: Jaya, a pillar of strength and and a beacon of positivity; Aashu, whose empathy and love knows no bounds; Rishabh, the harbinger of boundless laughter. Together, they form the tapestry of my cherished friendships, each thread a testament to the beauty of human connection. I owe a debt of gratitude to the radiant souls who have illuminated my path: Prateeksha, Pratibha, and Aditi. These three are muse of laughter and light in my life and their presence is truly invaluable. I am deeply grateful for the invaluable friendship and presence of Sahil, Bhawana, Garima, and Shriya, each bringing their unique brilliance into my life. I am deeply grateful to Jitendra sir, my teacher, whose guidance and support have been indispensable on my journey to this point. In the ebbs and flows of my PhD journey, my brothers Pawan and Ritik, alongside the guiding presence of my masi Saroj, provided steadfast guidance through the darkest lows and joined in the celebrations during the highest achievements.

In the culmination of my PhD journey, I am profoundly grateful for the support and encouragement bestowed upon me by my soon-to-be life partner Chandan Arora, who entered my life in the eleventh hour and yet, within a short span, offered unwavering support, love, and encouragement that fueled my success. In every trial and triumph, my family, especially my father, has been my rock, standing by me with unwavering love and understanding. Their collective presence, including my brothers, sisters, cousins, aunts, and uncles, has provided a sanctuary of support, sustaining me through the most challenging moments. Their presence has been a source of comfort and inspiration, reminding me of the importance of resilience and perseverance. I would like to extend my sincere gratitude to my Maa, who taught me the value of perseverance and hard work. Her endless love and support have been my greatest blessings. Lastly, I extend my sincerest thanks to the divine almighty for guiding me through this journey, for every blessing and opportunity bestowed upon me.

'नास्ति मातृसमा छाया, नास्ति मातृसमा गतिः ।
नास्ति मातृसमं त्राणं, नास्ति मातृसमा प्रिया ।।'

"There is no shadow, no shelter, no protector like a mother.
There is no life giver in this world like a mother."

Certificate

This is to certify that the thesis entitled **Generalized Time Series Models and Spectral Density Based Parameters Estimation** submitted by **Niharika Bhootna (2018MAZ0010)** for the award of the degree of **Doctor of Philosophy** to Indian Institute of Technology Ropar is a record of bonafide research work carried out under my guidance and supervision. To the best of my knowledge and belief, the work presented in this thesis is original and has not been submitted, either in part or full, for the award of any other degree, diploma, fellowship, associateship or similar title of any university or institution.

In my opinion, the thesis has reached the standard fulfilling the requirements of the regulations relating to the degree.

Signature

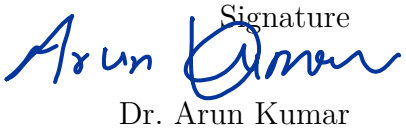

Dr. Arun Kumar
Department of Mathematics
Indian Institute of Technology Ropar
Rupnagar, Punjab 140001
Date: 02/04/2024

Lay Summary

A time series is a sequence of data points or observations, each one being recorded at a specified time. Time series analysis involves examining and interpreting the patterns to understand trends and fluctuations over time. A time series typically consists of four main components. In other words, a time series can be decomposed into four components namely, trend, seasonality, cyclic variations, and residuals. The trend component represents the long-term movement or direction of the time series. Seasonality refers to regular and predictable fluctuations that occur at specific intervals and cyclic variations involve fluctuations that may not follow a fixed time frame. Residuals capture the random, unpredictable fluctuations in the data that cannot be attributed to trend, seasonality, or cycle variations. This knowledge is used to predict the future.

A time series is stationary if the data doesn't change its statistical properties like mean or variance with time. On the other hand, if a time series has noticeable trends and fluctuations, or its statistical properties change over time, we say it's non-stationary. Time series modeling is predicting the future based on what has been learned from the past and it is widely used in various fields such as finance, economics, weather forecasting, and many others to make predictions, identify patterns, and gain insights into how variables change over time. In essence, time series helps us make sense of data that evolves over time, allowing us to extract valuable information for decision-making and forecasting.

There are several well-known models, like AR, MA, ARMA, and ARIMA, to name the few. In literature, these models are generalized in several directions to capture heavytaildness, the time-varying variance of innovation terms, long memory, and other inherent characteristics of empirical data. In this work, we extend the work available on long memory and non-Gaussian time series models and provide the stationarity, invertibility, and parameters estimation approach for the introduced models.

Abstract

This thesis endeavors to investigate and propose some generalized time series models to extend the work available on classical and long memory models. The exploration encompasses various aspects, including the study of stationarity, invertibility, spectral densities, autocovariance functions, parameter estimation, and asymptotic properties of estimators for the introduced models. In this thesis work, we extend some classical and long memory models existing in literature to several directions. Initial part of the study focuses on developing and exploring the TAR(1) model by assuming tempered stable marginals for the AR(1) process, with a specific emphasis on its behavior under stationarity assumptions. In this context, the marginal probability density function of the error term is derived and it is shown that the distribution of error term is infinitely divisibility. The TAR(1) process serves as a generalization of well-established inverse Gaussian and one-sided stable autoregressive models. Furthermore, we study an autoregressive model of order one assuming tempered stable innovations. The subsequent step involves parameter estimation for both processes, a crucial aspect of model validation and applicability. Two distinct methodologies, namely conditional least squares and the method of moments, are employed in this estimation process. These techniques are then rigorously assessed and validated through simulated data, providing insights into the model's performance under various conditions. The performance of the model is not only theoretically evaluated but also practically demonstrated through its application to both real and simulated datasets.

Next, we introduce the Gegenbauer autoregressive tempered fractionally integrated moving average (GARTFIMA) process, aiming to generalize the existing GARMA and ARTFIMA models. A key motivation behind this extension is to tackle the unbounded spectral density, observed in the GARMA process. The analysis begins by comprehensively exploring the spectral density of the GARTFIMA process. Understanding the frequency components and their strengths within the time series is crucial for evaluating the model's efficacy in capturing various patterns and behaviors. Subsequently, the autocovariance function is obtained using the spectral density of the process, providing insights into the temporal dependencies and relationships inherent in the data. To estimate the parameters of the GARTFIMA process, two distinct methodologies are employed. Firstly, a non-linear least square (NLS) based approach is utilized, which establishes a least square regression between empirical and theoretical spectral densities. Secondly, the Whittle likelihood estimation method is applied, emphasizing the statistical measure of discrepancy between the theoretical and observed spectral densities. The asymptotic properties of the Whittle likelihood estimators are obtained.

The performance of these techniques is assessed on simulated data, providing their effectiveness. Additionally, the relevance and practical applicability of the GARTFIMA process are demonstrated through its application to real-world data. A comparative analysis against other time series models is conducted, highlighting the slightly better performance of the introduced model.
Moreover, we extend the existing seasonal fractional ARUMA process by introducing a tempered fractional ARUMA process. This extension involves the incorporation of exponential tempering into the traditional seasonal fractional ARUMA model. The initial focus lies in establishing the fundamental characteristics of the introduced tempered fractional ARUMA process. This encompasses the conditions ensuring the stationarity and invertibility of the model. The analysis then delves into the spectral properties of the tempered fractional ARUMA model. To estimate the parameters of the tempered fractional ARUMA model, we again employ the Whittle likelihood estimation approach, which involves minimizing the contrast between the theoretical and observed spectral densities, providing a robust framework for parameter estimation. Additionally, the asymptotic properties of the estimators are investigated, offering valuable insights into their reliability and consistency as the sample size increases. Practical validation of the proposed estimation technique is conducted through a systematic assessment of its performance on simulated data.
Lastly, the study extends to generalized ARMA processes, characterized by the type 2 Humbert polynomials and called Horadam ARMA and Horadam-Pethe ARMA processes. We examine the autocovariance function and its inherent properties for these models. By leveraging the minimum contrast Whittle likelihood estimation, we estimate the parameters of the Horadam ARMA and Horadam-Pethe ARMA processes. In addition to the conventional minimum contrast Whittle likelihood estimation, we also use the debiased Whittle likelihood estimation. This computationally efficient technique is designed to reduce biases inherent in the standard Whittle likelihood method. The incorporation of debiasing mechanisms enhances the robustness and accuracy of parameter estimates, particularly in scenarios where biases might distort the results. The assessment of the proposed parameter estimation methods is conducted through the use of simulated data for the Horadam ARMA process. This empirical evaluation serves as a crucial benchmark to gauge the effectiveness and reliability of the Whittle likelihood and debiased Whittle likelihood techniques.

Keywords: Stationary processes, spectral density, positive tempered stable distribution, Humbert polynomials, fractional ARUMA processes, Gegenbauer processes, parameter estimation.

List of Publications

1. N. Bhootna and A. Kumar. *Tempered Stable Autoregressive Models*, Communications in Statistics - Theory and Methods. 53(2): 765-785 (2024).

2. N. Bhootna and A. Kumar. *GARTFIMA Process and its Empirical Spectral Density Based Estimation*, Journal of Applied Statistics (2023).

3. N. Bhootna, M.S. Dhull, A. Kumar and N. Leonenko. *Humbert Generalized Fractional Differenced ARMA Processes*, Communications in Nonlinear Science and Numerical Simulation. 125:107412 (2023). (Not a part of the Thesis)

4. N. Bhootna and A. Kumar. *Tempered Fractional ARUMA Process* (under review).

5. N. Bhootna and A. Kumar. *Parameter Estimation of Horadam ARMA and Horadam-Pethe ARMA Processes* (preprint).

Contents

List of Figures

List of Tables

List of Notations

List of Abbreviations

AR autoregressive

MA moving average

ARMA autoregressive moving average

ARIMA autoregressive integrated moving average

ARFIMA autoregressive fractionally integrated moving average

ARTFIMA autoregressive tempered fractionally integrated moving average

GARMA Gegenbauer autoregressive moving average

HARMA Humbert autoregressive moving average

GARTFIMA Gegenbauer ARTFIMA

NLS non-linear least square

CLS conditional least square

MOM method of moments

pdf probability density function

List of Symbols

$\mathbb{Z}$ the set of integers

$\mathbb{Q}$ the set of rational numbers

$\mathbb{R}$ the set of real numbers

$\in$ is an element of

$\notin$ is not an element of

Γ gamma function

$\mathcal{B}$ beta function

${}_2F_1$ hypergeometric function

Chapter 1

Introduction

Time series modeling is a continuously evolving field that has applications in different areas. A time series is a family of random variables $\{X_t : t \in T\}$, where T denotes the set of time points and X_t denotes the value at time t. In other words, a time series is series of observations recorded at specific times [18]. The essence of the time series analysis lies in the analysis of historical data and the development of a robust model capable of encapsulating the inherent characteristics such as meaningful statistics, trends, patterns, and revealing dependencies among observations of a given sequence. Understanding these dependencies is crucial, and various methods and models are employed to forecast future observations [16]. A time series is said to be strictly stationary when the joint probability distribution of any n observations is invariant to shifts in time. In other words, joint distribution of $\{X_{t+1}, X_{t+2}, \ldots, X_{t+n}\}$ is same as another set of n observations shifted by h time units, that is, $\{X_{t+1+h}, X_{t+2+h}, \ldots, X_{t+n+h}\}$, for all t. In weak sense, a time series X_t is deemed stationary if $\mathrm{E}(X_t) = \mu$ is constant regardless of t, and the autocovariance, denoted by $\gamma(h) = \mathrm{Cov}(X_{t+h}, X_t)$, is solely a function of lag h [13]. The time series is considered to be non-stationary if the statistical properties such as mean, variance, and autocovariance does not remain the same over time and the series includes time trends and random walks. In the frequency domain, the spectral density function; denoted as $f_x(\omega)$, for $\omega \in (-\pi, \pi)$; takes center stage in elucidating the characteristics of a time series $\{X_t\}$ [79]. The Wiener-Khintchine theorem encapsulates the connection between the spectral density function and the sequence of autocovariance, establishing a bridge between time-domain and frequency-domain analyses [15]. The autocovariance sequence can be derived through the inverse Fourier transform of the spectral density function, while conversely, the spectral density function is a result of the Fourier transform of the autocovariance. The spectral density for a time series $\{X_t\}$ is defined as follows:

Definition 1.1 (Spectral Density [85])**.** For a time series $\{X_t\}$ with autocovariance function $\gamma(h)$, the spectral density is defined as:

$$f_x(\omega) = \frac{1}{2\pi} \sum_{h=0}^{\infty} \gamma(h) e^{-\iota\omega h}, \quad \text{for } \omega \in (-\pi, \pi).$$

The autocovariance of a process can be obtained by taking the inverse Fourier transform of the spectral density, that is,

$$\gamma(h) = \int_{-\pi}^{\pi} f_x(\omega) e^{\iota\omega h} d\omega. \tag{1.1}$$

Transitioning from the fundamental concepts of time series analysis, we delve into the historical development of the classical time series models. The literature on the development of these models is outlined below.

1.1 Historical Development of Classical Time Series Models

Classical time series models play a crucial role in understanding and analyzing the behavior of time series data. These models serve as foundational tools in time series analysis and provide a framework for exploring and interpreting various temporal patterns and structures present in the data. The study of regularities and trends in data dates back to the early 20th century, with notable contributions from G. U. Yule and G. Walker [91,97]. They made important contributions to the theory and practice of correlation, regression, and the autoregressive models. The autoregressive (AR), moving average (MA), and autoregressive moving average (ARMA) models were introduced by Yule (1926) [97], Slutsky (1937) [82], and Wold (1938) [95], respectively, to model stationary time series data. A time series is stationary if its statistical properties remain unchanged over time. Next, we define some classical time series models.

Autoregressive (AR(p)) Process:

Yule aimed to model stationary time series data by demonstrating how a process could be represented as a sum of its own lagged values and a random term. For a time series $\{X_t\}$, the autoregressive process of order p, denoted by AR(p), is defined as follows:

$$\Phi(B)X_t = \epsilon_t, \tag{1.2}$$

where ϵ_t is Gaussian white noise with variance σ^2, B is the backward shift operator defined as: $B^j(X_t) = X_{t-j}$, $\Phi(B) = (1 - \sum_{j=1}^{p} \phi_j B^j)$, and $\phi_1, \phi_2, \ldots, \phi_p$ are model coefficients. Here, $\Phi(B)$ is also known as the characteristic polynomial of degree p of the process, and the AR(p) process is stationary if all roots of $\Phi(B)$ lie outside the unit circle.

Moving Average (MA(q)) Process:

Slutsky's contributions were crucial in expanding the understanding of stochastic processes and their applications in economics. His work addressed the study of cyclical fluctuations and their impact on economic theories and laid the groundwork for moving average models [82], where observed data are modeled as linear combinations of past and current random shocks or white noise with variance σ^2. The moving average process of order q, denoted by MA(q), is defined as follows:

$$X_t = \Theta(B)\epsilon_t, \tag{1.3}$$

where ϵ_t is again Gaussian white noise with variance σ^2, $\Theta(B) = 1 + \sum_{j=1}^{q} \theta_j B^j$ and $\theta_1, \theta_2, \ldots, \theta_q$ are model coefficients. Here, $\Theta(B)$ is also known as the characteristic polynomial of degree q of the process, and the MA(q) process is invertible if all roots of $\Theta(B)$ lie outside the unit circle.

Autoregressive Moving Average (ARMA(p, q)) Process:

In 1938, Wold made significant contributions to the field of time series analysis by introducing the concept of the autoregressive moving average process [95]. His work demonstrates how the autoregressive and moving average components could be combined to represent stationary time series. The ARMA process, denoted by ARMA(p, q), where p and q represent the order of AR and MA terms, respectively. Let ϵ_t be Gaussian white noise with variance σ^2. Then, the ARMA(p, q) is given by:

$$\Phi(B)X_t = \Theta(B)\epsilon_t, \tag{1.4}$$

where $\Phi(B)$ and $\Theta(B)$ are stationary AR and invertible MA operators, respectively, defined in (1.2) and (1.3). Throughout the thesis, we will be using the same notation for stationary AR and invertible MA operators. Wold's research provided a more comprehensive framework for modeling and understanding stationary time series data, which became fundamental in many areas including econometrics, signal processing, and engineering. These pioneering works continue to shape the field of time series analysis and serve as the basis for more advanced models and techniques developed in subsequent years. The above discussed classical models work on the assumption of stationarity of the dataset. However, in real-life scenarios, observed data often do not exhibit stationary behavior, that is, mean and variance and other statistical properties change over time. To address this limitation, Box and Jenkins (1976) developed the autoregressive integrated moving average (ARIMA) process, for detailed study one can refer to [17].

Autoregressive Integrated Moving Average (ARIMA(p, d, q)) Process:

The ARIMA process models a non-stationary time series by introducing an integer order difference operator d into the traditional ARMA(p, q) process and is denoted by ARIMA(p, d, q). The ARIMA process is defined as follows:

$$\Phi(B)(1 - B)^d X_t = \Theta(B)\epsilon_t, \tag{1.5}$$

where ϵ_t is Gaussian white noise with variance σ^2. This process transforms a non-stationary series into stationary ones through an integer order differencing. Their approach allowed for accurate forecasting by incorporating historical patterns, trends, and seasonality, thus enabling better predictions of future values based on past data. Trajectory plots for the classical time series models are given in Fig. 1.1. Various R libraries were employed to create these plots. The ARIMA approach is commonly known as the Box-Jenkins methodology. Their work stimulated further research in time series modeling and forecasting, leading to the development of more advanced models, such as seasonal ARIMA, state-space models, and non-linear time series models.however, the ARIMA(p, d, q) process fails to capture LRD in data with d as an integer. The data exhibiting LRD behaviors have been found in various fields such as Finance, Economics, Geophysics, and Agriculture [10,74]. The LRD series evinces substantial correlation after large lags. The LRD process is essential to study as they exhibit non-instinctive properties that may not be captured using the traditional AR, MA, ARMA, and ARIMA time series models.

1.2 Long Memory Processes

A long memory process, also known as a LRD process, is a stochastic process commonly found in time series data that exhibits long-term correlations or dependencies between observations across extended time intervals. This type of process is characterized by the presence of slow decay in autocorrelation, indicating that the influence of past observations persists over a considerable range of time. For seasonal long memory process $\{X_t\}$, the autocorrelation function for lag h, denoted by $\rho(h)$, behaves asymptotically as $\rho(h) \simeq \cos(h\omega_0)h^{-\alpha}$, when $h \to \infty$ for some positive $\alpha \in (0, 1)$ and $\omega_0 \in (0, \pi)$ [19]. An LRD process is characterized by an autocovariance function or autocorrelation function that is not absolutely summable. In the frequency domain, it represents a process where the power spectral density is unbounded across all frequencies. This signifies that the process exhibits correlations or dependencies over long ranges, extending to distant observations rather than

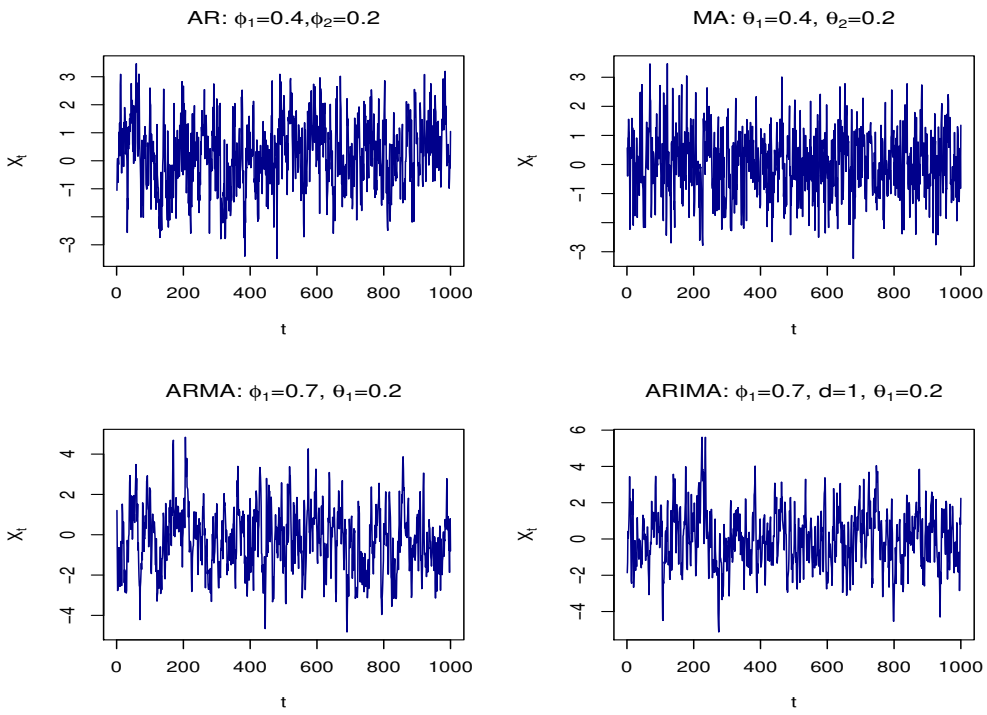

Figure 1.1: Trajectory plots for the classical time series models.

decaying rapidly. Some LRD processes are discussed as follows:

Autoregressive Fractionally Integrated Moving Average (ARFIMA(p, d, q)) Process:

The autocorrelation function for the classical time series models such as AR, MA, ARMA, and ARIMA processes decays exponentially, making them short memory processes. However, this characteristic does not appear to be common in many empirical time series. Some series appear to have a long memory property, which means that the correlation between data in a series can persist over longer time periods. The traditional models cannot be used in such scenarios. The ARFIMA(p, d, q) process is a generalized ARIMA(p, d, q) model defined in [46], which aims to explain both short-term and long-term persistence in data. The model is generalized by taking the order of differencing d to be any real value instead of being an integer in the traditional ARIMA process. For some recent articles with applications of the ARFIMA process in modeling of series with long memory, see [52,57,62,68,90]. The fractional ARIMA(p, d, q) or ARFIMA(p, d, q) process is expressed through the equation [46]:

$$\Phi(B)(1-B)^d X_t = \Theta(B)\epsilon_t, \tag{1.6}$$

where $(1-B)^d = \sum_{k=0}^{\infty} \frac{\Gamma(k-d)B^k}{\Gamma(-d)\Gamma(k+1)}$ and ϵ_t is Gaussian white noise with variance σ^2.

The process is stationary and invertible for $|d| < \frac{1}{2}$. Rewrite (1.6) as follows:

$$X_t = \Psi(B)\epsilon_t,$$

where $\Psi(B) = \frac{\Theta(B)}{\Phi(B)}\Delta^d$ and $\Delta^d = (1-B)^{-d}$. Then for $z = e^{-\iota\omega}$ the spectral density of X_t takes the following form [46]:

$$f_x(\omega) = |\Psi(z)|^2 f_\epsilon(\omega) = \frac{\sigma^2}{2\pi}\frac{|\Theta(z)|^2}{|\Phi(z)|^2}(2\sin(\omega/2))^{-2d}.$$

The corresponding autocorrelation function $\gamma(h)$ for lag h can be calculated by taking the inverse Fourier transform of spectral density. The relation between autocovariance function and spectral density is given in (1.1). For ARFIMA process with lags $p = 0$ and $q = 0$, the autocovariance is given by [46]:

$$\gamma(h) = \frac{(-1)^h(-2d)!}{(h-d)!(-h-d)!}.$$

Gegenbauer Autoregressive Moving Average (GARMA(p, q)) Process:

In subsequent years, Andel [4] and Gray et al. [38] introduced the concept of the GARMA process. This process also possesses seasonal long-range dependence [21]. GARMA is an extension of the Fractional ARIMA process which was proposed to model long-term seasonal and periodic behaviors. It uses the properties of generating function of Gegenbauer polynomials to model a time series. The Gegenbauer polynomials are generalizations of the Legendre polynomials. For $|u| \leq 1$, the Gegenbauer polynomials $C_n^d(u)$ are defined in terms of generating function as follows:

$$(1-2uZ+Z^2)^{-d} = \sum_{n=0}^{\infty} C_n^d(u)Z^n, \tag{1.7}$$

where $d \neq 0$, $|Z| < 1$, and $C_n^d(u)$ is represented by:

$$C_n^d(u) = \sum_{k=0}^{n/2}(-1)^k \frac{\Gamma(n-k+d)}{\Gamma(d)\Gamma(n+1)\Gamma(n-2k+1)}(2u)^{n-2k}. \tag{1.8}$$

The GARMA(p, q) process is defined as:

$$\Phi(B)(1 - 2uB + B^2)^d X_t = \Theta(B)\epsilon_t,$$

where ϵ_t is Gaussian white noise with variance σ^2. The process is stationary and invertible for $|u| \leq 1$ and $|d| < 1/2$. The spectral density of the GARMA process, for $z = e^{-\iota\omega}$, is outlined as:

$$f_x(\omega) = \frac{\sigma^2}{2\pi} \frac{|\Theta(z)|^2}{|\Phi(z)|^2} \left[4\left(\cos(\omega) - u\right)^2\right]^{-d}. \tag{1.9}$$

The study on the usefulness of the Gegenbauer stochastic process is done by Dissanayake et al. [23]. The limit theorems for stationary Gaussian processes and their non-linear transformations with covariance function are defined as:

$$\rho(h) \simeq \sum_{k=1}^{r} A_k \cos(h\omega_k) h^{-\alpha_k}, \sum_{k=1}^{r} A_k = 1,$$

where $A_k \geq 0,\ \alpha_k > 0, and\ \omega_k \in [0, \pi),\ when\ k = 1, \ldots, r$ have been considered in [50]. For different estimation methods related to the GARMA process, see the recent article [49]. In literature, many tempered distributions and processes are studied using the exponential tempering in the original distribution or process [8,36,56,75,76,88,99]. The fractionally integrated process with seasonal components is studied and maximum likelihood estimation is done by Reisen et al. [72]. The parametric spectral density with power-law behavior about a fractional pole at the unknown frequency ω is analyzed. Also, the Gaussian estimates and limiting distributional behavior of estimates are studied by Giraitis et al. [32]. Later, Giraitis and Leipus provided an extension to the fractional ARIMA process by introducing the seasonal fractional ARUMA process [34].

Fractional ARUMA Process:

The fractional ARUMA process introduced in [34], serves as a model for time series exhibiting long memory characteristics, characterized by persistent dependencies over long periods. This process specifically captures long-range periodic behavior observable at a finite number of frequencies within its spectrum. The formulation of this process is structured as follows:

$$\Phi(B)(1 - B)^{d_0} \prod_{j=1}^{k} (1 - 2u_j B + B^2)^{d_j} (1 + B)^{d_{k+1}} X_t = \Theta(B)\epsilon_t, \tag{1.10}$$

where ϵ_t is the Gaussian white noise with variance σ^2. The process is stationary and invertible for $|u_j| \leq 1$ and $|d_j| < 1/2\ \forall j$. Also, $\prod_{j=1}^{k}(1-2u_jB+B^2)^{d_j} = \sum_{n=0}^{\infty}\pi_n B^n$, where the coefficients π_n can be expressed in terms of Gegenbauer polynomials $\{C_k^d(u)\}$ as:

$$\pi_n = \sum_{\substack{0\leq r_1 \ldots r_k \leq n \\ r_1+r_2+\ldots+r_k=n}} C_{r_1}^{-d_1}(u_1)\, C_{r_2}^{-d_2}(u_2)\cdots C_{r_k}^{-d_k}(u_k)\,.$$

For $d_0 = 0$, $d_{k+1} = 0$, and $z = e^{\iota\omega}$, the spectral density of the process $\{X_t\}$ is defined as:

$$\begin{aligned} f_x(\omega) &= \frac{\sigma^2}{2\pi}\frac{|\Theta(z)|^2}{|\Phi(z)|^2}\prod_{j=1}^{k}\left[4\left(\cos(\omega)-u_j\right)^2\right]^{-d_j} \\ &= \frac{\sigma^2}{2\pi}\frac{|\Theta(z)|^2}{|\Phi(z)|^2}\prod_{j=1}^{k}\left[4\sin\left(\frac{\omega-\cos^{-1}(u_j)}{2}\right)\sin\left(\frac{\omega+\cos^{-1}(u_j)}{2}\right)\right]^{-2d_j}. \end{aligned} \tag{1.11}$$

For the parameter estimation of the ARUMA process, one can refer to [60].

Autoregressive Tempered Fractionally Integrated Moving Average (ARTFIMA) Process:

The ARTFIMA(p, d, λ, q) process defined by [76] generalizes the ARFIMA process defined in (1.6). The model is defined by introducing a tempering parameter λ in the ARFIMA model, that is, instead of taking the fractional shift operator $(1-B)^d$, the authors have considered a tempered fractional shift operator $(1-e^{-\lambda}B)^d$, where $\lambda > 0$. The series exhibits a semi long-range dependence structure, that is, for λ close to 0, the autocovariance function of the process behaves similarly to a long memory process and, for large λ, the autocovariance function decays exponentially [76]. The ARTFIMA process is defined by:

$$\Phi(B)(1-e^{-\lambda}B)^d X_t = \Theta(B)\epsilon_t. \tag{1.12}$$

The above equation is rewritten as:

$$X_t = \Psi(B)\epsilon_t,$$

where $\Psi(B) = \dfrac{\Theta(B)}{\Phi(B)}\Delta^{d,\lambda}$ and $\Delta^{d,\lambda} = (1-e^{-\lambda}B)^{-d}$. The spectral density of X_t takes the following form [76]:

$$f_x(\omega) = |\Psi(z)|^2 f_\epsilon(\omega) = \frac{\sigma^2}{2\pi}\frac{|\Theta(e^{-\iota\omega})|^2}{|\Phi(e^{-\iota\omega})|^2}|1 - e^{-(\lambda+\iota\omega)}|^{-2d}$$
$$= \frac{\sigma^2}{2\pi}\frac{|\Theta(e^{-\iota\omega})|^2}{|\Phi(e^{-\iota\omega})|^2}(1 - 2e^{-\lambda}\cos(\omega) + e^{-2\lambda})^{-d}. \tag{1.13}$$

Taking $Y_t = \Delta^{d,\lambda} X_t$, the model takes the following form:

$$Y_t - \sum_{j=1}^{p} \phi_j Y_{t-j} = \epsilon_t + \sum_{i=1}^{q} \theta_i \epsilon_{t-i},$$

which is the ARMA(p, q) process. The ARTFIMA process is stationary for $d \notin \mathbb{Z}$ and $\lambda > 0$ (see [76]). For $p = 0$ and $q = 0$, the autocovariance function of ARTFIMA$(0, d, \lambda, 0)$ process is defined by:

$$\gamma(h) = \frac{\sigma^2\Gamma(2d+h)}{\Gamma(2d)\Gamma(h+1)} {}_2F_1(2d, h+2d; h+1; e^{-2\lambda}),$$

where ${}_2F_1(a, b; c; z)$ is Gaussian hypergeometric function such that:

$${}_2F_1(a, b; c; z) = 1 + \frac{a.b}{c.1}z + \frac{a(a+1)b(b+1)}{c(c+1)2!}z^2 + \cdots .$$

Type 1 and Type 2 HARMA(p, ν, u, q) Processes:

The type 1 Humbert ARMA (HARMA) process was introduced by Bhootna et al. [11] using the generating function of type 1 and type 2 Humbert polynomials. The Gegenbauer and Pincherle polynomials are the particular cases of type 1 Humbert polynomials. The Horadam and Horadam-Pethe polynomials are the particular cases of type 2 Humbert polynomials. The work focus on the study of Pincherle ARMA, Horadam ARMA, and Horadam-Pethe ARMA processes. These processes possess seasonal long memory which helps to capture autocorrelation present in the data, leading to improved forecasting accuracy. The proposed model holds potential applications in various domains. It can be used in sales forecasting in e-commerce industries by effectively capturing seasonality, trends, and patterns in historical sales data. Furthermore, due to the long memory property of the model, it can be used in capturing autocorrelation patterns evident in financial returns, volatility, and other key indicators. Here is an overview of the study on the type 1 and type 2 HARMA processes.

Type 1 HARMA(p, ν, u, q) Process

To study the foundation of the type 1 Humbert ARMA or type 1 HARMA process, it is vital to study type 1 Humbert polynomials. The definition is as follows:

Definition 1.2 (Type 1 Humbert polynomials)**.** The Humbert polynomials of type 1, $\{\Pi^{\nu}_{n,m}\}_{n=0}^{\infty}$, are defined in terms of generating function as:

$$(1 - mut + t^m)^{-\nu} = \sum_{n=0}^{\infty} \Pi^{\nu}_{n,m}(u)t^n, m \in \mathbb{N}, |t| < 1, |u| \leq 1, \text{ and } |\nu| < \frac{1}{2}. \quad (1.14)$$

The type 1 HARMA(p, ν, u, q) process $\{X_t\}$ is defined by:

$$\Phi(B)(1 - muB + B^m)^{\nu} X_t = \Theta(B)\epsilon_t, \quad (1.15)$$

where ϵ_t is Gaussian white noise with variance σ^2, $0 \leq u < 2/m$, $|\nu| < 1/2$, and $\Phi(B)$, $\Theta(B)$ are stationary AR and invertible MA operators, respectively, defined in (1.2) and (1.3). In Def. 1.2, the polynomial $\Pi^{\nu}_{n,m}(u)$ can be explicitly written as [48]:

$$\Pi^{\nu}_{n,m}(u) = \sum_{k=0}^{\lfloor \frac{n}{m} \rfloor} \frac{(-mu)^{n-mk}}{\Gamma((1-\nu-n)+(m-1)k)(n-mk)!k!}, \text{ where } \left\lfloor \frac{n}{m} \right\rfloor \text{ is floor function.}$$

The hypergeometric representation of $\Pi^{\nu}_{n,m}(u)$ is given by:

$$\Pi^{\nu}_{n,m}(u) = \frac{(\nu)_n (mu)^n}{n!} {}_mF_{m-1}\left[\frac{-n}{m}, \frac{-n+1}{m}, \cdots, \frac{-n-1+m}{n}; \right.$$
$$\left. \frac{-\nu-n+1}{m-1}, \frac{-\nu-n+2}{m-2}, \cdots, \frac{-\nu-n+m-1}{m-1}; \frac{1}{(m-1)^{m-1}u^m}\right].$$

For $m = 2$, the Humbert polynomials reduces to Gegenbauer polynomials, which is generally denoted as $\{C^{\nu}_n(u)\}_{n=0}^{\infty}$. For $m = 3$, the polynomials reduce to Pincherle polynomials, denoted as $\{P^{\nu}_n(u)\}_{n=0}^{\infty}$, (see [69]).

Remark 1.2.1. *The type 1 HARMA process is stationary and invertible, for* $|\nu| < 1/2$, $0 \leq u \leq 2/m$, *and all roots of* $\Phi(B) = 0$ *and* $\Theta(B) = 0$ *lie outside the unit circle.*

Remark 1.2.2. *For a type 1* HARMA(p, ν, u, q) *process the spectral density takes the following form:*

$$f_x(\omega) = \frac{\sigma^2}{2\pi} \frac{|\Theta(z)|^2}{|\Phi(z)|^2} (2 + m^2u^2 - 2mu(\cos(\omega) + \cos((1-m)\omega)) + 2\cos(m\omega))^{-\nu},$$

where $z = e^{-\iota\omega}$, *for* $\omega \in (-\pi, \pi)$.

To delve into the examination of the process's seasonal long memory and singularities, it is essential to study the following definitions:

Definition 1.3 (Singular point [28])**.** The point $\omega = \omega_0$ is said to be singular point of function f, if at $\omega = \omega_0$, f fails to be analytic, that is, $f(\omega_0) = \infty$.

Definition 1.4 (Seasonal long memory)**.** The stationary time series $\{X_t\}$ is said to have seasonal long memory if there exist $\omega_0 \in \mathbb{R}$ and $\alpha \in (0, 1)$ such that

$$\rho(h) \simeq h^{-\alpha} \cos(h\omega_0), \text{ as } h \to \infty,$$

and $\cos(h\omega_0) \neq 1$.

Remark 1.2.3. *Let* $\{X_t\}$ *be the stationary type 1* HARMA(p, ν, u, q) *process. Then, under the assumptions of stationarity the spectral density of type 1* HARMA(p, ν, u, q) *has singular spectrum [11]*

1. *at* $u = 0$ *and* $\omega = \frac{4n\pi \pm \pi}{m}$, *for* $-\frac{m\pm 1}{4} < n < \frac{m\mp 1}{4}$,
2. *at* $u = \frac{2}{m}(-1)^n \cos(\frac{4n\pi}{m-2})$ *and* $\omega = \pm\frac{2n\pi}{m-2}$, *for* $m \neq 2$ *and* $-\frac{(m-2)}{4} < n < \frac{(m-2)}{4}$, *and*
3. *at* $\omega = \cos^{-1}(u)$, *for* $m = 2$.

Remark 1.2.4. *The stationary type* 1 *HARMA*$(p, \nu, 0, q)$ *process has seasonal long memory, for* $0 < \nu < 1/2$ *(see [11]).*

Type 2 HARMA process

The definition of the type 2 HARMA process involves the utilization of the generating function of type 2 Humbert polynomials, which is outlined below:

Definition 1.5 (Type 2 Humbert polynomials)**.** The type 2 Humbert polynomials $\{Q^{\nu}_{n,m}(u)\}_{n=0}^{\infty}$ are defined by the following generating function:

$$(1 - 2ut + t^m)^{-\nu} = \sum_{n=0}^{\infty} Q^{\nu}_{n,m}(u)t^n, \ |t| < 1, \ |\nu| < 1/2, \ |u| \leq 1. \tag{1.16}$$

Here, $Q^{\nu}_{n,m}(u) = \Pi^{\nu}_{n,m}(\frac{2u}{m})$ (see 1.14).

The type 2 HARMA process is established utilizing the generating function outlined in (1.16) in the following manner [11]:

$$\Phi(B)(1 - 2uB + B^m)^{\nu} X_t = \Theta(B)\epsilon_t, \tag{1.17}$$

where ϵ_t is Gaussian white noise with variance σ^2 and $0 \leq u \leq 1$. The explicit form of the polynomials $Q^{\nu}_{n,m}(u)$ is defined by:

$$Q^{\nu}_{n,m}(u) = \sum_{k=0}^{[\frac{n}{m}]} (-1)^k \frac{(\nu)_{(n-(m-1)k)}}{k!(n-mk)!} (2u)^{n-mk},$$

where $\nu_0 = 1$ and $(\nu)_n = \nu(\nu+1)\cdots(\nu+n-1)$. For $m = 2$, the above polynomials in (1.16) is Gegenbauer polynomials and $Q^{\nu}_{n,2}(u) = C^{\nu}_n(u)$. Also, for $m = 3$, the polynomials in (1.16) are known as Horadam-Pethe polynomials $\{Q^{\nu}_{n,3}\}_{n=0}^{\infty}$, and for $m = 1$, they are known as Horadam polynomials $\{Q^{\nu}_{n,1}\}_{n=0}^{\infty}$, see Gould (1965) [35], Horadam (1985) [44] and Horadam and Pethe (1981) [45].

Remark 1.2.5. *The type 2 HARMA process is stationary and invertible for* $|\nu| < 1/2$ *and* $0 \leq u \leq 1$ *and all roots of* $\Phi(B) = 0$ *and* $\Theta(B) = 0$ *lies outside the unit circle.*

Remark 1.2.6. *For a type 2 Humbert ARMA*(p, ν, u, q) *process the spectral density takes the following form:*

$$f_x(\omega) = \frac{\sigma^2}{2\pi} \frac{|\Theta(z)|^2}{|\Phi(z)|^2} (2 + 4u^2 - 4u(\cos(\omega) + \cos((1-m)\omega)) + 2\cos(m\omega))^{-\nu}, \quad (1.18)$$

where $z = e^{-\iota\omega}$.

Remark 1.2.7. *Under the assumption of stationarity the spectral density of* HARMA(p, ν, u, q) *process has singularities [11]*

1. *at* $u = 0$ *and* $\omega = \frac{4n\pi \pm \pi}{m}$, *for* $-\frac{m\pm1}{4} < n < \frac{m\mp1}{4}$ *and*
2. *at* $u = (-1)^n \cos(\frac{4n\pi}{m-2})$ *and* $\omega = \pm\frac{2n\pi}{m-2}$, *for* $m \neq 2$ *and* $-\frac{(m-2)}{4} < n < \frac{(m-2)}{4}$.

For the detailed study of the above defined processes and parameter estimation, refer to [11]. The trajectory plots for various long memory processes are given in Fig. 1.2.

1.3 Spectral Density Based Parameter Estimation

The spectral density based estimation methods use the theoretical spectral density $f_x(\omega)$ and empirical spectral density (periodogram), denoted by $I(\omega)$, to construct the contrast or likelihood function $D(f_x(\omega), I(\omega))$. The empirical spectral density provides a representation of the distribution of frequencies in the time series data. The estimation process starts by calculating the empirical spectral density. This

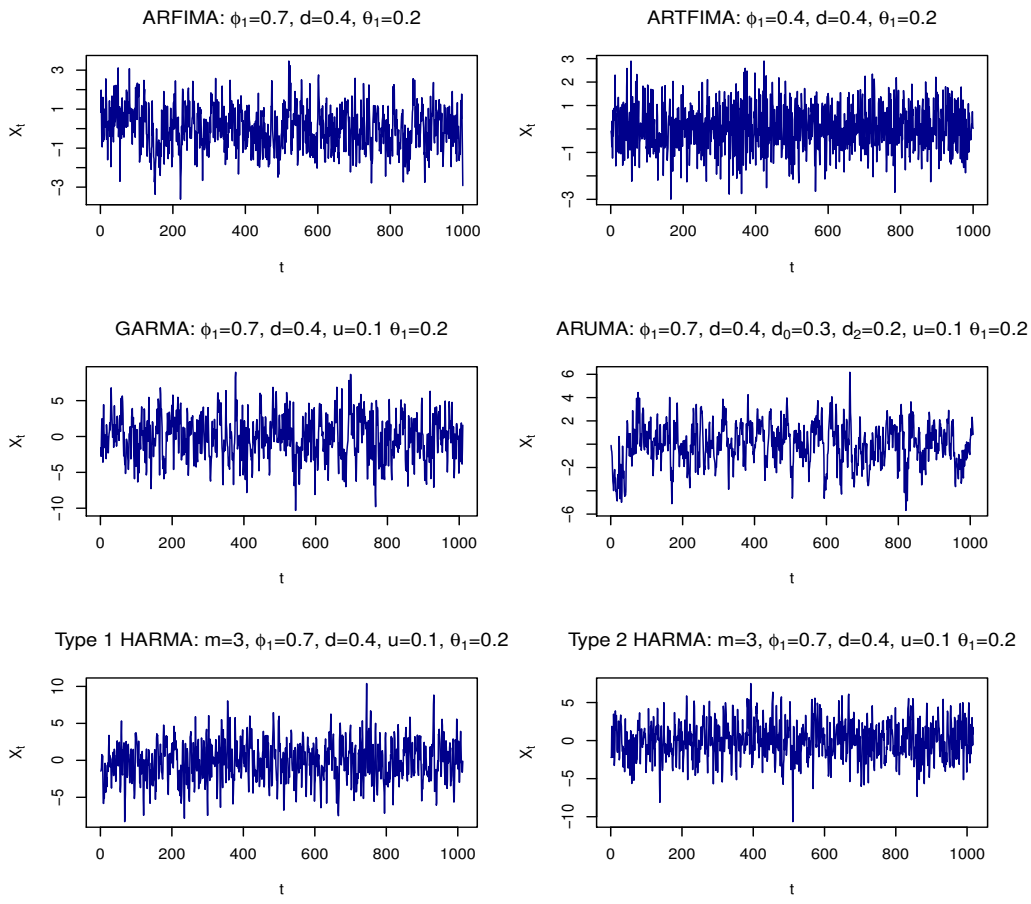

Figure 1.2: Trajectory plots for various long memory processes.

involves computing the periodogram, which is a commonly used estimator of the spectral density of a process $\{X_t\}$ and is expressed as:

$$I(\omega_j) = \frac{1}{2\pi}\left\{ R(0) + \sum_{s=1}^{n-1} R(s)\cos(s\omega_j) \right\}, \tag{1.19}$$

where $R(s) = \frac{\sum_{i=1}^{n-s}(X_i-\bar{X})(X_{i+s}-\bar{X})}{n}$, for $s = 0, 1, \ldots, (n-1)$ is the sample autocovariance function with sample mean $\bar{X}$, and $\omega_j = 2\pi j/n$, for $j = 0, 1, \ldots, \lfloor n/2 \rfloor$. The function $D(f_x(\omega), I(\omega))$ acts as a measure of dissimilarity or proximity between the theoretical and empirical spectral densities. The criteria to measure the nearness of $f_x(\omega)$ and $I(\omega)$ is given by [87] :

$$D(f_x(\omega), I(\omega)) = \int_{-\pi}^{\pi} K(I(\omega)/f_x(\omega))\, d\omega,$$

where $K(x)$ is three times continuously differentiable function on $(0, \infty)$ and has unique minima at $x = 1$. The contrast function $D(f_x(\omega), I(\omega))$ can take different

forms based on the assumption of the function $K(x)$ as discussed in [87], that is,

- $K(x) = x$,
- $K(x) = x - \log(x)$,
- $K(x) = \log(x) + \frac{1}{x}$,
- $K(x) = (\log(x))^2$,
- $K(x) = x\log(x) - x$,
- $K(x) = (x^\alpha - 1)^2$, where $0 < \alpha < \infty$.

Using the above-defined method, we study the Whittle likelihood and the debiased Whittle likelihood methods for parameter estimation. Both methods use the likelihood functions, which act as a measure of dissimilarity between true and empirical spectral density.

Whittle Likelihood Approach:

The Whittle estimation procedure, introduced by Whittle in 1951 [93,94], has significantly influenced parametric estimation within the frequency domain. Over time, substantial findings have been amassed, leading to the development of a comprehensive theory that incorporates diverse models exhibiting either short or long-range dependence. The asymptotic properties, that is, consistency and asymptotic normality of the Whittle likelihood estimators can be proved using the assumptions defined by Hannan in 1973 (see conditions A and B in [41]) and applying Theorem 8.2.1 in [33]. In 1986, Fox and Taqqu [26] adapted the approach of Whittle for parameter estimation of strongly dependent stationary time series. In 2008, Shitan and Peiris [81] used the Whittle likelihood estimation for a generalized autoregressive model of order 1. Several scholarly works have investigated the asymptotic behavior of the Whittle estimator, concluding a functional central limit theorem. For instance, Dahlhaus [20] presents this aspect in the context of weakly dependent time series. Expanding on theoretical properties, Heyde and Gay [42] as well as Hosoya [47], delve into the discussion of Whittle likelihood estimators for multivariate long memory processes, emphasizing their applicability beyond Gaussian processes. Addressing parameter estimation issues within the stable FARIMA(p, d, q) process, Kokoszka and Taqqu [54] have successfully employed a modified version of Whittle's method. Furthermore, Whittle estimation has garnered attention in studies by Anh et al. [6], Casas and Gao [21], Gao [29], Gao et al. [30], and Leonenko and Sakhno [59], which also serve as sources for additional references on this subject.

The Whittle likelihood technique leverages the empirical spectral density and theoretical spectral density to estimate the model parameters of the time series $\{X_t\}$. The process of estimation involves the minimization of a likelihood function, which centers around a set of harmonic frequencies denoted as ω_j, where $j = 0, 1, \ldots, \lfloor n/2 \rfloor$. These frequencies play a pivotal role in defining the empirical spectral density critical to Whittle likelihood estimation. This empirical spectral density serves as a depiction of frequency distribution within the time series data. The estimation procedure commences with the computation of this empirical spectral density, achieved through the calculation of the periodogram, a widely used estimator for spectral density. The formulation of the periodogram is represented by (1.19). The objective of the Whittle likelihood estimation method is to determine model parameters that minimize the disparity between the empirical $(I(\omega_j))$ and theoretical $(f_x(\omega_j))$ spectral densities. This is accomplished through the optimization of the following likelihood function:

$$l_w(\theta) = \sum_{j=1}^{n} \left(\frac{I(\omega_j)}{f_x(\omega_j)} + \log(f_x(\omega_j) \right), \tag{1.20}$$

where θ represents a vector of unknown parameters. The estimates of the parameters are obtained by minimizing the likelihood function $l_w(\theta)$ with respect to θ and depend on the sample size n, that is,

$$\hat{\theta}_n = \text{argmin}(l_w(\theta), \theta \in \Omega_0),$$

where $\Omega \subset \mathbb{R}^3$ and $\Omega_0 \subset \Omega$ is compact set. To prove the consistency and asymptotic normality of the Whittle likelihood estimator the following conditions, namely, *Conditions A* and *Conditions B* defined by Hannan [41] are required to establish, which are as follows:

Conditions A:

(a) The time series $\{X_t\}$ has the following moving average representation:

$$X_t = \sum_{k=0}^{\infty} a_k \epsilon_{t-k}, , \text{ where } \sum_{k=0}^{\infty} a_k^2 < \infty \text{ and } a_0 = 1. \tag{1.21}$$

(b) The spectral density $(f_x(\omega))$ of the process $\{X_t\}$ can be written as:

$$f_x(\omega) = \frac{\sigma^2}{2\pi} K(\omega)$$

and $\frac{1}{K(\omega)+a}$ is a continuous function, for $\omega \in (-\pi, \pi)$, $\forall\ a > 0$.

(c) Assuming the parameter space (Ω_0) is compact. Then the parameter vector $\theta \in \Omega_0$ defines the spectral density uniquely.

Conditions B:

(a) $K(\omega) > 0$, for all $\omega \in (-\pi, \pi)$ and $\theta \in \Omega_0$.

(b) $K(\omega)$ twice differentiable of all the parameters in parameter vector θ.

(c) The condition in (1.21) holds.

To prove the consistency of the Whittle likelihood using *Conditions A*, Fox and Taqqu gave a theorem (see Theorem 8.2.1 [26]), which is as follows:

Theorem 1.3.1. *Suppose an observable moving-average process* $\{X_t, t \in \mathbb{Z}\}$, *of* (1.21) *is ergodic and has the spectral density* $f_x(w) = \frac{\sigma^2}{2\pi} K(\omega)$, *and suppose the functions* $K(\omega)$, $\theta \in \Omega_0$ *satisfy Conditions A. Further, if additionally,* $1/f_x(\omega)$ *is continuous on* $(-\pi, \pi)$, *then,*

$$\hat{\theta}_n \xrightarrow{a.s.} \theta, \quad as\, n \to \infty.$$

The asymptotic normality of the Whittle likelihood can be proved using Theorem 2 defined by Hannan [41], which is as follows:

Theorem 1.3.2. *Under Conditions B,* $\sqrt{n}(\hat{\theta} - \theta)$ *converges in distribution to Gaussian random vectors with zero mean and covariance matrix* W^{-1}, *where*

$$W = \frac{1}{4\pi} \int_{-\pi}^{\pi} \left\{ \frac{\partial \log K(\omega)}{\partial \theta} \right\} \left\{ \frac{\partial \log K(\omega)}{\partial \theta} \right\}' d\omega.$$

Debiased Whittle Likelihood:

The debiased Whittle likelihood method is an improved computationally efficient method based on spectral density. Recently, the method was introduced by Sykulski et al. [85] to reduce the bias in the Whittle likelihood method. They present a pseudo-likelihood derived from the Whittle likelihood that promises remarkable reductions in bias and mean-squared error in practical applications. This improvement comes without imposing a significant increase in computational expense or compromising consistency and convergence rates. They term this pseudo-likelihood as the "de-biased Whittle likelihood". The method's performance in both simulation studies and its application to a vast oceanographic dataset is demonstrated. It has been further substantiated that the method yields consistent estimates even under less stringent assumptions. Importantly, there is no necessity

for the power spectral density to be continuous across frequencies. In both the scenarios, the debiased approach significantly reduces bias by up to two orders of magnitude. Dahlhaus's work [20] elucidated that the bias observed within the Whittle likelihood could be attributed to a phenomenon recognized as the leakage effect. This effect is alternatively termed as spectral blurring or spectral leakage. When a time series model is defined in continuous time but sampled at specific time intervals, there arises a potential issue known as aliasing. Aliasing occurs when high-frequency components in the continuous signal are incorrectly interpreted as lower frequencies in the discrete observations due to insufficient sampling rates [85]. In the context of Whittle estimation, aliasing introduces additional complexities. If not appropriately addressed or adjusted, aliasing can exacerbate the bias in Whittle estimates. Assuming $f_n(\omega;\theta)$ to be the theoretical spectral density of the process, the pseudo-likelihood function defined by Sykulski [85] has the form:

$$l_d(\theta) = \sum_{\omega} \Big\{ \log(\bar{f}_n(\omega;\theta)) + \frac{I(\omega)}{\bar{f}_n(\omega;\theta)} \Big\},$$

where

$$\bar{f}_n(\omega;\theta) \equiv \int_{-\pi}^{\pi} f(\omega';\theta)\mathcal{F}_n(\omega-\omega')d\omega'$$

is the expected periodogram, here,

$$\mathcal{F}_n(\omega) \equiv \frac{2\pi n \sin^2(n\omega/2)}{\sin^2(\omega/2)}$$

and $I(\omega)$ is the periodogram. The estimates are obtained by maximizing the function $l_d(\theta)$ as:

$$\hat{\theta}_n = \text{argmax}(l_d(\theta), \theta \in \Omega_0). \tag{1.22}$$

From [85], it is evident that the debiased estimator is computationally efficient and provides consistent estimates, and $\bar{f}_n(\omega;\theta)$ is the expected spectral representation, obtained by convolving the actual modeled spectrum with the Fejér kernel. However, the challenge lies in achieving this replacement of $f_x(\omega)$ with $\bar{f}_n(\omega;\theta)$, while ensuring computational efficiency as this replacement would often necessitate numerical approximation methods, which is efficient but can lead to computational inefficiencies and increased computational costs. In a study conducted in 2021, Grainger et al. [37] demonstrated, via numerical simulation, that the debiased Whittle likelihood method surpasses alternative techniques like least squares fitting in terms of both parameter recovery accuracy and precision. The consistency of the debiased whittle likelihood estimators can be proved using Prop. 1 defined by Sykulski et al. [85], which is as follows:

Proposition 1.3.1. *Assume that $\{X_t\}$ is an infinite sequence obtained from sampling a zero-mean continuous-time real-valued process $X(t;\theta)$, which satisfies the following assumptions:*

1. *The parameter set $\Omega_0 \in \mathbb{R}^p$ is compact with a non-null interior, and the true length-p parameter vector θ lies in the interior of Ω_0.*
2. *Assume that for all $\theta \in \Omega_0$ and $\omega \in [-\pi, \pi]$, the spectral density of the sequence $\{X_t\}$ is bounded below by $f(\omega;\theta) \geq f_{min} > 0$, and bounded above by $f(\omega;\theta) \leq f_{max}$.*
3. *If $\theta \neq \tilde{\theta}$, then there is a space of non-zero measure such that for all ω in this space $f(\omega;\theta) \neq f(\omega;\tilde{\theta})$.*
4. *The $f(\omega;\theta)$ is continuous in θ and Riemann integrable in ω.*
5. *The expected periodogram $\bar{f}_n(\omega:\theta)$ has two continuous derivatives in θ which are bounded above in magnitude uniformly for all n, where the first derivative in θ also has $\Omega_0(n)$ frequencies in $(-\pi, \pi)$ that are non-zero.*

Then, the estimator

$$\hat{\theta}_n = argmax(l_d(\theta), \theta \in \Omega_0),$$

for a process $\{X_t\}$, satisfies

$$\hat{\theta}_n \xrightarrow{a.s.} \theta, \quad as\, n \to \infty.$$

1.4 Aims and Objectives

The motive of this thesis is to study and introduce generalized time series models to extend the work available on classical and long memory time series models which are based on the assumptions of normality of the error terms, non-summability of the autocovariance (in case of long memory models), unbounded spectral densities, etc. We aim to study the properties such as stationarity, invertibility, form of spectral densities, autocovariance functions, parameter estimation, and asymptotic properties of the estimated parameters inherent in these generalized models. The examination of the stationarity and invertibility properties is conducted through a comprehensive approach that contains theoretical techniques. Also, the thesis focuses on parameter estimation of the generalized models using the empirical spectral densities of the processes and the likelihood functions, which measure the discrepancy between actual and empirical spectral densities. Outlined below are the main objectives of the thesis.

- Usually classical models such as AR, MA, and ARMA work on the assumptions of normality of the innovation terms. In many real-life scenarios, this might not be true. Many real-life time series probability distributions display heavy-tailed behavior or semi heavy-tailed behavior. Semi heavy-tailed probability density functions are those where tails are heavier than the Gaussian and lighter than the power law. In this thesis, our initial step involves defining a tempered stable autoregressive model of order 1 and denoting it by TAR(1) and AR(1) process with tempered stable distribution to overcome the issue of heavy-tailed datasets by assuming marginals and innovation distribution to be positive tempered stable. The TAR(1) process is a generalization of the inverse Gaussian autoregressive process discussed by Abraham and Balakrishna [1]. These models can give more flexibility in modeling datasets encountering extreme outcomes.

- Another generalization of long memory time series is done by introducing the Gegenbauer autoregressive tempered fractionally integrated moving average (GARTFIMA) process by introducing exponential tempering in the long memory GARMA process. The autocovariance function of the GARMA process is not absolutely summable and in finite variance cases, the spectral density becomes unbounded at some frequencies. It is more convenient to study the GARTFIMA model as the model overcomes these issues and the process can be used to model datasets with periodic behaviors having a bounded spectrum for frequencies near 0. Subsequently, we present an innovative generalization of the seasonal fractional ARUMA models, introducing the concept of "tempered fractional ARUMA model". This extension involves incorporating tempered fractional differencing within the traditional seasonal ARUMA framework, significantly enriching the model's flexibility and dynamics. The fundamental purpose of this extension is to address the inherent issue of a unit root within the classical ARUMA model. We feel a strong motivation to study these processes since tempering plays a pivotal role in circumventing the issue of the unit root within the classical and long memory models. Additionally, while the spectral density of seasonal fractional ARUMA is not bounded everywhere, tempering serves as a remedy, ensuring that the spectral density of the tempered processes remains bounded across all scenarios. The tempering transforms the spectral characteristics, conferring stability and control over the spectral properties of these models in various contexts.

- Further, we study the Horadam ARMA and Horadam-Pethe ARMA processes, which are the particular cases of type 2 Humbert ARMA processes. The type

2 Humbert ARMA process is defined by using type 2 Humbert polynomials. The type 1 and type 2 Humbert polynomials based on the type 1 and type 2 HARMA(p, ν, u, q) processes are studied in [11]. The Gegenbauer and the Pincherle polynomials are particular cases of type 1 Humbert polynomials. The Horadam and Horadam-Pethe polynomials are a particular case of type 2 Humbert polynomials. The Gegenbauer polynomials based time series model, namely, the GARMA process, has already been studied and applied in several real-world applications emanating from different areas. These processes possess seasonal long memory which helps to capture autocorrelation present in the data, leading to improved forecasting accuracy. Bhootna et al. [11] introduced the Pincherle ARMA, Horadam ARMA, and Horadam-Pethe ARMA processes and discussed the spectral density, stationarity, and invertibility conditions of the process. In this thesis, we propose to use the Whittle likelihood and the debiased Whittle likelihood techniques for the parameter estimation of Horadam ARMA and Horadam-Pethe ARMA processes. The debiased Whittle is an improved computationally efficient method based on spectral density. Recently, the method was introduced by Sykulski et.al [85] to reduce the bias in the Whittle likelihood method introduced by P. Whittle [94]

These new classes of time series models generalize the existing models like ARMA, ARIMA, ARFIMA, ARTFIMA, and GARMA in several directions. The possible areas of applications of the proposed model include sales forecasting in e-commerce industries as it can capture seasonality, trends, and other patterns in historical sales data. Also, the long memory property can capture autocorrelation patterns observed in financial returns, volatility, and other indicators. These models can be applied to analyze environmental monitoring data, such as water quality parameters, air pollution levels, and ecosystem dynamics. Overall, our study contributes to the advancement of time series analysis by introducing different generalized models, investigating their properties, providing parameter estimation techniques, and showcasing their efficacy through simulations and real data applications. The rest of the thesis is organized as follows:

In Chapter 2, we introduce and study a one-sided tempered stable first-order autoregressive model called TAR(1) and an autoregressive model featuring tempered stable innovations. Chapters 3 and 4 focus on the study of tempered processes namely, the Gegenbauer autoregressive tempered fractionally integrated moving average (GARTFIMA) process and the tempered fractional ARUMA process. These processes generalize the ARTFIMA, GARMA, and ARUMA processes, studied in

[34,38,63], respectively. In Chapter 5, we study the parameter estimation of type 1 and type 2 HARMA processes, using the spectral density based Whittle likelihood approach and the debiased Whittle likelihood approach. The last Chapter concludes the thesis and discusses some future directions.

Chapter 2

Tempered Stable Autoregressive Models

In this chapter, we introduce and study a one-sided tempered stable first order autoregressive model called TAR(1). Under the assumption of stationarity of the model, the marginal probability density function of the error term is obtained. It is shown that the distribution of the error term is infinitely divisible. Parameter estimation of the introduced TAR(1) process is done by adopting the conditional least square and method of moments based approach and the performance of the proposed methods is evaluated on simulated data. Also, we study an autoregressive model of order one with tempered stable innovations. Using appropriate test statistic it is shown that the model fits very well on real and simulated data. Our models generalize the inverse Gaussian and one-sided stable autoregressive models existing in the literature.

2.1 Introduction

Autoregressive models serve as eminent approach of modelling among different time-series methods. Many real life time-series data exhibits autoregressive behaviour. Classical autoregressive time series models are based on the assumption of normality of the innovation term. However, this assumption may not be true for all the real life scenarios. Many real life time series probability distributions display heavy-tailed behaviour or semi-heavy tailed behaviour. Semi-heavy tailed pdf are those where tails are heavier than the Gaussian and lighter than the power law, (see [65]). It is well known that series of counts, proportions, binary outcomes or non-negative observations are some examples of non-normal real life time-series data [39]. The autoregressive model of order 1, denoted by AR(1), is a simple, useful and interpretable model in a wide range of real life applications. Several AR(1) models with different marginal distributions are considered in literature. For example, Gaver and Lewis [31] considered linear additive first-order autoregressive scheme with gamma distributed marginals. The authors show that error distribution is same as the distribution of a non-negative random variable which has a point mass at 0 and

which is exponential if positive [31]. A more general exponential ARMA(p, q) model, called EARMA(p, q), is considered in [58]. A second order autoregressive model is considered by Dewald and Lewis, where Laplace distributed marginals are considered [22]. Abraham and Balakrishna considered inverse Gaussian autoregressive model, where the marginals are inverse Gaussian distributed [1]. The authors show that after fixing a parameter of the inverse Gaussian to 0 the error term is also inverse Gaussian distributed. The transition laws of tempered stable Ornstein-Uhlenbeck processes are discussed in [98].

In this chapter, we consider tempered stable autoregressive model of order 1 and denote it by TAR(1). This model generalizes the work discussed in Abraham and Balakrishna [1]. One parameter inverse Gaussian (also called Lévy distribution) is a particular case of the one-sided tempered stable distribution. We derive the explicit form of the error density. Further, we show that if the AR(1) series marginals are stable distributed, the error is also stable distributed with some scaling. A step-by-step procedure of the estimation of the parameters of the proposed model is given. Moreover, we consider an AR(1) model with one-sided tempered stable innovations. This model is different from the TAR(1) model where marginals are one-sided tempered stable, and here the innovations are positive tempered stable distributed. The application of this model is shown on real life power consumption data and drinking water treatment data. In particular, the introduction of the tempered stable autoregressive model of order 1 (TAR(1)) and AR(1) process with tempered stable innovation represent a novel contribution. Additionally, the introduction of an autoregressive model with positive tempered stable innovations presents another original contribution. While building upon prior research on inverse Gaussian autoregressive models, we extend the framework to incorporate one-sided tempered stable distributions, offering explicit formulations for error densities. The rest of the chapter is organized as follows: Section 2 defines the TAR(1) model where the explicit form of the density of the error term, infinite divisibility, moments, and parameter estimation methods of TAR(1) model are discussed. In Section 3, an AR(1) model with positive tempered stable innovations is introduced. The estimation procedure of the parameters of the introduced model is given based on the method of moments and conditional least square. The simulations study, where efficacy of the estimation procedure is discussed based on simulated data and real life application are discussed in this last section of the chapter.

2.2 Tempered Stable Autoregressive Model

In this section, we introduce the tempered stable autoregressive model and discuss the main properties. Consider an autoregressive process of order 1, defined as:

$$X_t = \rho X_{t-1} + \epsilon_t, \tag{2.1}$$

where $|\rho| < 1$ and $\{\epsilon_t, t \geq 1\}$ is sequence of i.i.d. random variables. Assuming marginals X_t s to be stationary positive tempered stable distributed. Then, there exist a distribution of ϵ_t s. The class of stable distributions is denoted by $Stable(\beta, \nu, \mu, \sigma)$, with parameter $\beta \in (0, 2]$ is the stability index, $\nu \in [-1, 1]$ is the skewness parameter, $\mu \in \mathbb{R}$ is the location parameter, and $\sigma > 0$ is the shape parameter. The stable class probability density functions do not possess closed-form except for three cases (Gaussian, Cauchy, and Lévy). Generally stable distributions are represented in terms of their characteristic functions or Laplace transforms. Stable distributions are infinitely divisible. The one-sided stable random variable S has following Laplace transform (see [78]):

$$\mathbb{E}(e^{-sS}) = e^{-s^\beta}, \ s > 0, \ \beta \in (0, 1).$$

The right tail of the S behaves (see [78]) as:

$$\mathbb{P}(S > x) \sim \frac{x^{-\beta}}{\Gamma(1-\beta)}, \text{ as } x \to \infty. \tag{2.2}$$

Next, we introduce the positive tempered stable distribution. The positive tempered stable random variable T, with tempering parameter $\lambda > 0$, and stability index $\beta \in (0, 1)$, has the Laplace transform (LT) (see [55,63]):

$$\mathbb{E}\left(e^{-sT}\right) = e^{-\left((s+\lambda)^\beta - \lambda^\beta\right)}. \tag{2.3}$$

Note that tempered stable distributions are obtained by exponential tempering in the distributions of α-stable distributions [75]. The advantage of tempered stable distribution over an α-stable distribution is that it has moments of all order and its density is also infinitely divisible. The probability density function for T is given by:

$$f_{\beta,\lambda}(x) = e^{-\lambda x + \lambda^\beta} f_\beta(x), \quad \lambda > 0, \ \beta \in (0, 1),$$

where $f_\beta(x)$ is the PDF of an α-stable distribution [89]. The tail probability of tempered stable distribution has the following asymptotic behavior:

$$\mathbb{P}(T > x) \sim c_{\beta,\lambda} \frac{e^{-\lambda x}}{x^{\beta}}, \text{ as } x \to \infty, \tag{2.4}$$

where $c_{\beta,\lambda} = \frac{1}{\beta\pi}\Gamma(1+\beta)\sin(\pi\beta)e^{\lambda^{\beta}}$. The first two moments of tempered stable distribution are given by:

$$\mathbb{E}(T) = \beta\lambda^{\beta-1}, \;\; \mathbb{E}(T)^2 = \beta(1-\beta)\lambda^{\beta-2} + (\beta\lambda^{\beta-1})^2.$$

A pdf $u(x)$ is called a semi-heavy tailed pdf if

$$u(x) \sim e^{-cx}v(x), \; c > 0,$$

where v is a regularly varying function [65]. Recall that a positive function v is regularly varying with index ν if

$$\lim_{x\to\infty} \frac{v(dx)}{v(x)} = d^{\nu}, \; d > 0.$$

Using (2.4), it is straightforward to show that

$$f_{\beta,\lambda}(x) \sim \lambda c_{\beta,\lambda} x^{-\beta} e^{-\lambda x}, \text{ as } x \to \infty,$$

and hence the tempered stable density function is semi-heavy tailed.

2.2.1 Distributional Properties

In this subsection, we discuss about the distributional properties related to the introduced TAR(1) process. If each X_t in (2.1) is positive tempered stable, then the Laplace transform of X_t is given by:

$$\Phi_{X_t}(s) = \mathbb{E}(\exp(-sX_t)) = \mathbb{E}(\exp(-s(\rho X_{t-1} + \epsilon_t))) = \Phi_{X_{t-1}}(\rho s)\Phi_{\epsilon_t}(s). \tag{2.5}$$

Assuming X_t s to be stationary distributed, it follows:

$$\Phi_X(s) = \exp\{-((\lambda+s)^{\beta} - \lambda^{\beta})\}, \quad \lambda > 0, \; \beta \in (0,1), \tag{2.6}$$

and

$$\Phi_X(\rho s) = \exp\{-((\lambda+\rho s)^{\beta} - \lambda^{\beta})\}, \quad \lambda > 0, \; \beta \in (0,1). \tag{2.7}$$

Using (2.5)

$$\Phi_X(s) = \Phi_{\epsilon}(s)\Phi_X(\rho s),$$

which implies

$$\Phi_\epsilon(s) = \frac{\Phi_X(s)}{\Phi_X(\rho s)}.$$

Putting values from (2.6) and (2.7), yields

$$\Phi_\epsilon(s) = \exp\{(\rho s + \lambda)^\beta - (s + \lambda)^\beta\}. \tag{2.8}$$

The k-th order moment, for the innovation term, can be extracted by taking the k-th order derivative of Laplace transform as follows:

$$\mathbb{E}[\epsilon^k] = (-1)^k \frac{d^k}{ds^k}\phi_\epsilon(s)|_{s=0},\ k \in \mathbb{N},$$

which yields

$$\mathbb{E}(\epsilon) = \beta\lambda^{\beta-1}(1-\rho), \tag{2.9}$$

and

$$\mathbb{E}(\epsilon^2) = (\beta\lambda^{\beta-1}(\rho-1))^2 + \beta(\beta-1)\lambda^{\beta-2}(\rho^2-1). \tag{2.10}$$

Remark 2.2.1. *For $\lambda = 0$, in (2.8), we have $\Phi_\epsilon(s) = e^{-(1-\rho^\beta)s^\beta}$, which is the Laplace transform of a positive stable random variable $(1-\rho^\beta)^{1/\beta}S$. Hence, it shows that the if the AR(1) series is stable the error term is also stable.*

Proposition 2.2.1. *The error distribution with Laplace transform (2.8) is infinitely divisible.*

Proof. By Feller (1971), a pdf $f(x)$, $x \geq 0$ is infinitely divisible iff its Laplace transform is of the form $F(s) = e^{-\phi(s)}$, $for\ s > 0$, where $\phi(s)$ has a completely monotone derivative. Further, a function $\psi(\cdot)$ is completely monotone if it possesses derivatives $\psi^{(n)}(\cdot)$ of all orders and $(-1)^n\psi^{(n)}(s) \geq 0$, $s > 0$, $n = 0, 1, \ldots$ (see [25], p. 439). For $\Phi_\epsilon(s)$, we have $\phi(s) = (s+\lambda)^\beta - (\rho s + \lambda)^\beta$, which gives $\phi'(s) = \beta(s+\lambda)^{\beta-1} - \beta\rho(\rho s+\lambda)^{\beta-1}$. Consider $\psi(s) = (s+\lambda)^{\beta-1}$, which yields to $\psi^{(n)}(s) = (\beta-1)(\beta-2)\cdots(\beta-n)(s+\lambda)^{\beta-n-1}$. Thus $(-1)^n\psi^{(n)}(s) \geq 0$, $n = 0, 1, 2, \ldots$. Similarly, considering $\zeta(s) = (\rho s + \lambda)^{\beta-1}$, we can show that $\zeta(s)$ is completely monotone. Moreover, $(-1)^n\phi^n(s) = (-1)^n\psi^n(s) - (-1)^n\zeta^n(s)$ and $\psi^n(s)$ is always greater than $\zeta^n(s)$ as $0 < \rho < 1$, this implies $(-1)^n\phi^n(s) \geq 0$. So, $\phi(s)$ has completely monotone derivative. □

Remark 2.2.2. *Using (2.8), it follows that the random variable ϵ can be written as the difference of two independent but not identically distributed tempered stable random variables. Hence the error distributions are infinitely divisible since, the*

difference of two infinitely divisible random variables is infinitely divisible (see [84], Prop. 2.1, p. 94).

Next, we provide the explicit form of the pdf of the error term using complex inversion formula, which generalize the corresponding results in [1].

Theorem 2.2.1. *For the stationary tempered stable autoregressive model defined in (2.1) with Laplace transform defined as:*

$$\mathbb{E}\left(e^{-sX_t}\right) = e^{-\left((s+\lambda)^\beta - \lambda^\beta\right)}, \tag{2.11}$$

the pdf of the innovation term has following integral form:

$$g(x) = \frac{1}{2\pi i}\Bigg[\int_0^\infty \left(e^{\frac{-\lambda x}{\rho}} e^{-wx} e^{\rho^\beta w^\beta e^{-\iota\pi\beta} - (we^{-\iota\pi}+\lambda-\frac{\lambda}{\rho})^\beta} - e^{\frac{-\lambda x}{\rho}} e^{-wx} e^{\rho^\beta w^\beta e^{\iota\pi\beta} - (we^{\iota\pi}+\lambda-\frac{\lambda}{\rho})^\beta}\right) dw$$
$$+ \int_0^{\frac{\lambda}{\rho}-\lambda} \left(- e^{-\lambda x} e^{-wx} e^{(-\lambda\rho+\rho we^{-\iota\pi}+\lambda)^\beta - (we^{-\iota\pi})^\beta} - e^{-\lambda x} e^{-wx} e^{(-\lambda\rho+\rho we^{\iota\pi}+\lambda)^\beta - (we^{\iota\pi})^\beta}\right) dw,\Bigg] \tag{2.12}$$

where $\lambda > 0$ and $\beta \in (0,1)$.

Proof. Inverse Laplace transform corresponding to $\Phi_\epsilon(s)$ provides the density of innovation term. The density for innovation can be computed using complex inversion formula for Laplace transform given by

$$g(x) = \frac{1}{2\pi i}\int_{x_0-i\infty}^{x_0+i\infty} e^{sx}\Phi_\epsilon(s)ds, \tag{2.13}$$

where point $x_0 > a$ for some a is taken in such a way that the integrand is analytic for $\mathcal{R}e(s) > a$. Note that the integrand $e^{sx}\Phi_\epsilon(s)$ is an exponential function which is analytic in whole complex plane. However, due to fractional power in the exponent the integrand $e^{sx}\Phi_\epsilon(s)$ has branch points at $s = -\lambda$ and $s = -\lambda/\rho$. Thus we take a branch cut along the non-positive real axis and consider a (single-valued) analytic branch of the integrand. To calculate (2.13), consider a closed double-key-hole contour C: ABCDEFGHIJA (Fig. 2.1) with branch points at $O = (-\lambda, 0)$ and $O' = (-\lambda/\rho, 0)$. The contour consists of following segments: AB and IJ are arcs of radius R, BC, DE, FG, and HI are line segment parallel to x-axis, CD, EF, and GH are arcs of circles with radius r, and JA is the line segment from $x_0 - iy$ to $x_0 + iy$ (see Fig. 1). The integrand is analytic within and on the contour C so that by

Cauchy's residue theorem (see [80])

$$\frac{1}{2\pi i}\int_C e^{sx}\Phi_\epsilon(s)ds = 0.$$

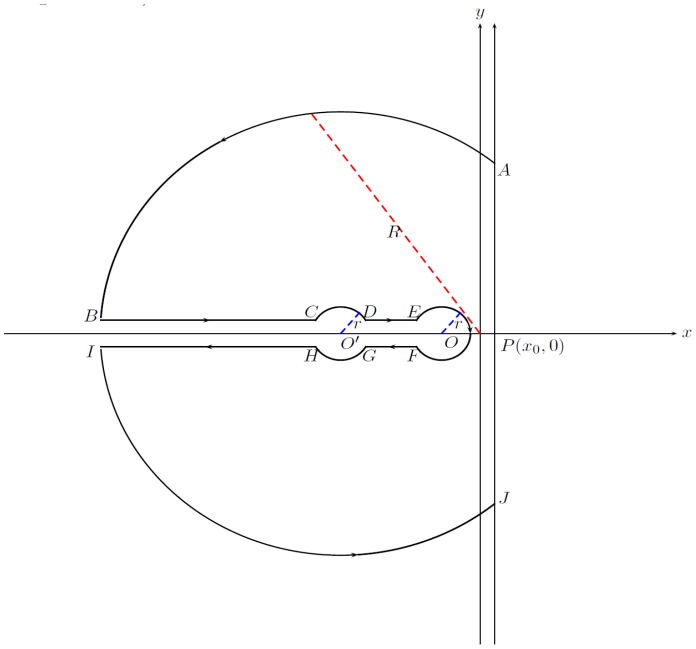

Figure 2.1: The double key hole contour

Using (Lemma 4.1 Schiff (1999), p. 154), the integral on circular arcs AB and IJ tend to 0 as $R \to \infty$. The integral over CD, EF, and GH are also zero as r goes to infinity. Thus, as $r \to 0$ and $R \to \infty$, we have

$$\begin{aligned}\frac{1}{2\pi i}\int_{x_0-i\infty}^{x_0+i\infty} e^{sx}\Phi_\epsilon(s) = -\frac{1}{2\pi i}\int_{BC} e^{sx}\Phi_\epsilon(s)ds - \frac{1}{2\pi i}\int_{DE} e^{sx}\Phi_\epsilon(s)ds \\ - \frac{1}{2\pi i}\int_{FG} e^{sx}\Phi_\epsilon(s)ds - \int_{HI} e^{sx}\Phi_\epsilon(s)ds. \qquad (2.14)\end{aligned}$$

Along BC, put $s = -\frac{\lambda}{\rho} + we^{\iota\pi}$, which implies $ds = -dw$, and hence

$$\int_{BC} e^{sx}\exp((\rho s+\lambda)^\beta - (s+\lambda)^\beta))ds = \int_r^{R-\lambda/\rho} e^{-\lambda x/\rho}e^{-wx}e^{\rho^\beta w^\beta e^{\iota\pi\beta} - (we^{\iota\pi}+\lambda-\lambda/\rho)^\beta}dw. \qquad (2.15)$$

Along HI, $s = -\dfrac{\lambda}{\rho} + we^{-\iota\pi}$ and $ds = -dw$

$$\int_{HI} e^{sx}\exp((\rho s+\lambda)^{\beta}-(s+\lambda)^{\beta}))ds = -\int_{r}^{R-\lambda/\rho} e^{-\lambda x/\rho}e^{-wx}e^{\rho^{\beta}w^{\beta}e^{-\iota\pi\beta}-(we^{-\iota\pi}+\lambda-\lambda/\rho)^{\beta}}dw. \tag{2.16}$$

Along DE, $s = -\lambda + we^{\iota\pi}$ and $ds = -dw$

$$\int_{DE} e^{sx}\exp((\rho s+\lambda)^{\beta}-(s+\lambda)^{\beta}))ds = \int_{r}^{-r+(\lambda/\rho)-\lambda} e^{-\lambda x}e^{-wx}e^{(-\lambda\rho+\rho we^{\iota\pi}+\lambda)^{\beta}-(we^{\iota\pi})^{\beta}}dw. \tag{2.17}$$

Along FG, $s = -\lambda + we^{-\iota\pi}$ and $ds = -dw$

$$\int_{FG} e^{sx}\exp((\rho s+\lambda)^{\beta}-(s+\lambda)^{\beta}))ds = -\int_{r}^{-r+(\lambda/\rho)-\lambda} e^{-\lambda x}e^{-wx}e^{(-\lambda\rho+\rho we^{-\iota\pi}+\lambda)^{\beta}-(we^{-\iota\pi})^{\beta}}dw \tag{2.18}$$

Substituting (2.15), (2.16), (2.17), and (2.18) in (2.14), the result follows as $r \to 0$ and $R \to \infty$. □

Remark 2.2.3. *For the special case $\lambda = 0$ and $\beta = \dfrac{1}{2}$, (2.12) reduces to:*

$$g(x) = \left(\frac{1-\sqrt{\rho}}{\sqrt{2}}\right)\left(\frac{1}{2\pi x^3}\right)^{1/2}\exp\left(\frac{(1-\sqrt{\rho})^2}{4x}\right),\ \ |\rho| < 1,$$

and is called Lévy probability density function see [7], which is a special case of the inverse Gaussian density. Abraham and Balakrishna [1] show that if the inverse Gaussian autoregressive model is stationary the error term is also inverse Gaussian distributed. Our results complement their findings.

Remark 2.2.4. *For $\lambda = 0$, the error density function in (2.12) reduces to:*

$$g(x) = \frac{1}{\pi}\int_{0}^{\infty} e^{-wx}e^{w^{\beta}(1-\rho^{\beta})\cos(\pi\beta)}\sin\left(w^{\beta}(1-\rho^{\beta})\sin(\pi\beta)\right),\ x > 0. \tag{2.19}$$

Proposition 2.2.2. *For $\lambda = 0$, the innovation term has the following fractional q-th order moment:*

$$\mathbb{E}(\epsilon^{q}) = \frac{\Gamma(1-q/\beta)}{\Gamma(1-q)}(1-\rho^{\beta})^{q/\beta},\ 0 < q < \beta < 1.$$

Proof. For a positive random variable X with a Laplace transform $\Phi(s)$, and for $p > 0$, it follows:

$$\int_{0}^{\infty}\frac{d^{n}}{ds^{n}}[\Phi(s)]s^{p-1} = \int_{0}^{\infty}\frac{d^{n}}{ds^{n}}\left[\mathbb{E}e^{-sX}\right]s^{p-1}ds = \mathbb{E}\int_{0}^{\infty}\frac{d^{n}}{ds^{n}}\left[e^{-sX}\right]s^{p-1}ds$$

$$= (-1)^n \mathbb{E}\left[\int_0^\infty X^n e^{-uX} u^{p-1} ds\right] = (-1)^n \Gamma(p) \mathbb{E}(X^{n-p}).$$

Thus for $q \in (n-1, n)$, for an integer n, we have:

$$\mathbb{E}(X^q) = \frac{(-1)^n}{\Gamma(n-q)} \int_0^\infty \frac{d^n}{ds^n} \left[\Phi(s)\right] s^{n-q-1} ds.$$

Using the relationship for $q \in (0, 1)$, it follows:

$$\begin{aligned}
\mathbb{E}(\epsilon^q) &= \frac{-1}{\Gamma(1-q)} \int_0^\infty \frac{d}{ds} \left[e^{(\rho s+\lambda)^\beta - (s+\lambda)^\beta}\right] s^{-q} ds \\
&= \frac{1}{\Gamma(1-q)} \int_0^\infty e^{(\rho s+\lambda)^\beta - (s+\lambda)^\beta} \left((s+\lambda)^{\beta-1} - \rho\beta(\rho s+\lambda)^{\beta-1}\right) s^{-q} ds,
\end{aligned}$$

which gives the q-th order fractional moment of the innovation term. For $\lambda = 0$, it can be written in the explicit form as follows:

$$\begin{aligned}
\mathbb{E}(\epsilon^q) &= \frac{1}{\Gamma(1-q)} \int_0^\infty e^{-(1-\rho^\beta)s^\beta} s^{\beta-q-1} \beta(1-\rho^\beta) ds \\
&= \frac{1}{\Gamma(1-q)} \int_0^\infty e^{-(1-\rho^\beta)u} u^{-q/\beta} (1-\rho^\beta) du \quad (\text{put } s^\beta = u) \\
&= \frac{(1-\rho^\beta)}{\Gamma(1-q)} \frac{\Gamma(1-q/\beta)}{(1-\rho^\beta)^{(1-q/\beta)}} = \frac{\Gamma(1-q/\beta)}{\Gamma(1-q)} (1-\rho^\beta)^{q/\beta}, \ 0 < q < \beta.
\end{aligned}$$

□

Proposition 2.2.3. *For the stationary TAR(1) model, defined in (2.1) the autocorrelation for r-th lag ρ_r has the following recursive form*

$$\rho_r = \rho^r.$$

Proof. For the given TAR(1) process $X_t = \rho X_{t-1} + \epsilon_t$, multiplying both the side by X_{t-r}, we get:

$$X_t X_{t-r} = \rho X_{t-1} X_{t-r} + \epsilon_t X_{t-r}.$$

Here X_t is independent of ϵ_j for $j > n$. Taking expectation on both the sides, yields

$$\mathbb{E}(X_t X_{t-r}) = \rho \mathbb{E}(X_{t-1} X_{t-r}) + \mathbb{E}(\epsilon_t X_{t-r}),$$

which gives

$$\begin{aligned}
\mathbb{E}(X_t X_{t-r}) - \mathbb{E}(X_t)\mathbb{E}(X_{t-r}) = \rho \mathbb{E}(X_{t-1} X_{t-r}) - \rho \mathbb{E}(X_{t-1})\mathbb{E}(X_{t-r}) + \rho \mathbb{E}(X_{t-1})\mathbb{E}(X_{t-r}) \\
- \mathbb{E}(X_t)\mathbb{E}(X_{t-r}) + \mathbb{E}(\epsilon_t)\mathbb{E}(X_{t-r}).
\end{aligned}$$

Thus,

$$\begin{aligned}\mathrm{Cov}(X_t, X_{t-r}) &= \rho\mathrm{Cov}(X_{t-1}X_{t-r}) + \mathbb{E}(X_{t-1})\mathbb{E}(X_{t-r})(\rho-1) + \mathbb{E}(\epsilon_t)\mathbb{E}(X_{t-r}) \\ &= \rho\mathrm{Cov}(X_{t-1}X_{t-r}) + \mathbb{E}(X_{t-r})(\mathbb{E}(X_t)(\rho-1) + \mathbb{E}(\epsilon_t)).\end{aligned}$$

Since, $\mathbb{E}(\epsilon_t) = (1-\rho)\beta\lambda^{\beta-1}$ and $\mathbb{E}(X_t) = \beta\lambda^{\beta-1}$, it follows:

$$\begin{aligned}\mathrm{Cov}(X_t, X_{t-r}) &= \rho\mathrm{Cov}(X_{t-1}, X_{t-r}) + \mathbb{E}(X_{t-r})(\beta\lambda^{\beta-1}(\rho-1) + (1-\rho)\beta\lambda^{\beta-1}) \\ &= \rho\mathrm{Cov}(X_{t-1}, X_{t-r}).\end{aligned}$$

Dividing both side by $\sqrt{\mathrm{Var}(X_t)\mathrm{Var}(X_{t-r})}$, yields

$$\frac{\mathrm{Cov}(X_tX_{t-r})}{\sqrt{\mathrm{Var}(X_t)Var(X_{t-r})}} = \frac{\mathrm{Cov}(X_{t-1}X_{t-r})}{\sqrt{\mathrm{Var}(X_{t-1})\mathrm{Var}(X_{t-r})}},$$

Using, $\mathrm{Var(X_t)}$=$\mathrm{Var(X_{t-1})}$=$\mathrm{Var(X_{t-r})}$, leads to

$$\rho_r = \rho\rho_{r-1} \implies \rho_r = \rho^r,$$

where $\rho_0 = 1$ and $\rho_1 = \rho$.

□

2.2.2 Parameter Estimation

Here, we discuss the estimation procedure of the parameters of the tempered stable autoregressive model. We consider conditional least square and moments based estimation methods.

Parameter estimation by conditional least square: The conditional least square method provides a straightforward procedure to estimate the parameters for dependent observations by minimizing the sum of square of deviations about conditional expectation [9,53]. To estimate the parameter ρ of process (2.1) the conditional least square (CLS) method is used. The CLS estimator of parameter vector $\theta = (\rho, \lambda, \beta)$ is obtained by minimizing

$$Q_n(\theta) = \sum_{i=1}^{n} \left[X_{i+1} - \mathbb{E}(X_{i+1}|X_i, X_{i-1}, \cdots, X_1)\right]^2, \tag{2.20}$$

with respect to θ. For an AR(1) sequence, due to Markovian property

$$\mathbb{E}(X_{i+1}|X_i, X_{i-1}, \cdots, X_1) = \mathbb{E}(X_{i+1}|X_i), \tag{2.21}$$

which yields

$$\mathbb{E}(X_{i+1}|X_i) = \rho X_i + \mathbb{E}(\epsilon_i), \tag{2.22}$$

where $\mathbb{E}(\epsilon_i) = \beta\lambda^{\beta-1}(1-\rho)$. Using (2.20) and (2.21), we can write

$$Q_n(\theta) = \sum_{i=1}^{n} \left[X_{i+1} - \rho X_i - (1-\rho)\beta\lambda^{\beta-1}\right]^2. \tag{2.23}$$

Minimising (2.23) w.r.t ρ, β, and λ gives the following relation for β and λ:

$$\beta\lambda^{\beta-1} = \frac{\sum_{i=1}^{n}(X_{i+1} - \hat{\rho}X_i)}{n(1-\hat{\rho})}. \tag{2.24}$$

and estimate for ρ using above equation (2.24) is

$$\hat{\rho} = \frac{\sum_{i=1}^{n}(X_i - \bar{X})(X_{i+1} - \bar{X})}{\sum_{i=1}^{n}(X_i - \bar{X})^2}, \tag{2.25}$$

The estimate $\hat{\rho}$ can be easily calculated from the observed sample using (2.25). However, some numerical method which minimizes the squared difference between left and right hand sides is required to estimate β and λ from (2.24). Next, we prove the asymptotic normality of the estimator $\hat{\rho}_n$, which is otherwise denoted by $\hat{\rho}$ for ease of notation.

Proposition 2.2.4. *The CLS estimator $\hat{\rho}_n$ for ρ is asymptotically normal, that is,*

$$\sqrt{n}(\hat{\rho}_n - \rho) \xrightarrow{\mathcal{L}} \mathcal{N}(0, 1-\rho^2), \quad \text{as } n \to \infty.$$

Proof. TAR(1) process satisfies the regularity conditions defined by Klimkov and Nelson [53], so one can say that the CLS estimator of ρ is consistent and normal, that is,

$$\sqrt{n}(\hat{\rho}_n - \rho) \xrightarrow{\mathcal{L}} \mathcal{N}(0, D),$$

where $D = \frac{W}{V^2}$ and the value of W and V can be calculated using the method defined by Klimkov and Nelson [53]. Define:

$$\begin{aligned} g(\theta, X_{t-1}) &= \rho X_{t-1} + (1-\rho)\beta\lambda^{(\beta-1)}, \\ V &= \mathbb{E}\left[\left(\frac{\partial g(\theta, X_{t-1})}{\partial \rho}\right)^2\right] = \mathbb{E}[X_{t-1}^2] - \beta\lambda^{\beta-1}, \text{ and} \\ W &= \mathbb{E}\left[U_n^2\left(\frac{\partial g(\theta, X_{t-1})}{\partial \rho}\right)^2\right], \end{aligned}$$

where

$$U_n = X_t - \rho X_{t-1} - (1-\rho)\beta\lambda^{(\beta-1)} = \varepsilon_n - (1-\rho)\beta\lambda^{(\beta-1)}.$$

This implies that

$$\begin{aligned} W &= \mathbb{E}[(\varepsilon_n - (1-\rho)\beta\lambda^{(\beta-1)})^2 (X_{t-1} - \beta\lambda^{(\beta-1)})^2] \\ &= \mathbb{E}[(\varepsilon_n - (1-\rho)\beta\lambda^{(\beta-1)})^2]\mathbb{E}[(X_{t-1} - \beta\lambda^{(\beta-1)})^2]. \end{aligned}$$

Thus,

$$\begin{aligned} \frac{W}{V^2} &= \frac{\mathbb{E}[(\varepsilon_n - (1-\rho)\beta\lambda^{(\beta-1)})^2]}{\mathbb{E}[X_{t-1}^2 - \beta\lambda^{(\beta-1)})^2]} \\ &= \frac{\mathbb{E}[(\varepsilon_n)^2 - ((1-\rho)\beta\lambda^{(\beta-1)})^2 - 2\varepsilon_n(1-\rho)(\beta\lambda^{(\beta-1)})]}{\mathbb{E}[X_{t-1}^2] - (\beta\lambda^{(\beta-1)})^2} \\ &= \frac{\mathbb{E}[\varepsilon_n^2] - (1-\rho)^2(\beta\lambda^{(\beta-1)})^2}{\mathbb{E}[X_{t-1}^2] - (\beta\lambda^{(\beta-1)})^2} \\ &= \frac{(\beta\lambda^{\beta-1}(1-\rho))^2 + \beta(1-\beta)\lambda^{\beta-2}(1-\rho^2) - ((1-\rho)\beta\lambda^{\beta-1})^2}{\beta(1-\beta)\lambda^{\beta-2} + (\beta\lambda^{\beta-1})^2 - (\beta\lambda^{\beta-1})^2} = (1-\rho^2). \end{aligned}$$

□

Using (2.24), it is evident that for parameters β and λ, the estimators are not in closed-form and hence the estimates are obtained by optimization. Thus, in our opinion, the asymptotic properties of the estimators for β and λ are not possible to established. To check the asymptotic property of estimator $\hat{\rho}_n$ we simulate 1000 datasets, each with length $n = 5000$, for $\rho = 0.9$ and find out the simulated values of $\hat{\rho}_n$ for each simulation. For $\sqrt{n}(\hat{\rho}_n - \rho)$, the sample mean is 0 and sample variance is 0.194, which shows the convergence discussed in Prop. 2.2.4. The histogram for simulated values of $\sqrt{n}(\hat{\rho}_n - \rho)$ is given in Fig. 2.2.

Moments based estimation: The parameters of positive tempered stable distribution cannot be estimated by classical maximum likelihood estimation methods due to non-availability of closed from probability density function. Also, the CLS estimator provides an estimate for ρ only. Here, we use method of moments to estimate the parameters β and λ. The general idea used by Pearson [67] is the population moments about the origin are equal to the corresponding moments of the sample data. In case of TAR(1) process, moments for innovation distribution can be extracted using the corresponding Laplace transform as the density (2.12) is in complex form. The idea is to apply the method of moments on the error sample, which can be easily obtained from the original series by first estimating the ρ using

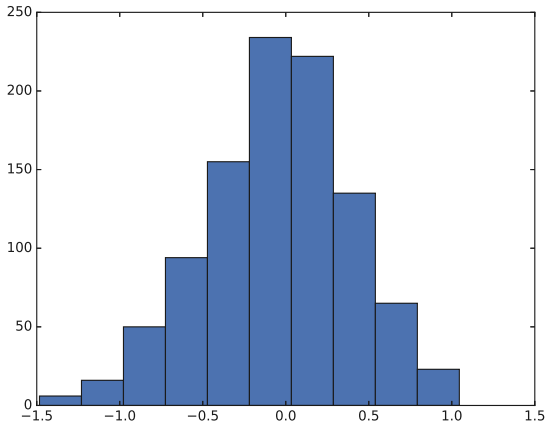

Figure 2.2: Histogram plot for $\sqrt{n}(\hat{\rho}_n - \rho)$

CLS method. The sample estimates for $\mathbb{E}(\epsilon_i)$ and $\mathbb{E}(\epsilon_i^2)$ are given by:

$$m_1 = \frac{\sum_{i=1}^{n} \epsilon_i}{n} = \frac{\sum_{i=1}^{n} (X_{i+1} - \rho X_i)}{n}, \tag{2.26}$$

$$m_2 = \frac{\sum_{i=1}^{n} \epsilon_i^2}{n} = \frac{\sum_{i=1}^{n} (X_{i+1} - \rho X_i)^2}{n}. \tag{2.27}$$

Taking $z = \frac{\sum_{i=1}^{n} (X_{i+1} - \rho X_i)}{n}$ and $r = \frac{\sum_{i=1}^{n} (X_{i+1} - \rho X_i)^2}{n}$ and using (2.9), (2.10), (2.26), and (2.27) we get the following relations:

$$\beta \lambda^{\beta - 1} = \frac{z}{1 - \rho}, \quad \beta = 1 + \frac{(z^2 - r)\lambda}{z(1 + \rho)}.$$

After some manipulation, the above two equations leads to following non-linear equations:

$$\beta \left(\frac{\beta - 1}{d} \right)^{(\beta - 1)} - \left(\frac{z}{1 - \rho} \right) = 0$$
$$(1 + d\lambda)\lambda^{d\lambda} - \left(\frac{z}{1 - \rho} \right) = 0$$

We use sequential least square optimization technique (SLSQP) to solve these equations, which is an iterative method to optimize a non-linear model using the non-linear least square model and sequential quadratic programming model [27]. We use "scipy.optimize", which use "SLSQP" as an inbuilt method in python to solve non-linear equations that gives the estimates for β and λ.

Parameter estimation by tail index: The parameter estimation, for the case $\lambda = 0$ (corresponding density given by (2.19)) is done by using the right tail behaviour of S, for the TAR(1) process. For the TAR(1) process, we have a positive stable innovation random variable $(1-\rho^\beta)^{1/\beta}S$ with corresponding Laplace transform $e^{-(1-\rho^\beta)s^\beta}$. Note that the innovation terms are independent and hence the estimation can be done using empirical and theoretical tails. Using (2.2), it follows:

$$\mathbb{P}((1-\rho^\beta)^{1/\beta}S > x) = \mathbb{P}(S > (1-\rho^\beta)^{-1/\beta}x) \sim \frac{((1-\rho^\beta)^{-1/\beta}x)^{-\beta}}{\Gamma(1-\beta)}, \text{ as } x \to \infty. \tag{2.28}$$

Taking log on both sides of (2.28) and replacing $\mathbb{P}(S > (1-\rho^\beta)^{-1/\beta}x) = G_\epsilon(x)$, where $G_\epsilon(x)$ represents the empirical tail for ϵ, we get

$$\log(G_\epsilon(x)) = -\beta\log(x) + \log(1-\rho^\beta) - \log(\Gamma(1-\beta)),\ 0 < \beta < 1. \tag{2.29}$$

Consider $Y = \log(G_\epsilon(x))$ and $X = -\log(x)$, which yields β as slope of the regressing Y on X.

2.2.3 Simulation Study

To check the efficacy of the estimation procedure, we perform simulation. Here, we have considered an AR(1) model with marginals to be distributed as one-sided tempered stable distribution and the corresponding Laplace transform for error term ϵ_t is given in (2.8). In order to simulate a tempered stable AR(1) series, first we simulate data for innovation using the Laplace transform (see [73]). Ridout discussed the simulation of a continuous distribution function using its Laplace transform which turns out to be very helpful if the probability density function is not in closed-form. We consider 1000 simulations each with length $n = 10,000$, for three different different parameter combinations. For each case single trajectory is used for estimation and the results are summarized in the following Table 2.1.

	Actual	**Estimated**
Case 1	$\rho = 0.9,\ \lambda = 1,\ \beta = 0.5$	$\hat{\rho} = 0.895,\ \hat{\lambda} = 1.13,\ \hat{\beta} = 0.489$
Case 2	$\rho = 0.8,\ \lambda = 2,\ \beta = 0.7$	$\hat{\rho} = 0.795,\ \hat{\lambda} = 1.93,\ \hat{\beta} = 0.70$
Case 3	$\rho = 0.75,\ \lambda = 1.5,\ \beta = 0.9$	$\hat{\rho} = 0.755,\ \hat{\lambda} = 1.60,\ \hat{\beta} = 0.90$

Table 2.1: Actual and estimated parameter values for single trajectory with different choices of parameters.

The sample trajectory for an AR(1) process for positive tempered stable distribution with parameters $\rho = 0.9$, $\lambda = 2$, and $\beta = 0.5$ is given in Fig. 2.3a. Next, we generate

1000 samples of TAR(1) process with size 10,000 each to assess the performance of the estimation method. To ensure the stationarity, here, we assume AR(1) process with parameter $\rho < |1|$. Consider $\rho = 0.9$ and take tempered stable distribution parameters as $\beta = 0.5$ and $\lambda = 2$. The parameters λ and β are estimated using method of moments. On the other hand, the conditional least square is used to estimate ρ, considering different samples. The corresponding box-plots for estimated parameter values are shown in Fig. 2.3b. For the particular case $\lambda = 0$, which

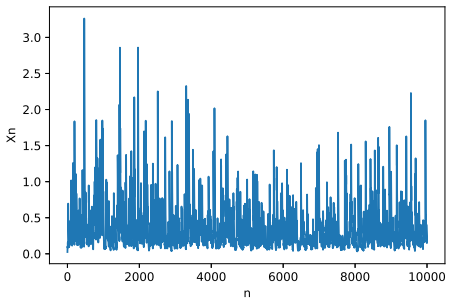

(a) Sample trajectory TAR(1)

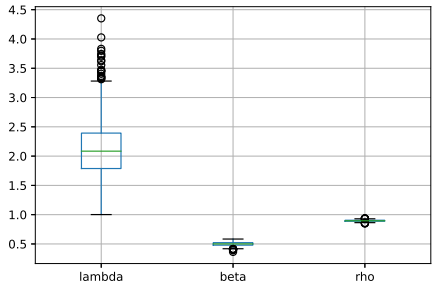

(b) Box-plot of estimated parameters of TAR(1) process using MoM

Figure 2.3: Sample path of TAR(1) process (left panel) and the box plot of estimated parameters using method of moments (right panel).

leads to one-sided positive stable autoregressive model, simulation is again done by the method given in [73], and parameter estimation is done by the tail index method using (2.29). We simulate a sample of $10,000$ observations for $\rho = 0.5$ and $\beta = 0.5$. By taking values greater than a particular threshold such that we have some percentage of the sorted dataset greater than that threshold value, we get regression based estimate for β. Taking a cutoff value of 0.009 gives the 30% of observation greater than the cutoff and gives the corresponding estimate of 0.36 for β. For cutoff value 0.019, we get almost 20% of the observation greater than threshold value and corresponding estimate is 0.41 for β, which is more close to true parameter value. Further, for $k = 0.06$ the estimated β is 0.49, which is even more closer to the actual value. This clearly indicates that the accuracy of the estimated parameter depend on the threshold selected. The results are summarized in Table 2.2, where k represents the threshold value.

	Threshold	**Actual**β	**Estimated**β
Case 1	k=0.009	0.5	0.36
Case 2	k=0.019	0.5	0.41
Case 3	k=0.06	0.5	0.49

Table 2.2: Actual and estimated parameter values for single trajectory with different choices of parameters based on tail index, for $\lambda = 0$.

2.3 AR(1) Process with Tempered Stable Innovations

Consider the stationary AR(1) process

$$X_t = \rho X_{t-1} + \epsilon_t, \quad |\rho| < 1, \tag{2.30}$$

where ϵ_t s are i.i.d positive tempered stable random variables defined in (2.3) and independent of X_{t-1}. Let $\Phi_{X_t}(s)$ and $\Phi_{\epsilon_t}(s)$ are Laplace transform of X_t and ϵ_t, respectively. Now, assuming $X_0 \overset{\mathrm{d}}{=} \epsilon_0$ and recursively writing (2.30), we get a moving average representation of AR(1) process as follows:

$$X_t = \sum_{i=0}^{n} \rho^i \epsilon_{t-i}, \ \lambda > 0, \ \beta \in (0,1).$$

The Laplace transform of X_t is

$$\Phi_{X_t}(s) = \prod_{i=0}^{n} \Phi_{\epsilon}(\rho^i s) = \prod_{i=0}^{n} e^{\lambda^\beta - (\lambda+\rho^i s)^\beta} = e^{n\lambda^\beta - \sum_{i=0}^{n}(\lambda+\rho^i s)^\beta}.$$

Proposition 2.3.1. *For $\lambda = 0$, the q-th order moment of X_t is given by:*

$$\mathbb{E}(X_t^q) = \frac{\Gamma(1-q/\beta)}{\Gamma(1-q)} (\sum_{i=0}^{n} \rho^{i\beta})^{q/\beta}, \ 0 < q < \beta < 1.$$

Proof. Using Prop. 2.2.2, for a positive random variable X with corresponding Laplace transform $\Phi(s)$, and for $p > 0$, it follows:

$$\int_0^\infty \frac{d^m}{ds^m}[\Phi(s)] s^{p-1} = (-1)^n \Gamma(p) \mathbb{E}(X^{n-p}).$$

Thus, for $q \in (m-1, m)$, for an integer m, we have:

$$\mathbb{E}(X^q) = \frac{(-1)^m}{\Gamma(n-q)} \int_0^\infty \frac{d^m}{ds^m} [\Phi(s)] \, s^{n-q-1} ds.$$

For $q \in (0,1)$, it follows:

$$\begin{aligned}\mathbb{E}(X_t^q) &= \frac{-1}{\Gamma(1-q)} \int_0^\infty \frac{d}{ds}\left[e^{n\lambda^\beta - \sum_{i=0}^n (\rho^i s+\lambda)^\beta}\right] s^{-q} ds \\ &= \frac{1}{\Gamma(1-q)} \int_0^\infty e^{n\lambda^\beta - \sum_{i=0}^n (\rho^i s+\lambda)^\beta} \sum_{i=0}^n \beta\rho^i(\rho^i s+\lambda)^{\beta-1} s^{-q} ds.\end{aligned}$$

For $\lambda = 0$, it yields

$$\begin{aligned}\mathbb{E}(X_t^q) &= \frac{1}{\Gamma(1-q)} \int_0^\infty e^{\sum_{i=0}^n \rho^{i\beta} s^\beta} s^{\beta-q-1} \beta\big(\sum_{i=0}^n \rho^{i\beta}\big) ds \\ &= \frac{1}{\Gamma(1-q)} \int_0^\infty e^{-\sum_{i=0}^n \rho^{i\beta} u} u^{-q/\beta} \beta\big(\sum_{i=0}^n \rho^{i\beta}\big) du \quad (\text{put } s^\beta = u) \\ &= \frac{\sum_{i=0}^n \rho^{i\beta}}{\Gamma(1-q)} \frac{\Gamma(1-q/\beta)}{\big(\sum_{i=0}^n \rho^{i\beta}\big)^{(1-q/\beta)}} = \frac{\Gamma(1-q/\beta)}{\Gamma(1-q)} \big(\sum_{i=0}^n \rho^{i\beta}\big)^{q/\beta}, \ 0 < q < \beta.\end{aligned}$$

□

Remark 2.3.1. *Using same argument as in Prop. 2.2.1, we show that the marginal distributions of X_t are infinitely divisible. It is easy to show that for $e^{n\lambda^\beta - \sum_{i=0}^n (\lambda+\rho^i s)^\beta}$, the exponent $\phi(s) = \sum_{i=0}^n (\lambda+\rho^i s)^\beta - n\lambda^\beta$ has completely monotone derivative, that is $(-1)^n \phi^n(s) \geq 0, \ n = 0, 1, 2, \ldots$.*

Remark 2.3.2. *The index of dispersion for X_t is $ID(X_t) = \dfrac{\mathrm{Var}(X_t)}{\mathbb{E}(X_t)}$. Using the mean and variance of the process X_t, given by $\mathbb{E}(X_t) = \dfrac{\beta\lambda^{\beta-1}}{1-\rho}$ and $\mathrm{Var}(X_t) = \dfrac{\beta(1-\beta)\lambda^{(\beta-2)}}{1-\rho^2}$, yields $ID(X_t) = \dfrac{1-\beta}{\lambda(1+\rho)}$, where $0 < \rho < 1, \beta \in (0,1)$ and $\lambda > 0$. For $\lambda > 1$ the $ID(X_t) < 1$, which implies that the marginal distributions of X_t are under-dispersed for $\lambda > 1$.*

2.3.1 Parameter Estimation

To estimate the parameter ρ of the process (2.30), the conditional least square method discussed in previous section is used, which minimize (2.20) with respect to θ. Using the mean of ϵ_t and (2.20), (2.21), and (2.22), we can write

$$Q_n(\theta) = \sum_{i=1}^n \left[X_{i+1} - \rho X_i - \beta\lambda^{\beta-1}\right]^2. \tag{2.31}$$

Minimizing (2.31) w.r.t ρ gives the following estimate:

$$\hat{\rho} = \frac{\sum_{i=1}^n (X_i - \bar{X})(X_{i+1} - \bar{X})}{\sum_{i=1}^n (X_i - \bar{X})^2}.$$

The parameter estimation for β and λ is done again using method of moments for ϵ_t, which leads to

$$m_1 = \beta\lambda^{\beta-1}, \quad m_2 = (\beta\lambda^{\beta-1})^2 + \beta(1-\beta)\lambda^{\beta-2},$$

where m_1 and m_2 are first and second order sample moments for ϵ_t, respectively. After some manipulation, we get the following non-linear equations:

$$\beta(c(\beta-1))^{(\beta-1)} - m_1 = 0, \quad \left(\frac{\lambda}{c}+1\right)\lambda^{(\lambda/c)+1} - m_1 = 0,$$

where $c = \dfrac{m_1}{m_2^2 - m1}$. Using the optimization technique SLSQP, discussed in Section 2.2.2, these equations are solved in python to obtain the estimates $\hat{\lambda}$ and $\hat{\beta}$. The estimate of λ can also be obtained using the estimate $\hat{\beta}$, denoted by:

$$\hat{\lambda} = \left(\frac{m_1}{\hat{\beta}}\right)^{\frac{1}{\hat{\beta}-1}} - m_1 = 0.$$

2.3.2 Simulation Study and Real Data Application

To check the performance of the estimation method, we use simulated dataset. Using the method discussed in [73], we simulate an independent sample of size 10,000 for error term using the Laplace transform of positive tempered stable random variable defined in (2.3). Then, we recursively simulate AR(1) series by using fixed value of ρ and letting $\epsilon_0 = X_0$. The performance of the estimation method for three different sets of parameters is summarized in Table 2.3. For each case single trajectory is used for estimation. The sample trajectory for AR(1) process with tempered stable innovations is given in Fig. 2.4a. Further, to assess the performance of the estimation method, box plots of the estimated parameters $\hat{\rho}, \hat{\beta}$, and $\hat{\lambda}$ are plotted by taking multiple simulated random samples of innovations and generating multiple AR(1) time-series. Here, we generate 1000 samples each of length $n = 10,000$ for $\rho = 0.9, \beta = 0.5$, and $\lambda = 2$ and estimate parameters for each sample. The box plot of estimated parameters is shown in Fig. 2.4b.

Real data application for power consumption data: The power consumption data during the time of COVID-19 is extracted from Kaggle. The data contains the daily state-wise power consumption in India during the time period Jan 2, 2019 to May 23, 2020 that is for a period of 17 months and each data-point represents the power consumption at that time in Mega Units (MU). We work on the data during the period Apr 14, 2019 to Apr 29, 2020 for the Indian state Arunachal Pradesh.

	Actual	**Estimated**
Case 1	$\rho = 0.9,\ \lambda = 1,\ \beta = 0.5$	$\hat{\rho} = 0.8909,\ \hat{\lambda} = 1.01,\ \hat{\beta} = 0.5002$
Case 2	$\rho = 0.8,\ \lambda = 2,\ \beta = 0.7$	$\hat{\rho} = 0.804,\ \hat{\lambda} = 2.037,\ \hat{\beta} = 0.69$
Case 3	$\rho = 0.75,\ \lambda = 1.5,\ \beta = 0.9$	$\hat{\rho} = 0.75131,\ \hat{\lambda} = 1.56,\ \hat{\beta} = 0.89$

Table 2.3: Actual and estimated parameter values for single trajectory with different choices of parameters.

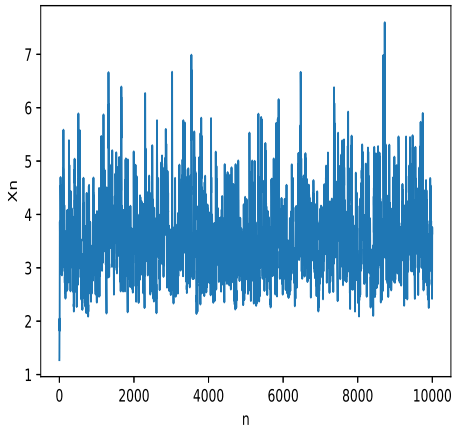

(a) Sample trajectory AR(1) process with tempered stable innovations

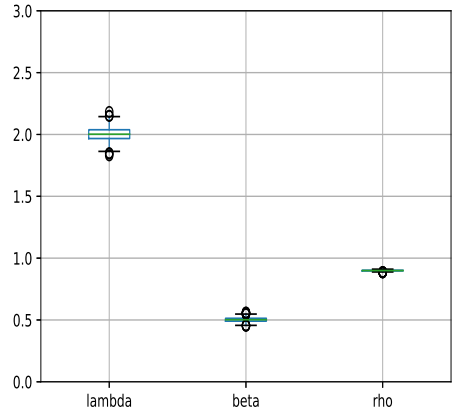

(b) Box plot of parameters using MoM

Figure 2.4: Sample path of AR(1) process with tempered stable innovations (left panel) and the box plot of estimated parameters (right panel).

The sample path of the data is plotted in Fig. 2.5a.

By simply looking at the data we can visualize the stationarity with some sharp spikes suggesting non-Gaussian behavior. We have applied Augmented Dickey–Fuller (ADF) test to check the stationarity of the data and the p-value comes out to be less than 0.05, which indicates that the null hypothesis of ADF test is rejected at 5% significance level and implies that the data is stationary. To determine the appropriate time series model, ACF and PACF plots are given in Fig. 2.5b and Fig. 2.6a, respectively, which determines the appropriate time series model with significant lag.

Clearly, PACF plot for the dataset is significant till lag 1 and the ACF plot tails off, this means that AR(1) model would be a good fit for this data. We assume that the innovation term ϵ_t follows one-sided tempered stable distribution. We fit the proposed AR(1) model with tempered stable distribution on the dataset. The estimated parameters using the above described methods are $\hat{\beta} = 0.91, \hat{\lambda} = 2.9$, and $\hat{\rho} = 0.60$. Using these estimated values, we simulate a dataset to assess the accuracy of the results. We simulate a data sample for $\hat{\lambda} = 2.8$ and $\hat{\beta} = 0.92$. Considering the

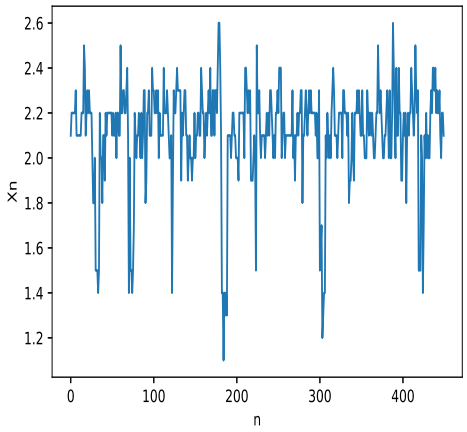

(a) Power consumption series

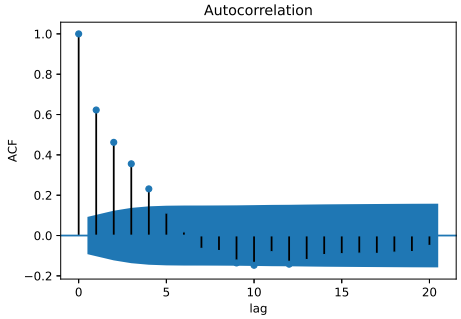

(b) ACF plot

Figure 2.5: Time series plot of the power consumption data (left panel) and the corresponding ACF plot (right panel).

relation $\epsilon_t = X_t - \rho X_{t-1}$, we generate a dataset for the innovation term. To check whether both the simulated data using estimated parameters values and the actual data set follow same distribution or not we use two sample Kolmogorov–Smirnov (K-S) test and Mann–Whitney U test. The two sample K-S and Mann–Whitney U test both are non-parametric tests which compare the distribution of two datasets. The two sample K-S test applied on actual error dataset and simulated error dataset, gives a p-value 0.056, and Mann–Whitney U test gives the p-value 0.377. Thus the null hypothesis for both the tests are accepted at 5% level of significance. This indicates that both the samples are from same distributions. Hence, it is appropriate to model the considered power consumption time-series using AR(1) model with positive tempered stable innovations.

Using the estimated parameters from empirical power consumption dataset, we generate synthetic tempered stable errors series of same length as of empirical dataset. Also, we generate another synthetic errors series by assuming the innovations to be Gaussian with mean μ and variance σ^2, where μ and σ^2 are estimated using empirical errors. The estimated parameters for tempered stable innovations are $\lambda = 2.89$ and $\beta = 0.92$, and the estimated parameters for Gaussian innovation are $\mu = 0.84$ and $\sigma^2 = 0.049$. The KDE plots for empirical errors, tempered stable errors, and Gaussian errors are given in Fig. 2.6b.

It is clearly evident that the density plot for Gaussian innovations does not matches with the density plot for empirical innovations. However, the density plot for tempered stable innovations better model the empirical innovations. Moreover, the K-S test and Mann Whitney U test is accepted at 5% level of significance, which justify to use AR(1) model with tempered stable innovations. To measure

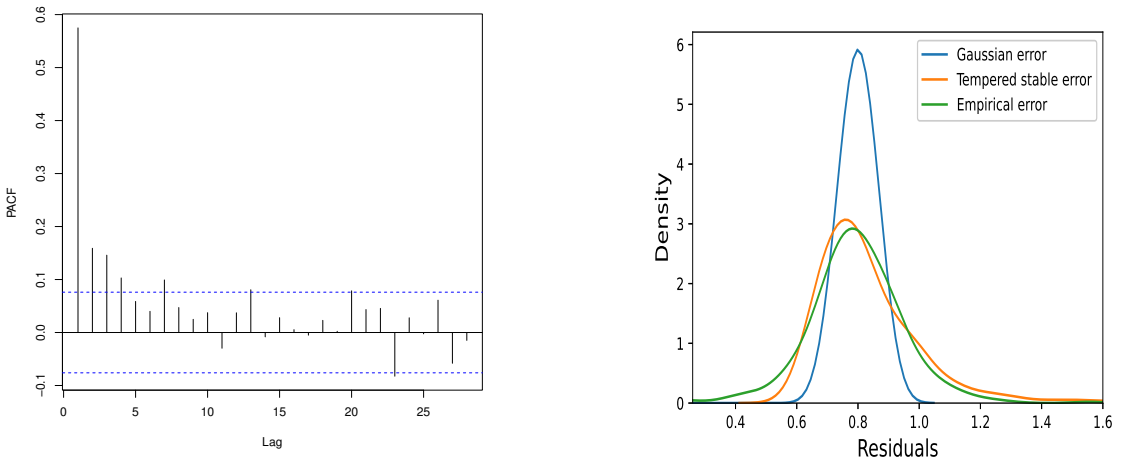

(a) PACF plot (b) KDE plot

Figure 2.6: PACF plot of the power consumption data (left panel) and the KDE plots of the empirical errors, simulated Gaussian errors, simulated tempered stable errors (right panel).

the model performance, Theil's U test is applied, which measures the accuracy based on distance between actual values and predicted values [14]. The model is said to performs well if the statistic value is close to 0. The two types of Theil's U statistics are defined below.

The type 1 statistic is defined as:

$$U_1 = \frac{\sqrt{\frac{1}{n}\sum_{i=1}^{n}(F_i - X_i)^2}}{\sqrt{\frac{1}{n}\sum_{i=1}^{n}F_i^2} + \sqrt{\frac{1}{n}\sum_{i=1}^{n}X_i^2}},$$

where F_i is the forcasted value at time $t = i$ and X_i is the corresponding actual value. Further, the type 2 statistic is defined as:

$$U_2 = \frac{\left[\sum_{i=1}^{n}(F_i - X_i)^2\right]^{1/2}}{\left[\sum_{i=1}^{n}X_i^2\right]^{1/2}}.$$

By allocating 80% of the power consumption data to training set and 20% data to testing set, and using the forcasted values from AR(1) model with tempered stable innovations the U_1 and U_2 statistics, respectively are 0.04 and 0.2, which indicates that the proposed model performs well for this dataset.

Real data application for drinking water treatment data: We study another

dataset that is drinking water treatment plant (DWTP) data, which has a daily frequency. The dataset is extracted from Data World. We study daily Turbidity data which is a measure of water clarity for a time period of 1000 days, that is , from May 15, 2008 to Feb 09, 2011. The sample path of the data is given in Fig. 2.7a. The ACF and PACF of the data are shown in Fig. 2.7b and 2.8a, respectively. One can observe that the PACF is significant for lag 1 and the ACF plot tails off indicating that the AR(1) would be a good fit for the data.

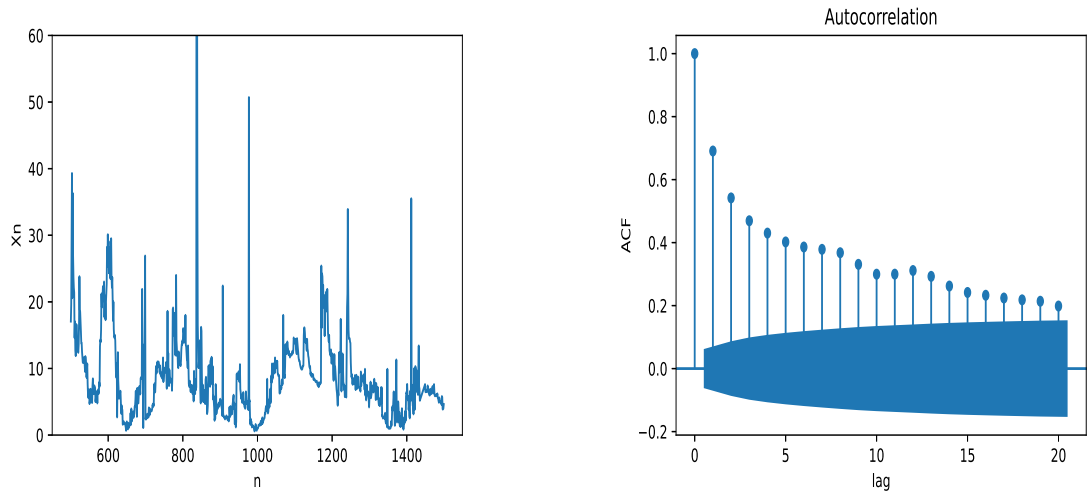

(a) Water turbidity series

(b) ACF plot

Figure 2.7: Time series plot of the water turbidity data (left panel) and the corresponding ACF plot (right panel).

The p-value for the ADF test statistic is less than 0.05 indicating the stationarity of the data. The estimated parameters for the proposed AR(1) model with tempered stable innovations are $\hat{\rho} = 0.69$, $\hat{\beta} = 0.49$, and $\hat{\lambda} = 0.04$. These estimated parameters are further used to simulate tempered stable innovations for KDE plot. Assuming the error distribution to be Gaussian the estimated parameters are $\mu = 2.68$ and $\sigma^2 = 28.64$. The KDE plots for empirical errors, simulated tempered stable errors and simulated Gaussian errors are given in Fig. 2.8b.

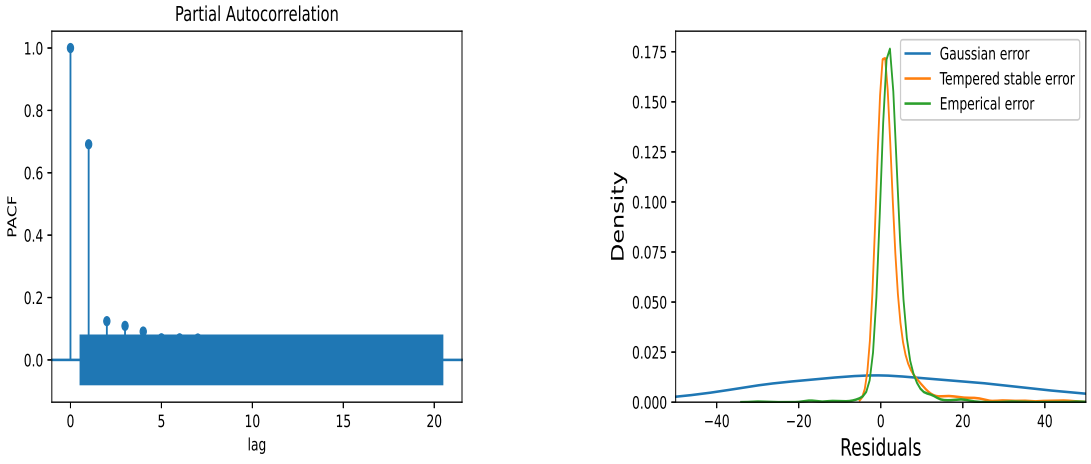

(a) PACF plot

(b) KDE plot

Figure 2.8: PACF plot of the power consumption data (left panel) and the KDE plots of the empirical errors, simulated Gaussian errors, simulated tempered stable errors (right panel).

Chapter 3

GARTFIMA Process: Empirical Spectral Density Based Estimation

In this chapter, we introduce a Gegenbauer autoregressive tempered fractionally integrated moving average (GARTFIMA) process. We work on the spectral density and autocovariance function for the introduced process. The parameter estimation is done using the empirical spectral density with the help of the non-linear least square technique and the Whittle likelihood estimation technique. The performance of the proposed estimation techniques is assessed on simulated data. Further, the introduced process is shown to better model the real-world data in comparison to other time series models.

3.1 Introduction

In Chapter 1, we extensively explored the foundational concepts of time series modeling, particularly focusing on the ARIMA(p, d, q) and ARFIMA(p, d, q) processes. While these models offer valuable insights into non-stationary time series, their effectiveness diminishes when confronted with data exhibiting long-range dependence. This phenomenon, characterized by substantial correlation persisting over large lag intervals, is prevalent in diverse fields such as finance, economics, geophysics, and agriculture [10,74]. To address the limitations of ARIMA and ARFIMA processes in capturing LRD, we turn our attention to the innovative approach introduced by Hosking in [46]. He extended the Box and Jenkins framework by incorporating a fractional differencing operator, giving rise to the Autoregressive Fractionally Integrated Moving Average (ARFIMA(p, d, q)) process. This process, with $d \in \mathbb{R}$, emerges as stationary for $|d| < 1/2$ and exhibits LRD characteristics for $d \in (0, 0.5)$. An LRD process is a process whose autocovariance function or autocorrelation function is not absolutely summable or in the frequency domain and power spectral density is not everywhere bounded. In recent years, tempered processes have been studied in great detail [12,40,56,75,77]. These processes are obtained by exponential tempering in the original process. The ARTFIMA models were introduced as a generalization of the ARFIMA model in

[76]. According to [76], it is more convenient to study ARTFIMA time series as the covariance function is absolutely summable in finite variance cases and the spectral density converges to zero [38]. Also, the spectral density of the ARFIMA process is unbounded as the frequency approaches 0. In many scenarios, there exist many datasets for which the power spectrum is bounded as the frequency approaches 0 and these types of datasets cannot be modelled using the ARFIMA process. An extension of the Fractional ARIMA process is proposed to model long-term seasonal and periodic behaviors and is referred to as the Gegenbauer autoregressive moving average (GARMA) process [38]. The GARMA process uses the properties of the Gegenbauer generating function to model a time series. For the Gegenbauer random fields, one can refer to [24].

In this chapter, we introduce and study the Gegenbauer autoregressive tempered fractionally integrated moving average (GARTFIMA) process, which is a further extension to the GARMA process as well as the ARTFIMA process by including the tempering parameter λ and Gegenbauer shift operator in ARFIMA process. The GARTFIMA process can be used to model datasets with periodic behaviors having a bounded spectrum for frequencies near 0. Our contribution involves both the introduction of a new model namely GARTFIMA model and the development of a novel parameter estimation techniques, namely non-linear least square approach. Additionally, we investigate an existing parameter estimation technique for GARTFIMA process, namely Whittle likelihood estimation method. The rest of the chapter is organized as follows:

Section 3.2 includes a new parameter estimation technique for the ARTFIMA process which is inspired from the non-linear regression technique introduced by Reisen [71]. A simulation study is also done to check the performance of the estimation method. In Section 3.3, the GARTFIMA process is introduced and the corresponding form of spectral density is obtained. Further, the autocovariance of the process is found by taking the inverse Fourier transform of the spectral density which does not have an explicit closed-form expression and can be represented using the coefficients of Gegenbauer polynomials. Moreover, the stationarity and invertibility conditions are also discussed for the GARTFIMA process. The parameter estimation techniques for the GARTFIMA process are provided in Section 3.4. To estimate the parameters of the process first approach is based on non-linear regression and the second is based on the Whittle likelihood estimation and the performance is assessed by doing a simulation study for both the methods, where the comparison of actual and estimated parameters are demonstrated using the box plots. The comparison of the defined model with ARFIMA and ARTFIMA models is also presented in this section.

3.2 Parameter Estimation for ARTFIMA Process

The parameter estimation for the ARTFIMA process is discussed in [76] using the Whittle likelihood based estimation technique. Here, we provide an alternative estimation technique based on empirical spectral density using the non-linear least square approach to estimate the parameters d and λ. We establish a non-linear regression equation between empirical and actual spectral densities to estimate the unknown parameters. In (1.12), assuming $(1-e^{-\lambda}B)X_t = U_t$, the spectral density for the ARMA(p,q) process $\Phi(B)U_t = \Theta(B)\epsilon_t$, is given by:

$$f_u(\omega_j) = \frac{\sigma^2}{2\pi}\frac{|\Theta(e^{-\iota\omega_j})|^2}{|\Phi(e^{-\iota\omega_j})|^2}. \tag{3.1}$$

Using (3.1) and (1.13), the spectral density of X_t can be written as:

$$f_x(\omega_j) = f_u(\omega_j)(1-2e^{-\lambda}\cos(\omega_j)+e^{-2\lambda})^{-d}. \tag{3.2}$$

Consider $\omega_j = \dfrac{2\pi j}{n}$, $j = 0, 1, \ldots, \lfloor n/2 \rfloor$ to be a set of Harmonic frequencies. Here, n is the sample size and ω_j is the set of harmonic frequencies. Taking natural logarithm on both sides of (3.2) and with some manipulation, it follows:

$$\begin{aligned}\log\{f_x(\omega_j)\} &= \log\{f_u(0)\} + \log\{f_u(\omega_j)\} - d\log\{(1-2e^{-\lambda}\cos(\omega_j)+e^{-2\lambda})\} - \log\{f_u(0)\} \\ &= \log\{f_u(0)\} - d\log\{(1-2e^{-\lambda}\cos(\omega_j)+e^{-2\lambda})\} + \log\left\{\frac{f_u(\omega_j)}{f_u(0)}\right\}.\end{aligned}$$

Adding $\log\{I(\omega_j)\}$ on both sides yields

$$\begin{aligned}\log\{I(\omega_j)\} = \log\{f_u(0)\} - d\log\{(1-2e^{-\lambda}\cos(\omega_j)+e^{-2\lambda})\} + \log\left\{\frac{f_u(\omega_j)}{f_u(0)}\right\} \\ + \log\left\{\frac{I(\omega_j)}{f_x(\omega_j)}\right\},\end{aligned} \tag{3.3}$$

where $I(\omega_j)$ is known as the periodogram or empirical spectral density of the process $\{X_t\}$ stated as:

$$I(\omega_j) = \frac{1}{2\pi}\left\{R(0) + \sum_{s=1}^{n-1} R(s)\cos(s\omega_j)\right\} \quad \omega \in [-\pi, \pi], \tag{3.4}$$

where $R(s) = \dfrac{1}{n}\sum_{i=1}^{n-s}(X_i - \bar{X})(X_{i+s} - \bar{X})$, $s = 0, 1, \ldots, (n-1)$ is the sample

autocovariance function with sample mean $\bar{X}$. Using (3.1), we have:

$$f_u(0) = \frac{\sigma^2}{2\pi} \frac{(1-\theta_1-\cdots-\theta_q)^2}{(1-\phi_1-\cdots-\phi_p)^2}.$$

Assuming $\log(I(\omega_j)/f_x(\omega_j))$ to be the error term for the non-linear equation given in (3.3) and minimizing the sum of squared errors for the equation, the parameters d and λ are estimated. Also, choosing the ω_j near 0, the term $\log(f_u(\omega_j)/f_u(0))$ will be negligible. So, another way for the estimation is to choose the upper limit of j such that the ω_j is small or near zero. Considering ω_j close to 0, the (3.3) can be rewritten as:

$$\log\{I(\omega_j)\} = \log\{f_u(0)\} - d\log\{(1-2e^{-\lambda}\cos(\omega_j)+e^{-2\lambda})\} + \log\left\{\frac{I(\omega_j)}{f_x(\omega_j)}\right\}. \quad (3.5)$$

The above equation can be expressed in form of a non-linear regression equation, where $\log(I(\omega_j)/f_x(\omega_j))$ can be expressed as error term $\log\{f_u(0)\}$ can be expressed as intercept and the parameters d and λ can be estimated by applying the non-linear least square regression or minimizing the sum of squared errors using generalized simulated annealing with "GenSa" package in R.

Simulation study

A simulation study is carried out to assess the performance of the stated estimation approach. Assuming the innovation distribution to be Gaussian with mean $\mu = 0$ and variance $\sigma^2 = 2$, a sample with size 1000 is simulated for an ARTFIMA(p, d, λ, q) process. The simulations are carried out using the artfima package available in R. For each case single trajectory is used for estimation. We run two distinct simulations using different parameter combinations to test the performance of the specified estimation approach. The results are summarized in Table 3.1.

	Actual	**Estimated**
Case 1	$d = 0.4$, $\lambda = 0.2$	$\hat{d} = 0.41$, $\hat{\lambda} = 0.18$
Case 2	$d = 0.5$, $\lambda = 0.4$	$\hat{d} = 0.52$, $\hat{\lambda} = 0.39$
Case 3	$d = 0.3$, $\lambda = 0.25$	$\hat{d} = 0.29$, $\hat{\lambda} = 0.30$
Case 4	$d = 0.25$, $\lambda = 0.1$	$\hat{d} = 0.24$, $\hat{\lambda} = 0.16$
Case 5	$d = 0.35$, $\lambda = 0.3$	$\hat{d} = 0.31$, $\hat{\lambda} = 0.34$

Table 3.1: Actual and Estimated values for single trajectory with differencing parameter d and tempering parameter λ.

Furthermore, using the ARTFIMA$(1, 0.4, 0.2, 1)$ process, we simulate 1000 samples

each with size 1000 and construct box-plots of estimated parameters using simulated data. The plot is shown in the left panel of Fig. 3.1. From Fig. 3.1, it is evident that the median of the estimated parameters is equal to the true values with some outliers also. Similarly, using the ARTFIMA$(1, 0.5, 0.4, 1)$ another simulation is performed and the box plot for the same is given in the right panel of Fig. 3.1. The performance of the estimation method also depends on the optimization method used in minimizing the errors in the non-linear optimization and the initial guess used for the parameters.

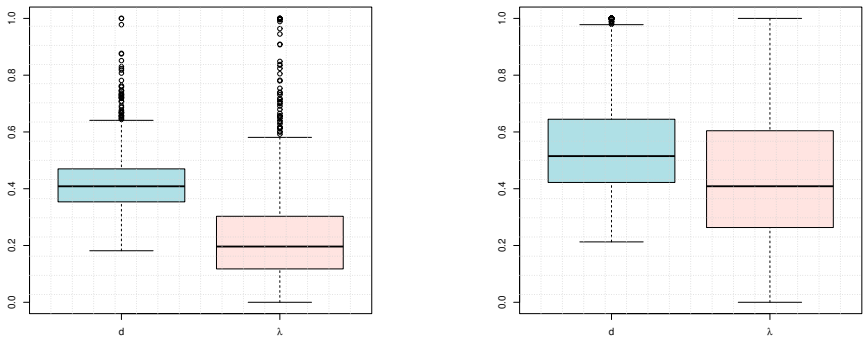

(a) (b)

Figure 3.1: Box plot of parameters using 1000 samples for $d = 0.4$ and $\lambda = 0.2$ (left panel) and for $d = 0.5$ and $\lambda = 0.4$ (right panel).

3.2.1 Gegenbauer process

The Gegenbauer polynomials are generalizations of the Legendre polynomials. For $|u| \leq 1$, the Gegenbauer polynomials $C_n^d(u)$ are defined in terms of generating function as follows:

$$(1 - 2uZ + Z^2)^{-d} = \sum_{n=0}^{\infty} C_n^d(u) Z^n, \tag{3.6}$$

where $d \neq 0$, $|Z| < 1$ and $C_n^d(u)$ is given by:

$$C_n^d(u) = \sum_{k=0}^{n/2} (-1)^k \frac{\Gamma(n-k+d)}{\Gamma(d)\Gamma(n+1)\Gamma(n-2k+1)} (2u)^{n-2k}. \tag{3.7}$$

The concept of the Gegenbauer process was developed by Andel [4]. The Gegenbauer process is defined using the generating function of Gegenbauer polynomials. For a general linear process $\{X_t\}$, the Gegenbauer process is given by:

$$X_t = \sum_{n=0}^{\infty} C_n^d(u)\epsilon_{t-n}, \tag{3.8}$$

where ϵ_t is white noise with mean 0 and variance σ^2. In terms of backward shift operator B, (3.8) can be written as:

$$X_t = (1 - 2uB + B^2)^{-d}\epsilon_t.$$

Remark 3.2.1. *The Gegenbauer process is stationary for* $|u| < 1$ *and* $d < 1/2$ *or* $|u| = \pm 1$ *and* $d < 1/4$.

The spectral density or the power spectrum of the Gegenbauer process is given by [38]:

$$f_x(\omega) = \frac{\sigma^2}{\pi}\{4(\cos(\omega) - u)^2\}^{-d},$$

and the autocovariance function of the Gegenbauer process takes the following form:

$$\gamma(h) = \frac{2^{1-2d}\sigma^2}{\pi}\sin^{-2d}(\omega_0)\sin(d\pi)\Gamma(1-2d)\cos(h\omega_0)\frac{\Gamma(h+2d)}{\Gamma(h+1)}.$$

An extension to the Gegenbauer process is known as the Gegenbauer autoregressive integrated moving average (GARMA) process. The GARMA process is a class of stationary long memory processes which generalize the ARIMA and ARFIMA processes. For the usefulness of generalized fractionally differenced Gegenbauer processes in time series modelling, see [23] and for different estimation methods related to the GARMA process, see the recent article [49]. The process is defined as follows:

$$\Phi(B)(1 - 2uB + B^2)^d X_t = \Theta(B)\epsilon_t,$$

where ϵ_t is Gaussian white noise with variance σ^2, B is the lag operator, $|u| \leq 1$, and $|d| < 1/2$. Again, $\Phi(B)$ and $\Theta(B)$ are stationary AR and invertible MA operators defined in (1.2) and (1.3).

3.3 Gegenbauer ARTFIMA Process

In this section, we introduce a new stochastic process, namely, the Gegenbauer autoregressive tempered fractionally integrated moving average (GARTFIMA)

process which is defined as follows:

$$\Phi(B)(1-2ue^{-\lambda}B+e^{-2\lambda}B^2)^d X_t = \Theta(B)\epsilon_t, \tag{3.9}$$

where ϵ_t is Gaussian white noise with variance σ^2, B is the lag operator, $|u|<1$, $\lambda \geq 0$, $|d|<1/2$, and $\Phi(B)$, $\Theta(B)$ are stationary AR and invertible MA operators defined in (1.2) and (1.3), respectively. This process generalizes the ARIMA, ARFIMA, ARTFIMA, and GARMA processes. In short, this process is denoted by the GARTFIMA(p,d,λ,u,q).

Theorem 3.3.1. *Let* $\{X_t\}$ *be the* GARTFIMA(p,d,λ,u,q) *process and all roots of* $\Phi(B)=0$ *and* $\Theta(B)=0$ *lie outside the unit circle. Then, the* GARTFIMA(p,d,λ,u,q) *process is stationary and invertible for* $|d|<1/2$ *and* $\lambda \geq 0$, *when* $|u|<1$.

Proof. Using (3.9), it follows:

$$X_t = \left(\frac{\Theta(B)}{\Phi(B)}\right)(1-2ue^{-\lambda}B+e^{-2\lambda}B^2)^{-d}\epsilon_t,$$

where we can write

$$(1-2ue^{-\lambda}z+e^{-2\lambda}z^2)^{-d} = \sum_{n=0}^{\infty} C_n^d(u)(e^{-\lambda}z)^n \text{ and } \mathrm{Var}(\epsilon_t)=\sigma^2. \tag{3.10}$$

For large n, the Gegenbauer polynomials $C_n^d(u)$ can be approximated as:

$$C_n^d(u) \sim \frac{\cos\left((n+d)\phi - d\pi/2\right) n^{d-1}}{\Gamma(d)\sin^d(\phi)}. \tag{3.11}$$

Here, $\phi = \cos^{-1}(u)$ and $\frac{\Theta(B)}{\Phi(B)} = \Psi(B) = \sum_{j=0}^{\infty}\psi_j B^j$. The variance of the process is given by:

$$\mathrm{Var}(X_t) = \sigma^2 \sum_{j=0}^{\infty}\psi_j^2 \sum_{n=0}^{\infty}(C_n^d(u))^2 e^{-2\lambda n}$$

and the variance will converge for $d<1/2$ and $\lambda \geq 0$, when $|u|<1$. To prove the invertibility condition, we define the process (3.9) as:

$$\epsilon_t = \pi(B)X_t,$$

where $\pi(z) = (1-2ue^{-\lambda}z+e^{-2\lambda}z^2)^d \frac{\Phi(z)}{\Theta(z)}$, and again using the same argument discussed above the, $\pi(z)$ will converge for $d>-1/2$ and $\lambda \geq 0$, when $|u|<1$. □

Theorem 3.3.2. *For a GARTFIMA(p, d, λ, u, q) process defined in (3.9), the spectral density takes the following form:*

$$f_x(\omega) = \frac{\sigma^2}{2\pi} \sum_{l=-q}^{q} \sum_{j=1}^{p} \psi(l) z^{l+p} \zeta_j \left[\frac{\rho_j^{2p}}{1 - \rho_j e^{-\iota\omega}} - \frac{1}{1 - \rho_j^{-1} e^{-\iota\omega}} \right] (A - B\cos(\omega) + C\cos^2(\omega))^{-d},$$

where $A = (1 + 4u^2 e^{-2\lambda} - 2e^{-2\lambda} + e^{-4\lambda})$, $B = 4ue^{-\lambda}(1 + e^{-2\lambda})$, $C = 4e^{-2\lambda}$,

$$\psi(l) = \sum_{s=\min[0,l]}^{\max[q,q+l]} \theta_s \theta_{s-l}$$

, and

$$\zeta_j = \frac{\sigma^2}{2\pi} \left[\rho_j \prod_{i=1}^{p} (1 - \rho_i \rho_j) \prod_{m \neq j,\ 1 \leq m \leq p} (\rho_j - \rho_m) \right]^{-1}.$$

Proof. Rewrite (3.9) as follows:

$$X_t = \Psi(B)\epsilon_t,$$

where $\Psi(B) = \dfrac{\Theta(B)}{\Phi(B)} \Delta^{d,\lambda}$ and $\Delta^{d,\lambda} = (1 - 2ue^{-\lambda}B + B^2)^{-d}$. Then, using the definition of the spectral density of linear process, we have:

$$f_x(\omega) = |\Psi(z)|^2 f_\epsilon(\omega),$$

where $z = e^{-\iota\omega}$ and $f_\epsilon(\omega)$ is spectral density of the innovation term. The spectral density of the innovation process ϵ_t is given by $\sigma^2/2\pi$, which implies

$$f_x(\omega) = \frac{\sigma^2}{2\pi} |\Psi(z)|^2 = \frac{\sigma^2}{2\pi} \frac{|\Theta(z)|^2}{|\Phi(z)|^2} \left| (1 - 2ue^{-(\lambda+\iota\omega)} + e^{-2(\lambda+\iota\omega)}) \right|^{-2d}. \tag{3.12}$$

Note that $\Phi(x)$ can be written as:

$$\Phi(x) = \prod_{j=1}^{p} (1 - \rho_j x), \tag{3.13}$$

where $\rho_1, \rho_2, \ldots, \rho_p$ are complex numbers such that $|\rho_j| < 1$, for $j = 1, 2, \ldots, p$. Using (3.13) in (3.12), it follows:

$$f_x(\omega) = \frac{\sigma^2 |\Theta(e^{-\iota\omega})|^2 \left| (1 - 2ue^{-(\lambda+\iota\omega)} + e^{-2(\lambda+\iota\omega)}) \right|^{-2d}}{2\pi \prod_{j=1}^{p} (1 - \rho_j z)(1 - \rho_j z^{-1})}.$$

Using the results from [83], the spectral density is given by:

$$f_x(\omega) = \frac{\sigma^2}{2\pi} \sum_{l=-q}^{q} \sum_{j=1}^{p} \psi(l) z^{l+p} \zeta_j \left[\frac{\rho_j^{2p}}{1-\rho_j e^{-\iota\omega}} - \frac{1}{1-\rho^{-1} e^{-\iota\omega}} \right] \left| (1 - 2ue^{-(\lambda+\iota\omega)} + e^{-2(\lambda+\iota\omega)}) \right|^{-2d},$$

where

$$\psi(l) = \sum_{s=\min[0,l]}^{\max[q,q+l]} \theta_s \theta_{s-l}$$

and

$$\zeta_j = \frac{\sigma^2}{2\pi} \left[\rho_j \prod_{i=1}^{p} (1-\rho_i \rho_j) \prod_{m \neq j,\, 1 \leq m \leq p} (\rho_j - \rho_m) \right]^{-1}.$$

The spectral density takes the following form:

$$f_x(\omega) = \frac{\sigma^2}{2\pi} \sum_{l=-q}^{q} \sum_{j=1}^{p} \psi(l) z^{l+p} \zeta_j \left[\frac{\rho_j^{2p}}{1-\rho_j e^{-\iota\omega}} - \frac{1}{1-\rho^{-1} e^{-\iota\omega}} \right] (A - B\cos(\omega) + C\cos^2(\omega))^{-d},$$

where $A = (1 + 4u^2 e^{-2\lambda} - 2e^{-2\lambda} + e^{-4\lambda})$, $B = 4ue^{-\lambda}(1 + e^{-2\lambda})$, and $C = 4e^{-2\lambda}$. □

Theorem 3.3.3. *For the GARTFIMA(p, d, λ, u, q) process defined in (3.9), the autocovariance function is given by:*

$$\gamma(h) = \sum_{l=-q}^{q} \sum_{j=1}^{p} \psi(l) \zeta_j \left[\rho^{2p} \sum_{m=0}^{\infty} \rho^m \gamma_w(h-m) d\omega + \sum_{n=1}^{\infty} \rho^n \gamma_w(h+n) \right],$$

where $\gamma_w(h-m) = \sigma^2 \sum_{n=0}^{\infty} C_n^d(u) C_{n+h}^d(t) e^{-(2n+(h-m)\lambda)}$ and $C_n^d(u)$ are defined in (3.7).

Proof. The autocovariance function can be calculated by taking the inverse Fourier transform of the spectral density of the process X_t using the following form:

$$\begin{aligned}
\gamma(h) &= \int_{-\pi}^{\pi} f_x(\omega) e^{\iota\omega h} d\omega \\
&= \frac{\sigma^2}{2\pi} \int_{-\pi}^{\pi} \left[\sum_{l=-q}^{q} \sum_{j=1}^{p} \psi(l) \zeta_j \left(\frac{\rho_j^{2p}}{1-\rho_j e^{-\iota\omega}} - \frac{1}{1-\rho_j^{-1} e^{-\iota\omega}} \right) \right. \\
&\qquad \left. \left| (1 - 2ue^{-(\lambda+\iota\omega)} + e^{-2(\lambda+\iota\omega)}) \right|^{-2d} z^{p+l} \right] e^{\iota\omega h} d\omega.
\end{aligned}$$

We can write another form using the following expansions:

$$\frac{\rho^{2p}}{1-\rho e^{-\iota\omega}} = \rho^{2p} \sum_{m=0}^{\infty} (\rho e^{-\iota\omega})^m,$$

$$\frac{-1}{1-\rho^{-1}e^{-\iota\omega}} = -1 + \sum_{n=0}^{\infty}(\rho e^{-\iota\omega})^n = \sum_{n=1}^{\infty}(\rho e^{\iota\omega})^n.$$

The spectral density of GARTFIMA$(0, d, \lambda, u, 0)$ process, defined by, $W_t = (1 - 2ue^{-\lambda}B + e^{-2\lambda}B^2)^{-d}\epsilon_t$ is given by:

$$f_w(\omega) = \frac{\sigma^2}{2\pi}\left|(1 - 2ue^{-(\lambda+\iota\omega)} + e^{-2(\lambda+\iota\omega)})\right|^{-2d}.$$

We can write

$$\begin{aligned}\gamma(h) &= \frac{\sigma^2}{2\pi}\int_{-\pi}^{\pi}\left[\sum_{l=-q}^{q}\sum_{j=1}^{p}\psi(l)\zeta_j\left(\rho_j^{2p}\sum_{m=0}^{\infty}(\rho_j e^{-\iota\omega})^m + \sum_{n=1}^{\infty}(\rho_j e^{\iota\omega})^n\right)\right. \qquad (3.14)\\ &\qquad \left.\left|(1 - 2ue^{-(\lambda+\iota\omega)} + e^{-2(\lambda+\iota\omega)})\right|^{-2d} z^{p+l}\right]e^{\iota\omega h}d\omega\\ &= \frac{\sigma^2}{2\pi}\sum_{l=-q}^{q}\sum_{j=1}^{p}\psi(l)\zeta_j\left[\int_{-\pi}^{\pi}\rho_j^{2p}\sum_{m=0}^{\infty}(\rho_j e^{-\iota\omega})^m\left|(1 - 2ue^{-(\lambda+\iota\omega)} + e^{-2(\lambda+\iota\omega)})\right|^{-2d}e^{\iota\omega h}d\omega\right.\\ &\qquad \left.+\int_{-\pi}^{\pi}\sum_{n=1}^{\infty}(\rho_j e^{\iota\omega})^n\left|(1 - 2ue^{-(\lambda+\iota\omega)} + e^{-2(\lambda+\iota\omega)})\right|^{-2d}e^{\iota\omega h}d\omega\right]\\ &= \frac{\sigma^2}{2\pi}\sum_{l=-q}^{q}\sum_{j=1}^{p}\psi(l)\zeta_j\left[\rho^{2p}\sum_{m=0}^{\infty}\rho_j^m\int_{-\pi}^{\pi}\frac{2\pi}{\sigma^2}f_w(\omega)e^{\iota(h-m)}d\omega + \sum_{n=1}^{\infty}\rho_j^n\int_{-\pi}^{\pi}\frac{2\pi}{\sigma^2}f_w(\omega)e^{\iota(h+n)}d\omega\right]\\ &= \sum_{l=-q}^{q}\sum_{j=1}^{p}\psi(l)\zeta_j\left[\rho_j^{2p}\sum_{m=0}^{\infty}\rho_j^m\gamma_w(h-m)d\omega + \sum_{n=1}^{\infty}\rho_j^n\gamma_w(h+n)\right]. \qquad (3.15)\end{aligned}$$

The autocovariance function for GARTFIMA $(0, d, \lambda, u, 0)$ process $W_t = (1 - 2ue^{-\lambda}B + e^{-2\lambda}B^2)^{-d}\epsilon_t$ is given as:

$$\begin{aligned}\gamma_w(k) &= \int_{-\pi}^{\pi}\cos(k\omega)f_w(\omega)d\omega = \frac{\sigma^2}{2\pi}\int_{-\pi}^{\pi}\cos(k\omega)\left|(1 - 2ue^{-(\lambda+\iota\omega)} + e^{-2(\lambda+\iota\omega)})\right|^{-2d}d\omega\\ &= \frac{\sigma^2}{2\pi}\int_{-\pi}^{\pi}\cos(h\omega)\left|\sum_{n=0}^{\infty}C_n^d(u)(e^{-\lambda-\iota\omega})^n\right|^2 d\omega. \qquad (3.16)\end{aligned}$$

For ease of notation, let $C_n^d(u) = a_n$. Then,

$$\begin{aligned}\left|\sum_{n=0}^{\infty}C_n^d(u)(e^{-\lambda-\iota\omega})^n\right|^2 &= (a_0 + a_1e^{-\lambda-\iota\omega} + a_2e^{-2\lambda-2\iota\omega} + \ldots)(a_0 + a_1e^{-\lambda+\iota\omega} + a_2e^{-2\lambda+2\iota\omega} + \cdots)\\ &= \sum_{n=0}^{\infty}a_n^2e^{-2n\lambda} + 2\sum_{n=0}^{\infty}a_na_{n+1}e^{-(2n+1)\lambda}\cos(\omega)\end{aligned}$$

$$+ 2\sum_{n=0}^{\infty} a_n a_{n+2} e^{-(2n+2)\lambda}\cos(2\omega) + \cdots$$
$$= \sum_{n=0}^{\infty} a_n^2 e^{-2n\lambda} + 2\sum_{r=1}^{\infty}\sum_{n=0}^{\infty} a_n a_{n+r} e^{-(2n+r)\lambda}\cos(\omega r). \tag{3.17}$$

Using (3.17) and (3.16), it follows:

$$\gamma_w(k) = \frac{\sigma^2}{\pi}\int_{-\pi}^{\pi}\cos(k\omega)\sum_{r=1}^{\infty}\sum_{n=0}^{\infty} a_n a_{n+r} e^{-(2n+r)\lambda}\cos(\omega r)d\omega$$
$$= \frac{\sigma^2}{\pi}\sum_{r=1}^{\infty}\sum_{n=0}^{\infty} a_n a_{n+r} e^{-(2n+r)\lambda}\int_{-\pi}^{\pi}\cos(k\omega)\cos(\omega r)d\omega = \sigma^2\sum_{n=0}^{\infty} a_n a_{n+h} e^{-(2n+k)\lambda}. \tag{3.18}$$

Finally, taking $k = h-m$ and $k = h+n$ in (3.18) and putting the values of $\gamma_w(h-m)$ and $\gamma_w(h+n)$ in (3.14), one gets the desired result. □

Proposition 3.3.1. *For $u = 1$, the GARTFIMA(p, d, λ, u, q) process reduced to ARTFIMA$(p, 2d, \lambda, q)$ process.*

Proof. For $u = 1$ the process defined in (3.9) can be rewritten as:

$$\Phi(B)(1 - e^{-\lambda}B)^{2d}X_t = \Theta(B)\epsilon_t.$$

For $u = 1$, the autocovariance function $\gamma_w(h)$ for GARTFIMA$(0, d, \lambda, u, 0)$ takes the following form:

$$\gamma_w(k) = \sigma^2\sum_{n=0}^{\infty} C_n^d(1)C_{n+h}^d(1)e^{-(2n+k)\lambda},$$

where $C_n^d(1) = \binom{2d+n-1}{n}$ and $C_n^d(1) = \binom{2d+n+k-1}{n+k}$. Now,

$$\gamma_w(k) = \sigma^2(C_0^d(1)C_k^d(1)e^{-k\lambda} + C_1^d(1)C_{k+1}^d(1)e^{-(k+1)\lambda} + C_2^d(1)C_{k+2}^d(1)e^{-(k+2)\lambda} + \cdots)$$
$$= \sigma^2\left[\binom{2d+k-1}{k}e^{-k\lambda} + \binom{2d}{1}\binom{2d+k}{k+1}e^{-(k+2)\lambda}\right.$$
$$\left. + \binom{2d+1}{2}\binom{2d+k+1}{k+2}e^{-(k+4)}\lambda + \cdots\right]$$
$$= \sigma^2\left[\frac{(2d+k-1)!e^{-k\lambda}}{(2d-1)!k!} + \frac{2d(2d+k)!e^{-(k+2)\lambda}}{(k+1)!(2d-1)!} + \frac{(2d+1)!(2d+k+1)!e^{-(k+4)\lambda}}{2!(2d-1)!(k+2)!(2d-1)!}\right.$$
$$\left. + \cdots\right]$$

$$= \sigma^2 e^{-k\lambda} \frac{2d(2d+1)\dots(2d+k-1)}{k!} \left[1 + \frac{2d(2d+k)e^{-2\lambda}}{(k+1)} + \frac{2d(2d+1)(k+2d)(k+2d+1)e^{-4\lambda}}{(k+1)(k+2)2!} + \cdots \right]$$

$$= \frac{\sigma^2 \Gamma(2d+k)}{\Gamma(2d)\Gamma(k+1)} {}_2F_1(2d, k+2d; k+1; e^{-2\lambda}), \tag{3.19}$$

which is the autocovariance function for ARTFIMA$(0, 2d, \lambda, 0)$ process defined in [76]. According to Sabzikar et al. [76], the autocovariance function of ARTFIMA$(p, 2d, \lambda, q)$ process is given by:

$$\gamma(h) = \frac{\sigma^2}{2\pi} \sum_{l=-q}^{q} \sum_{j=1}^{p} \psi(l)\zeta_j \left[\rho^{2p} \sum_{m=0}^{\infty} \rho^m \frac{2\pi}{\sigma^2} \gamma_w(h-m) + \sum_{n=1}^{\infty} \rho^n \frac{2\pi}{\sigma^2} \gamma_w(h+n) \right],$$

where $\gamma_w(k)$ for $k = h - m$ and $k = h + n$ is defined in (3.19). Using the $\gamma_w(k)$ from (3.19), the autocovariance of ARTFIMA$(p, 2d, \lambda, q)$ takes a similar form to GARTFIMA(p, d, λ, u, q) process for u=1.

□

Proposition 3.3.2. *For $\lambda = 0$, the GARTFIMA(p, d, λ, u, q) process reduce to GARMA(p, d, u, q) process.*

Proof. For $\lambda = 0$, (3.9) can be written as:

$$\Phi(B)(1 - 2uB + B^2)^d X_t = \Theta(B)\epsilon_t,$$

and for $\lambda = 0$ in (3.18) the autocovariance for GARMA$(0, d, u, 0)$ process W_t takes the following form [96]:

$$\gamma_w(k) = \sigma^2 \sum_{n=0}^{\infty} C_n^d(u) C_{n+k}^d(u).$$

With the help of (3.14), one can write the autocovariance function of GARMA(p, d, u, q) in terms of autocovariance function of GARMA$(0, d, u, 0)$ denoted by $\gamma_w(h)$. □

Theorem 3.3.4. *For a GARTFIMA(p, d, λ, q) process, $\sum_{h=0}^{\infty} |\gamma(h)| < \infty$, if $|d| < \frac{1}{2}, \lambda > 0$, and $|u| < 1$.*

Proof. Note that the process is stationary, when $|d| < \frac{1}{2}, \lambda > 0$, and $|u| < 1$. We have:

$$\sum_{h=0}^{\infty} \gamma(h) = \sigma^2 \sum_{h=0}^{\infty} \sum_{n=0}^{\infty} C_n^d(u) e^{-n\lambda} C_{n+h}^d(u) e^{-(n+h)\lambda}.$$

Hence,

$$\sum_{h=0}^{\infty}|\gamma(h)| \leq \sigma^2 \sum_{h=0}^{\infty}\sum_{n=0}^{\infty}|C_n^d(u)e^{-n\lambda}||C_{n+h}^d(u)e^{-(n+h)\lambda}|.$$

For large n, $C_n^d(u)$ can be approximated by:

$$C_n^d(u) \sim \frac{\cos\left((n+d)\phi - d\pi/2\right) n^{d-1}}{\Gamma(d)\sin^d(\phi)}, \quad \phi = \cos^{-1}(u). \tag{3.20}$$

Note that

$$C_n^d(u)C_{n+h}^d(u)e^{-(2n+h)\lambda} \sim \begin{cases} C_1(d)n^{2d-2}e^{-2n\lambda}, & \text{as } n \to \infty, \text{ and } h \text{ finite}, \\ C_2(d)h^{d-1}e^{-h\lambda}, & \text{as } h \to \infty, \text{ and } n \text{ finite}, \\ C_3(d)n^{2d-2}e^{-3n\lambda}, & \text{as } n \to \infty, \text{ and } h \to \infty, \end{cases} \tag{3.21}$$

for constants $C_1(d), C_2(d), C_3(d) > 0$. Thus, $\sum_{h=0}^{\infty}|\gamma(h)| < \infty$, for all d which completes the proof. □

3.4 Parameter Estimation and Real-World Application

In this section, the methodology for parameter estimation of the GARTFIMA process is discussed. The parameter estimation of the GARTFIMA process is done by adopting the non-linear least square (NLS) based approach discussed for the ARTFIMA process in Section 3.2. Further, the parameter estimation is done using the Whittle likelihood method. These methods are adopted for estimating parameters d, λ, and u. Firstly, we will discuss the estimation using the NLS approach.

Non-linear least square (NLS) approach:
Similar to the procedure discussed for ARTFIMA process, let $(1 - 2ue^{-\lambda}B + e^{-2\lambda}B^2)^d X_t = U_t$ and the spectral density of this process $U_t = \dfrac{\Theta(B)}{\Phi(B)}\epsilon_t$ is given by:

$$f_u(\omega) = \frac{\sigma^2}{2\pi}\frac{|\Theta(e^{-\iota\omega})|^2}{|\Phi(e^{-\iota\omega})|^2}. \tag{3.22}$$

Substituting (3.22) in (3.12), the spectral density of X_t can be written as:

$$f_x(\omega) = f_u(\omega)\left|(1-2ue^{-(\lambda+\iota\omega)}+e^{-2(\lambda+\iota\omega)})\right|^{-2d} = f_u(\omega)(A-B\cos(\omega)+C\cos^2(\omega))^{-d}, \tag{3.23}$$

where $A = (1+4u^2e^{-2\lambda}-2e^{-2\lambda}+e^{-4\lambda})$, $B = 4ue^{-\lambda}(1+e^{-2\lambda})$, and $C = 4e^{-2\lambda}$. Consider $\omega_j = \dfrac{2\pi j}{n}$, where $j = 0, 1, \ldots, [n/2]$. Here, n is the sample size and ω_j is the set of harmonic frequencies. Taking natural logarithm on the both sides of (3.23) with some manipulation leads to

$$\begin{aligned}\log\{f_x(\omega_j)\} &= \log\{f_u(0)\} + \log\{f_u(\omega_j)\} \\ &\quad - d\log\{(A-B\cos(\omega_j)+C\cos^2(\omega_j))\} - \log\{f_u(0)\} \\ &= \log\{f_u(0)\} - d\log\{(A-B\cos(\omega_j)+C\cos^2(\omega_j))\} + \log\left\{\frac{f_u(\omega_j)}{f_u(0)}\right\}.\end{aligned}$$

Adding $\log\{I(\omega_j)\}$ on the both sides, it follows:

$$\log\{I(\omega_j)\} = \log\{f_u(0)\} - d\log\{(A-B\cos(\omega_j)+C\cos^2(\omega_j))\} \tag{3.24}$$

$$+\log\left\{\frac{f_u(\omega_j)}{f_u(0)}\right\} + \log\left\{\frac{I(\omega_j)}{f_x(\omega_j)}\right\}, \tag{3.25}$$

where $I(\omega_j)$ is the periodogram or empirical spectral density of the process stated in (3.4). Using (3.22), $f_u(0)$ can be written as:

$$f_u(0) = \frac{\sigma^2}{2\pi}\frac{(1-\theta_1-\cdots-\theta_q)^2}{(1-\phi_1-\cdots-\phi_p)^2}.$$

Now, the estimation is done by minimizing the sum of squared errors in (3.24), where the error is given by: $\log(I(\omega_j)/f_x(\omega_j))$ and $\log\{f_u(0)\}$ is the intercept term for the equation. Also, choosing the ω_j near 0, the term $\log\left\{\dfrac{f_u(\omega_j)}{f_u(0)}\right\}$ will be negligible. So, the upper limit of j should be chosen such that the ω_j is small or near zero. From (3.24), we have:

$$\log\{I(\omega_j)\} = \log\{f_u(0)\} - d\log\{(A-B\cos(\omega_j)+C\cos^2(\omega_j))\} + \log\left\{\frac{I(\omega_j)}{f_x(\omega_j)}\right\}. \tag{3.26}$$

One can estimate the parameters d, λ, and u by using (3.24) or (3.26). Generally, the estimates using (3.24) are better since it uses all the terms. In this chapter, we have done the parameter estimation by minimizing the squared error based

on (3.24), by using the R package *nloptr* which uses *nlxb* function for non-linear optimization.

Whittle likelihood estimation: To estimate the parameters of the process the Whittle likelihood technique is employed which is a spectral density based approach defined in Chapter 1. The Whittle likelihood estimation is a periodogram based technique. It employs spectral techniques to approximate the spatial likelihood which can be calculated using the Fast Fourier transform or spectral density of the time series $\{X_t\}$. The idea is to minimize the likelihood function defined in (1.20), which uses both the empirical and actual spectral densities. The approach is also implemented by Sabzikar et al. to estimate the parameters of ARTFIMA time series [76]. In this chapter, the methods are considered without any prior assumptions on spectral densities of the processes. The methods are applied directly on simulated series and the results appear to be promising. Consider the set of harmonic frequencies ω_j, $j = 0, 1, \ldots, n/2$, recall the empirical spectral density

$$I_x(\omega_j) = \frac{1}{2\pi}\left\{ R(0) + \sum_{s=1}^{n-1} R(s)\cos(s\omega_j) \right\},$$

where $\omega_j = 2\pi j/n$, $j = 0, 1, \ldots, \lfloor n/2 \rfloor$. The spectral density of the GARTFIMA$(0, d, \lambda, u, 0)$ process is:

$$f_x(\omega) = \frac{\sigma^2}{2\pi}|\Psi(z)|^2 = \frac{\sigma^2}{2\pi}\frac{|\Theta(z)|^2}{|\Phi(z)|^2}(A - B\cos(\omega) + C\cos^2(\omega))^{-d}. \tag{3.27}$$

The whittle likelihood denoted by $l_w(\theta)$ is defined as:

$$l_w(\theta) = \sum_{j=1}^{n} \frac{I_x(\omega_j)}{f_x(\omega_j)} + \log(f_x(\omega_j)),$$

where θ is the unknown parameters vector given by $\theta = (d, \lambda, u)$. The estimates of the parameters d, λ, and u are obtained by minimizing the likelihood function $l_w(\theta)$ with respect to θ. That is,

$$\hat{\theta} = \text{argmin}(l_w(\theta), \theta \in \Omega_0),$$

where $\Omega = \{d, \lambda, u : |d| < 1/2, \lambda > 0, |u| < 1\} \subset \mathbb{R}^3$. Let $\Omega_0 \subset \Omega$ is compact set and $\theta = (d, \lambda, u) \in \Omega_0$.

Theorem 3.4.1. *Under the assumptions of theorem 3.3.1, the Whittle likelihood*

estimators are consistent. That is,

$$\lim_{n\to\infty} \hat{\theta} = \theta.$$

Proof. The consistency of the Whittle likelihood estimator can be proved using the result by Hannan (see Theorem 1 in [41]). We assume that the parameter vector θ belong to a compact parametric space Ω_0 and the spectral density defined in (3.12) is written as follows:

$$f_x(\omega) = \frac{\sigma^2}{2\pi} K(\omega), \text{ where } K(\omega) = \frac{|\Theta(z)|^2}{|\Phi(z)|^2}(A - B\cos(\omega) + C\cos^2(\omega))^{-d}.$$

We need to verify the following conditions to prove the result:

(a) The time series defined in 3.9 can be written as: $X_t = \sum_{k=0}^{\infty} a_k \epsilon_{t-k}$, $\sum_{k=0}^{\infty} |a_k| < \infty$, and $a_0 = 1$

(b) $\frac{1}{K(\omega)+a}$ is a continuous function for $\omega \in (-\pi, \pi)$, for all $a > 0$.

(c) The parameter vector $\theta \in \Omega_0$ define the spectral density uniquely.

First, we prove Condition (a). Using (3.9), the series $\{X_t\}$ can be written as:

$$\begin{aligned} X_t &= \frac{\Theta(B)}{\Phi(B)}(1 - 2ue^{-\lambda}B + e^{-2\lambda}B^2)^{-d}\epsilon_t = \left(\sum_{j=0}^{\infty} \psi_j B^j\right)\left(\sum_{n=0}^{\infty} C_n^d(u)(e^{-n\lambda}B^n)\right)\epsilon_t \\ &= \sum_{k=0}^{\infty} a_k \epsilon_{t-k}, \text{ where } a_k = \sum_{s=0}^{k} e^{-s\lambda}\psi_{k-s}C_s^d(u), \end{aligned}$$

which is a moving average representation of the GARTFIMA time series. Now, we know that the $\Theta(B)$ and $\Phi(B)$ are stationary autoregressive and invertible moving average operators, respectively and $\frac{\Theta(z)}{\Phi(z)} = \sum_{j=0}^{\infty} \psi_j z^j$, where $\sum_{j=0}^{\infty} \psi_j < \infty$, for $|z| \leq 1 + \epsilon$. This implies $|\psi_j| < C(1+\epsilon)^{-j}$, for some constant C. Further,

$$\sum_{k=0}^{\infty} |a_k| \leq \sum_{k=0}^{\infty}\sum_{s=0}^{k} |\psi_{k-s}||e^{-s\lambda}C_s^d(u)| = \sum_{s=0}^{\infty}\sum_{k=s}^{\infty} |\psi_{k-s}||e^{-s\lambda}C_s^d(u)| \tag{3.28}$$

$$= \sum_{s=0}^{\infty}\sum_{r=0}^{\infty} |\psi_r||e^{-s\lambda}C_s^d(u)|. \tag{3.29}$$

Since using (3.11) it can be proved that the series $\sum_{n=0}^{\infty} e^{-s\lambda}C_n^d(u)$ is finite, which implies $\sum_{k=0}^{\infty} |a_k| < \infty$. This proves Condition (a).
The function $K(\omega)$ is continuous, for $|u| < 1$, $|d| < 1/2$, and $\lambda > 0$, since the function does not have any singularity. Thus, it can easily be shown that part (b) is true. The parameter $|d| < 1/2$, which justifies Condition (c).

□

Theorem 3.4.2. *For the Whittle likelihood estimators,* $\sqrt{n}(\hat{\theta}-\theta) \sim \mathcal{N}(0, W^{-1})$, *where* W^{-1} *represents the variance covariance matrix having the following form:*

$$W = \frac{1}{4\pi}\int_{-\pi}^{\pi}\left\{\frac{\partial \log K(\omega)}{\partial\theta}\right\}\left\{\frac{\partial \log K(\omega)}{\partial\theta}\right\}' d\omega.$$

Proof. Using the results defined by Hannan (see Theorem 2 in [41]), we need to verify the following conditions to verify the asymptotic normality of the parameters:

(a) $K(\omega) > 0$, for all $\omega \in (-\pi, \pi)$ and $\theta \in \Omega_0$.

(b) $K(\omega)$ twice differentiable of parameters d, λ, and u.

(c) The time series defined in (3.9) can be written as: $X_t = \sum_{k=0}^{\infty} a_k \epsilon_{t-k}$, $\sum_{k=0}^{\infty} a_k^2 < \infty$, and $a_0 = 1$.

Condition (a) can be proved by rewriting $K(\omega)$ as follows:

$$\begin{aligned}
K(\omega) &= \frac{|\Theta(z)|^2}{|\Phi(z)|^2}(1+e^{-4\lambda}+4u^2e^{-2\lambda}+2e^{-2\lambda}\cos(2\omega)-4ue^{-\lambda}(1+e^{-2\lambda})\cos(\omega))^{-d} \\
&= \frac{|\Theta(z)|^2}{|\Phi(z)|^2}(1+e^{-4\lambda}+(2ue^{-\lambda}-(1+e^{-2\lambda})\cos(\omega))^2-((1+e^{-2\lambda})\cos(\omega))^2)^{-d} \\
&= \frac{|\Theta(z)|^2}{|\Phi(z)|^2}(\sin^2(\omega)+e^{-4\lambda}+2e^{-2\lambda}\cos(2\omega)-e^{-2\lambda}\cos^2(\omega) \\
&\quad +(2ue^{-\lambda}-(1+e^{-2\lambda})\cos(\omega))^2)^{-d} \\
&= \frac{|\Theta(z)|^2}{|\Phi(z)|^2}(\sin^2(\omega)+e^{-4\lambda}+3e^{-2\lambda}\cos^2(\omega)-2e^{-2\lambda}+(2ue^{-\lambda}-(1+e^{-2\lambda})\cos(\omega))^2)^{-d}
\end{aligned} \tag{3.30}$$

The term $(2ue^{-\lambda}-(1+e^{-2\lambda})\cos(\omega))^2)$ in (3.30) is positive. Now, we only need to prove that the term $K_1(\omega) = (\sin^2(\omega)+e^{-4\lambda}+3e^{-2\lambda}\cos^2(\omega)-2e^{-2\lambda}) > 0$, which can be proved by showing that $K_1(\omega)$ has positive value at the extreme points. By taking derivative of the function $K_1(\omega)$ with respect to ω, the extreme points are $\omega = \pm n\pi$, $\omega = (n\pi \pm \frac{\pi}{2})$, and $\lambda = (-1/2)\log(1/3)$ and the function $K_1(\omega) > 0$ at these values, which implies that $K(\omega) > 0$. The part (b) is easy to check that the function $K(\omega)$ is twice differentiable of parameters d, λ, and u. Condition (c) is similar to Condition (a) of Theorem 3.4.1. This proves the desired result. □

3.5 Simulation Study

To assess the performance of the introduced parameter estimation techniques, we use simulated data. The simulation study is done to obtain empirical evidence

regarding the effectiveness of statistical techniques. Using an appropriate simulation technique a synthetic series is generated for an initial set of parameters and the parameters are estimated from the simulated series using the defined estimation techniques. For each case single trajectory is used for estimation. The performance of the applied techniques can be simply assessed by comparing the estimated and actual parameters.

Procedure of simulation:
The GARTFIMA process defined in (3.9) can be written as:

$$\Phi(B)X_t = \Theta(B)(1 - 2ue^{-\lambda}B + e^{-2\lambda}B^2)^{-d}\epsilon_t. \tag{3.31}$$

To simulate a series from the GARTFIMA process, first we simulate an innovation series $\epsilon_t \sim N(\mu, \sigma^2)$. Then, we generate another series $\eta_t = (1 - 2ue^{-\lambda}B + e^{-2\lambda}B^2)^{-d}\epsilon_t$ by taking the binomial expansion of $(1 - 2ue^{-\lambda}B + e^{-2\lambda}B^2)^{-d}$ and ignoring higher order terms. The series $\eta_t = (1-2ue^{-\lambda}B+e^{-2\lambda}B^2)^{-d}\epsilon_t$ is generated using the simulated innovation series $\epsilon_t \sim \mathcal{N}(0, \sigma^2)$ and approximating η_t by considering first 4 terms in the binomial expansion of $(1 - 2ue^{-\lambda}B + e^{-2\lambda}B^2)^{-d}$, which is

$$\eta_t = (1 - 2ue^{-\lambda}B + e^{-2\lambda}B^2)^{-d}\epsilon_t = \sum_{n=0}^{\infty}\sum_{j=0}^{n}(-1)^j\frac{(\nu)_n}{n!}\binom{n}{j}(2ue^{-\lambda})^{n-j}B^{j+n}\epsilon_t \tag{3.32}$$

$$\approx \sum_{n=0}^{4}\sum_{j=0}^{n}(-1)^j\frac{(\nu)_n}{n!}\binom{n}{j}(2ue^{-\lambda})^{n-j}\epsilon_{t-n-j}. \tag{3.33}$$

Now, by generating the series η_t, the process (3.31) takes the following form:

$$X_t = \frac{\Theta(B)}{\Phi(B)}\eta_t,$$

which is an ARMA(p, q) process. Then, using the package arima in R the GARTFIMA process can be simulated.

Results:
We generate two series using different parameter combinations and evaluate the model performance using the parameter estimation based on non-linear regression. Assuming the innovation $\epsilon_t \sim \mathcal{N}(0, 2)$ and taking $d = 0.4$, $\lambda = 0.2$, and $u = 0.1$ the series η_t is simulated and then taking lags $p = 1$ and $q = 0$ we generate a synthetic GARTFIMA$(1, 0.4, 0.2, 0.1, 0)$ series. We also consider a synthetic GARTFIMA$(1, 0.5, 0.3, 0.2, 0)$ series. The actual and estimated parameters are

shown in Table 3.2.

	Actual	**Estimated**
Case 1	$d = 0.4,\ \lambda = 0.2,\ u = 0.1$	$\hat{d} = 0.41,\ \hat{\lambda} = 0.18,\ \hat{u} = 0.11$
Case 2	$d = 0.5,\ \lambda = 0.3,\ u = 0.2$	$\hat{d} = 0.51,\ \hat{\lambda} = 0.30,\ \hat{u} = 0.19$
Case 3	$d = 0.3,\ \lambda = 0.05,\ u = 0.1$	$\hat{d} = 0.36,\ \hat{\lambda} = 0.09,\ \hat{u} = 0.13$
Case 4	$d = 0.25,\ \lambda = 0.15,\ u = 0.3$	$\hat{d} = 0.22,\ \hat{\lambda} = 0.06,\ \hat{u} = 0.17$
Case 5	$d = -0.25,\ \lambda = 0.09,\ u = 0.8$	$\hat{d} = -0.27,\ \hat{\lambda} = 0.07,\ \hat{u} = 0.75$
Case 6	$d = -0.4,\ \lambda = 0.5,\ u = 0.9$	$\hat{d} = -0.46,\ \hat{\lambda} = 0.55,\ \hat{u} = 1$
Case 7	$d = -0.38,\ \lambda = 0.4,\ u = 0.8$	$\hat{d} = -0.34,\ \hat{\lambda} = 0.46,\ \hat{u} = 0.78$
Case 8	$d = 0.28,\ \lambda = 0.01,\ u = 0.7$	$\hat{d} = 0.22,\ \hat{\lambda} = 0.01,\ \hat{u} = 0.39$
Case 9	$d = 0.17,\ \lambda = 0.18,\ u = 0.28$	$\hat{d} = 0.2,\ \hat{\lambda} = 0.17,\ \hat{u} = 0.25$
Case 10	$d = -0.2,\ \lambda = 0.6,\ u = 0.2$	$\hat{d} = -0.17,\ \hat{\lambda} = 0.58,\ \hat{u} = 0.195$

Table 3.2: Actual and estimated parameter values for single trajectory with different choices of parameters using NLS approach.

Moreover, to measure the effectiveness of the NLS technique based on empirical spectral density, box plots for different parameters are constructed. To construct the box plots a simulation of 1000 series assuming the parameters $d = 0.4$, $\lambda = 0.2$, and $u = 0.1$ is done each with 1000 observations and the parameters d, λ, and u are estimated using the NLS based estimation and the corresponding box plot for these estimated parameters from each simulation are shown in Fig. 3.2 (left panel). Also, a simulation is performed for another combination of parameters, that is, $d = 0.5$, $\lambda = 0.3$, and $u = 0.1$, and the box-plots for 1000 simulations are given in Fig. 3.2 (right panel).

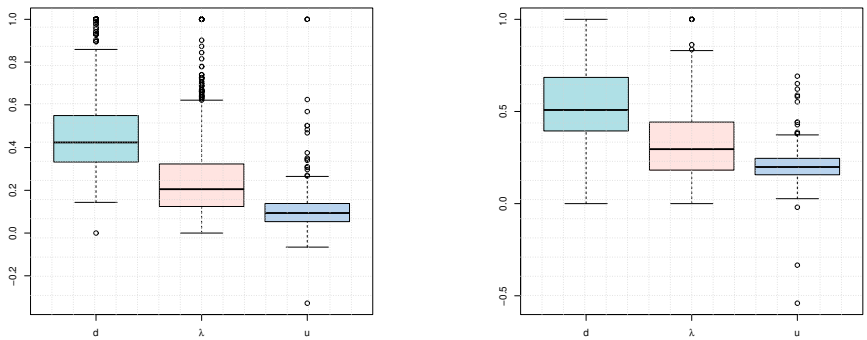

(a) (b)

Figure 3.2: Box plot of parameters using 1000 samples for $d = 0.4$, $\lambda = 0.2$, and $u = 0.1$ (Fig. 3.2a) and for $d = 0.5$, $\lambda = 0.3$, and $u = 0.2$ (Fig. 3.2b) based on NLS approach.

Next, we apply the Whittle likelihood technique on the same generated

series with the same parameters combinations given above, that is, GARTFIMA$(1, 0.4, 0.2, 0.1, 0)$ and GARTFIMA$(1, 0.5, 0.3, 0.2, 0)$, and the corresponding estimates are summarized in Table 3.3.

	Actual	**Estimated**
Case 1	$d = 0.4,\ \lambda = 0.1,\ u = 0.2$	$\hat{d} = 0.37,\ \hat{\lambda} = 0.08,\ \hat{u} = 0.2$
Case 2	$d = 0.5,\ \lambda = 0.3,\ u = 0.1$	$\hat{d} = 0.49,\ \hat{\lambda} = 0.33,\ \hat{u} = 0.08$
Case 3	$d = 0.3,\ \lambda = 0.05,\ u = 0.1$	$\hat{d} = 0.28,\ \hat{\lambda} = 0.08,\ \hat{u} = 0.16$
Case 4	$d = 0.25,\ \lambda = 0.15,\ u = 0.3$	$\hat{d} = 0.21,\ \hat{\lambda} = 0.1,\ \hat{u} = 0.34$
Case 5	$d = -0.25,\ \lambda = 0.09,\ u = 0.8$	$\hat{d} = -0.29,\ \hat{\lambda} = 0.08,\ \hat{u} = 0.70$
Case 6	$d = -0.4,\ \lambda = 0.5,\ u = 0.9$	$\hat{d} = -0.44,\ \hat{\lambda} = 0.56,\ \hat{u} = 0.85$
Case 7	$d = -0.38,\ \lambda = 0.4,\ u = 0.8$	$\hat{d} = -0.4,\ \hat{\lambda} = 0.45,\ \hat{u} = 0.78$
Case 8	$d = 0.28,\ \lambda = 0.01,\ u = 0.7$	$\hat{d} = 0.24,\ \hat{\lambda} = 0.01,\ \hat{u} = 0.65$
Case 9	$d = 0.17,\ \lambda = 0.18,\ u = 0.28$	$\hat{d} = 0.21,\ \hat{\lambda} = 0.15,\ \hat{u} = 0.22$
Case 10	$d = -0.2,\ \lambda = 0.6,\ u = 0.2$	$\hat{d} = -0.18,\ \hat{\lambda} = 0.57,\ \hat{u} = 0.14$

Table 3.3: Actual and estimated parameter values for single trajectory with different choices of parameters based on the Whittle likelihood.

Further, similar to the NLS estimation technique, the parameters are estimated for 1000 simulations and each sample with 1000 observations using the Whittle likelihood approach and box-plots are constructed for the same. The box-plots are shown in Fig. 3.3.

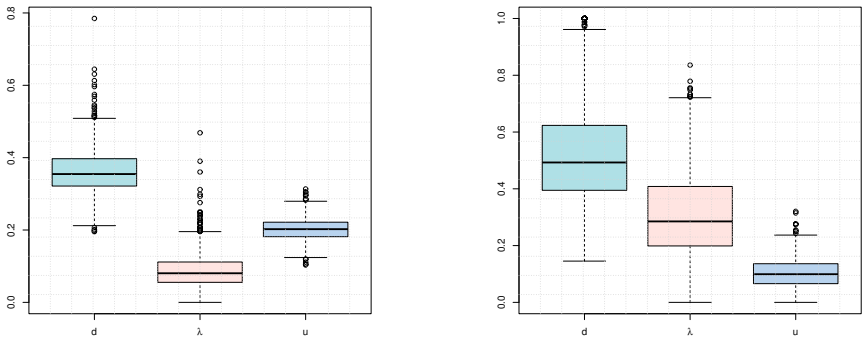

(a) (b)

Figure 3.3: Box plot of parameters using 1000 samples for $d = 0.4$, $\lambda = 0.1$, and $u = 0.2$ (Fig. 3.3a) and for $d = 0.5$, $\lambda = 0.3$, and $u = 0.2$ (Fig. 3.3b) based on the Whittle likelihood.

3.6 Real Data Application

To compare the performance of the introduced GARTFIMA process with existing time series models, two real-world datasets are considered. In this section, the comparison of the introduced model is done with existing time series models namely ARIMA, ARFIMA, ARTFIMA, and GARMA. We use two datasets for the comparison task and the first is the "Nile annual minima" dataset which is a dataset of the annual minimum flow of the Nile river from 622 AD to 1284 AD. The "Nile annual minima" dataset is already defined in R containing 663 observations. The dataset was recorded over the centuries and was given by an Egyptian prince Omar Toussoun in 1925 in a book named "Mémoire sur l'Histoire du Nil". Beran, Percival, and Walden (2000) analyzed that the dataset from 622 AD to 1284 AD is more homogeneous than the full dataset. The observations were recorded by a tool called Nilometer, which measures the height reached by the Nile River. The observations were taken and measured at the Roda gauge near Cairo. In this chapter, we are working on the dataset scaled by 1/100 containing 663 observations. Another dataset is Spain's 10-year treasury bond daily percentage yield data from July 2nd, 2012 to Feb 16th, 2017. The study of treasury bond daily percentage yield data is important to comprehend how present-day yields measure up to historical rates. The dataset is a daily dataset containing 1443 observations. Financial markets commonly use the 10-year maturity as a benchmark, which is why it is selected. The comparison study is given as follows:

Nile river data

The GARTFIMA model is applied to the "Nile Annual Minima" dataset which is a dataset of the annual minimum flow of the Nile river from the sample path of data is plotted in Fig. 3.4a. Also, the ACF and PACF plots are given in Fig. 3.4b and 3.4c. The ACF plot is significant for large lag values, this indicates the presence of long memory property in the dataset. The AR and MA lags are $p = 3$ and $q = 0$, respectively.

We apply the ARFIMA, ARTFIMA, and GARTFIMA models to the Nile minima dataset and check the performance of each model on the dataset by looking at the root mean squared errors for each model. By taking almost 75% of the data for the training set and 25% of data in the test set we will train ARIMA, ARFIMA, and ARTFIMA model using the R packages "auto.arima", "arfima", and "artfima", respectively and check the performance on the test set using root mean square error (RMSE), mean absolute error(MAE), mean absolute percentage error (MAPE), and root mean square percentage error (RMSPE) values. Further, using the non-linear least square estimation technique for the GARTFIMA process the

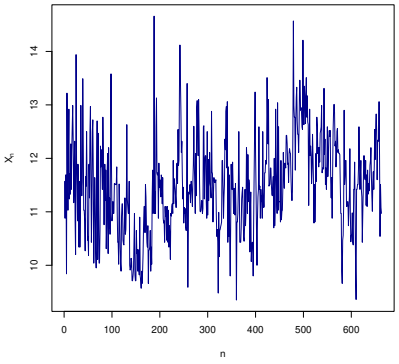

(a) Nile river annual minimum flow series

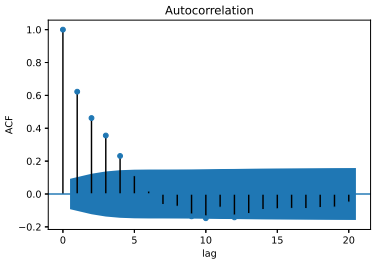

(b) ACF

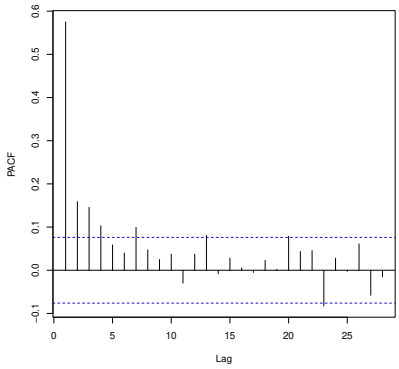

(c) PACF

Figure 3.4: Annual minimum flow series, ACF, and PACF plot for Nile annual minima data from left to right, respectively.

results are summarized in Table 3.4.

	Estimated parameters	**RMSE**	**MAE**	**MAPE**	**RMSPE**
ARIMA process	$\hat{d} = 0$	0.73	0.59	0.05	0.06
ARFIMA process	$\hat{d} = 0.39$	0.72	0.55	0.05	0.06
ARTFIMA process	$\hat{d} = 0.35$, $\hat{\lambda} = 0.007$	0.69	0.54	0.046	0.06
GARMA process	$\hat{d} = 0.2$, $\hat{u} = 0.99$	0.74	0.60	0.051	0.07
GARTFIMA process	$\hat{d} = -0.16$, $\hat{\lambda} = 0$, $\hat{u} = 0.89$	0.68	0.52	0.045	0.05

Table 3.4: Model performance comparison where ARFIMA, ARTFIMA and GARMA are estimated using inbuilt R packages and GARTFIMA parameters are estimated using NLS estimation.

This indicates that the GARTFIMA process with NLS estimation approach fits the model equivalent to ARFIMA and ARTFIMA processes. Further, the white noise can be plotted using actual and predicted values of the time series, and to look for the normality of the white noise series, we plot the density of actual white noise

with a synthetic white noise series. A synthetic random series of noise is generated from using the mean and variance of the actual series, which are 0.063 and 0.47, respectively. The density plots for both the series are given in Fig. 3.5, where the blue plot is for the actual and the black is for the synthetic dataset.

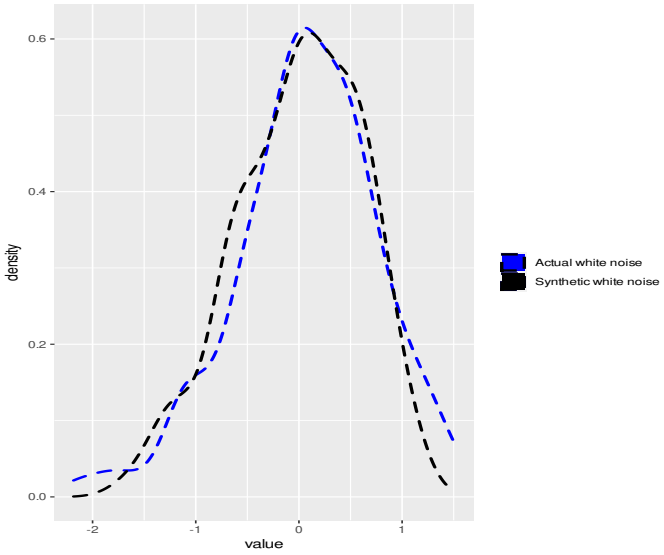

Figure 3.5: Density plot for actual and synthetic white noise series of the Nile annual minima dataset.

Spain's 10-year treasury bond data

The other dataset used for comparison is the 10-year bond yield of Spain which contains 1443 observations. The trajectory, ACF, and PACF plots of the dataset are given in Fig. 3.6a, 3.6b, and 3.6c. We get the AR and MA lags denoted by p and q using the Akaike information criterion (AIC) which comes out to be $p = 3$ and $q = 2$.

Similar to the previous approach defined for Nile annual minima data, we use R to compare the performance of ARIMA, ARFIMA, ARTFIMA, and GARTFIMA models. The results are summarized in Table 3.5. It indicates that the GARTFIMA

	Estimated parameters	**RMSE**	**MAE**	**RMSPE**
ARIMA process	$\hat{d} = 0$	3.25	2.35	33.713
ARFIMA process	$\hat{d} = -0.03$	3.24	2.36	88.7
ARTFIMA process	$\hat{d} = -0.23$, $\hat{\lambda} = 0.27$	3.26	2.35	68.263
GARMA process	$\hat{d} = 0.07$, $\hat{u} = 0.27$	3.24	2.35	138.36
GARTFIMA process	$\hat{d} = 0.06$, $\hat{\lambda} = 0.21$, $\hat{u} = 0.41$	3.20	2.29	31.99

Table 3.5: Model performance comparison for GARTFIMA using the NLS estimation.

process using the NLS technique for estimation performs slightly better than the

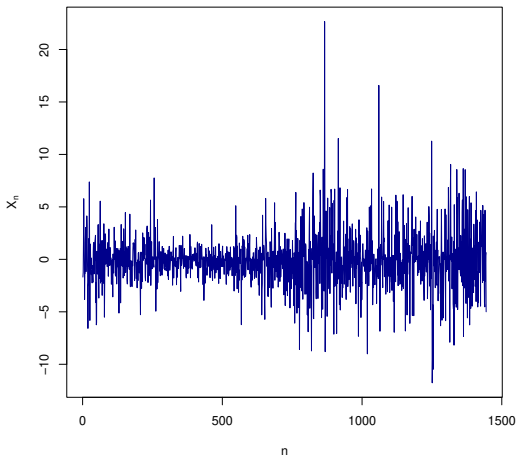

(a) Spain's treasury yield series

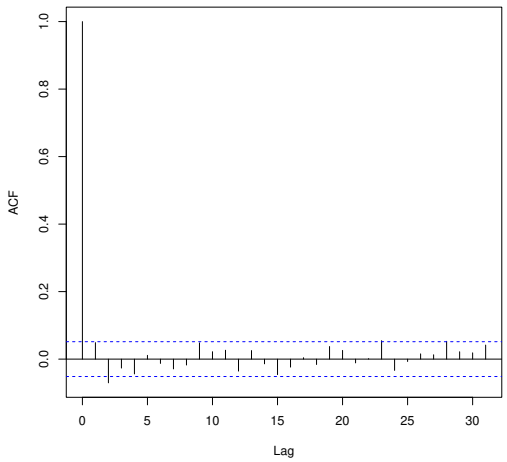

(b) ACF

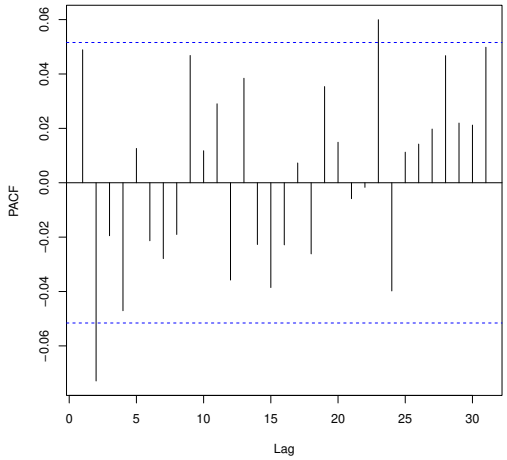

(c) PACF

Figure 3.6: Treasury yield series, ACF, and PACF plots for Spain's 10-year bond data from left to right, respectively.

ARFIMA and ARTFIMA processes. Moreover, a synthetic white noise series is generated using the mean and variance of actual white noise, which are 0.48 and 12.19, respectively. Also, the density plots for both the actual and synthetic white noise series are given in Fig. 3.7, where the blue plot is for the actual and the black is for the synthetic dataset.

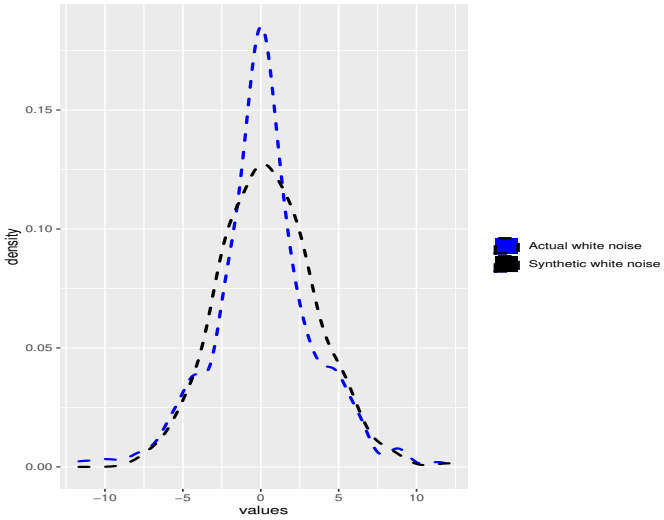

Figure 3.7: Density plot for actual and synthetic white noise series of Spain's 10-year treasury bond dataset.

Chapter 4

Tempered Fractional ARUMA Process

In this chapter, we introduce a new variation of the seasonal fractional ARUMA process, which we call the tempered fractional ARUMA process. This is achieved by introducing exponential tempering in the seasonal fractional ARUMA model. The stationarity and invertibility conditions of the introduced model are given and derive its spectral density. To estimate the model parameters, we utilize minimum contrast based Whittle likelihood estimation approach and investigate the asymptotic properties of the estimators of the model parameters. The estimation technique's performance is assessed on simulated data.

4.1 Introduction

The spectral density of a time series represents the distribution of its frequency components. By extending the ARMA framework, GARMA models offer flexibility in capturing various types of seasonality, including periodic and non-periodic patterns [38]. Researchers have utilized these models effectively in economics, finance, meteorology, and social sciences. Giraitis and Leipus provided an extension to the fractional ARIMA process, utilizing the GARMA framework, by introducing the seasonal fractional ARUMA process [34]. To study the parameter estimation for the ARUMA process one can refer to [60]. Meerschaert et al. in [64], proposed the ARTFIMA process with exponential tempering for improved flexibility and convenience in estimation and analysis. It is more convenient to study the tempered process rather than the original process as the covariance function is absolutely summable in finite variance cases and the spectral density converges to 0. Further, the tempering parameter provides modelling flexibility. Motivated by the work of [64], We present an innovative extension of the existing seasonal fractional ARUMA models, introducing the concept of "tempered fractional ARUMA models." This introduced extension involves incorporating tempered fractional differencing within the traditional seasonal ARUMA framework, significantly enriching the model's flexibility and dynamics. Tempering serves a crucial role in addressing

the unit root challenge inherent in the classical ARUMA model. Furthermore, in cases where the spectral density of seasonal fractional ARUMA is not universally bounded. Tempering acts as an effective remedy, ensuring that the tempered fractional ARUMA process maintains bounded spectral density in all scenarios. The distinctive feature of tempering brings about a transformation in the spectral characteristics and control to the spectral properties of the ARUMA model across diverse contexts. We discuss the stationarity and invertibility conditions of the introduced models to ensure their reliability and feasibility. Furthermore, we derive the spectral density of the tempered fractional ARUMA models, allowing us to gain deeper insights into the frequency components and their strengths within the time series. Estimating the model parameters is accomplished using minimum contrast based the Whittle likelihood estimation approach, which minimizes the contrast between the theoretical and observed spectral densities. Additionally, we investigate the asymptotic properties of the estimators to understand their reliability and consistency as the sample size increases. In summary, the novel contributions in this study lie in the introduction of tempered fractional ARUMA model. Other aspects, such as the, parameter estimation, theoretical framework, methodology, and empirical evaluation through simulation study, are likely built upon existing literature and standard practices in time-series analysis. The chapter is organized as follows. Section 2 introduces the tempered fractional ARUMA model and establishes its stationarity and invertibility conditions. In Section 3, the parameter estimation procedure is discussed. Further, Section 4 deals with the simulation study to assess the performance of the estimation method.

4.2 Tempered Fractional ARUMA Process

The fractional ARUMA process introduced by [34] is discussed in Chapter 1 and is given by (1.10). In this chapter, we introduce the concept of exponential tempering by incorporate the the tempering paramtere into the fractional ARUMA process, leading to the development of the tempered fractional ARUMA$(p, d_0, \ldots, d_{k+1}, \lambda, u_1, \ldots, u_k, q)$ process. By introducing the concept of tempering, we introduce an additional parameter that controls the decay rate within the fractional differencing process. The tempered fractional ARUMA process takes the given form:

$$\Phi(B)(1-e^{-\lambda}B)^{d_0}\prod_{j=1}^{k}(1-2u_je^{-\lambda}B+e^{-2\lambda}B^2)^{d_j}(1+e^{-\lambda}B)^{d_{k+1}}X_t=\Theta(B)\epsilon_t, \quad (4.1)$$

where ϵ_t is Gaussian white noise with variance σ^2, B is the lag operator, $|u_j| \leq 1$, $\lambda > 0$ and $d_i \notin \mathbb{Z}$, $i = 0, \ldots, k+1$. Again, $\Phi(B)$ and $\Theta(B)$ are stationary AR and invertible MA operators with lag order p and q, respectively. The Gegenbauer polynomials can be expressed in terms of generating functions as: $(1-2uz+z^2)^{-d} = \sum_{n=0}^{\infty} C_n^d(u) z^n$ where $d \neq 0$, $|z| < 1$ and $C_n^d(u)$ is given by

$$C_n^d(u) = \sum_{k=0}^{\lfloor n/2 \rfloor} (-1)^k \frac{\Gamma(n-k+d)}{\Gamma(d)\Gamma(n+1)\Gamma(n-2k+1)} (2u)^{n-2k} \sim \frac{\cos\left((n+d)\phi - d\pi/2\right) n^{d-1}}{\Gamma(d)\sin^d(\phi)}, \tag{4.2}$$

where $n \to \infty$ and $\phi = \cos^{-1}(u)$. The tempered fractional ARUMA process is a generalization of the following existing processes.

Remark 4.2.1. *For $d_0 = 0$, $d_{k+1} = 0$, $k = 1$, and $\lambda = 0$, the tempered fractional ARUMA process with lags $p = 0$ and $q = 0$ takes the form $(1 - 2u_1 B + B^2)^{d_1} X_t = \epsilon_t$, which is a Gegenbauer process defined by [19]. The Gegenbauer process is stationary and long memory for $|u_1| < 1$ and $0 < d_1 < 1/2$ or $|u| = 1$ and $0 < d_1 < 1/4$. The spectral density of the Gegenbauer process is given by $f_x(\omega) = \frac{\sigma^2}{2\pi} \{4[\cos(\omega) - \cos(\phi)]^2\}^{-d_1}$.*

Remark 4.2.2. *For $d_0 = 0$, $d_{k+1} = 0$, and $\lambda = 0$, the tempered fractional ARUMA process for $p = 0$ and $q = 0$ takes the following form:*

$$\prod_{j=1}^{k} (1 - 2u_j B + B^2)^{d_j} X_t = \epsilon_t, \tag{4.3}$$

which is a k factor Gegenbauer process defined by [96]. The k factor Gegenbauer process is stationary and long memory for $|u_j| < 1$ and $0 < d_j < 1/2$ or $|u_j| = 1$ and $0 < d_j < 1/4$, for each $j = 1, 2, \ldots, k$. The spectral density of the k factor Gegenbauer process is given by

$$f_x(\omega) = \frac{\sigma^2}{2\pi} \prod_{j=1}^{k} \{4[\cos(\omega) - \cos(\phi_j)]^2\}^{-d_j},$$

where $\phi_j = \cos^{-1}(u)$ is known as Gegenbauer frequencies for $j = 1, 2, \ldots, k$ which implies that the spectral density has k unbounded peaks. For $k = 1$ the k factor Gegenbauer process reduces to the Gegenbauer process.

Theorem 4.2.1. *The tempered fractional ARUMA$(p, d_0, \ldots, d_{k+1}, \lambda, u_1, \ldots, u_k, q)$ process $\{X_t\}$ is stationary and invertible if all roots of $\Phi(B)$ and $\Theta(B)$ lie outside the unit circle, $d_0, d_{k+1}, d_j \notin \mathbb{Z}$, and $\lambda > 0$, for $|u_j| \leq 1$ for each $j = 1, 2, \ldots k$.*

Proof. Using (4.1) the process can be rewritten as follows:

$$X_t = \left(\frac{\Theta(B)}{\Phi(B)}\right)(1-e^{-\lambda}B)^{-d_0}\prod_{j=1}^{k}(1-2u_je^{-\lambda}B+e^{-2\lambda}B^2)^{-d_j}(1+e^{-\lambda}B)^{-d_{k+1}}\epsilon_t. \tag{4.4}$$

We can write $\frac{\Theta(B)}{\Phi(B)} = \sum_{r=0}^{\infty}\psi_r B^r$ and $\left(1-e^{-\lambda}B\right)^{-d_0}\left(1+e^{-\lambda}B\right)^{-d_{k+1}} = \sum_{s=0}^{\infty}\alpha_s B^s$, where

$$\alpha_s = \sum_{l=0}^{s} e^{-l\lambda}\frac{\Gamma(s-l+d_0)}{\Gamma(d_0)\Gamma(s-l+1)}\frac{\Gamma(l+d_{k+1})}{\Gamma(d_{k+1})\Gamma(l+1)}. \tag{4.5}$$

Further, $\prod_{j=1}^{k}\left(1-2u_je^{-\lambda}B+e^{-2\lambda}B^2\right)^{-d_j} = \sum_{n=0}^{\infty}\pi_n B^n$, where

$$\pi_n = \sum_{\substack{0\le r_1\ldots r_k\le n\\ r_1+r_2+\ldots+r_k=n}} e^{-(r_1+r_2+\ldots+r_k)\lambda}C_{r_1}^{-d_1}(u_1)\,C_{r_2}^{-d_2}(u_2)\cdots C_{r_k}^{-d_k}(u_k). \tag{4.6}$$

Now (4.4) can be written as:

$$X_t = \sum_{r=0}^{\infty}\sum_{s=0}^{\infty}\sum_{n=0}^{\infty}\psi_r\alpha_s\pi_n B^{r+s+n}\epsilon_t = \sum_{r=0}^{\infty}\sum_{s=0}^{\infty}\sum_{n=0}^{\infty}\psi_r\alpha_s\pi_n\epsilon_{t-(r+s+n)}. \tag{4.7}$$

The variance of the process is given by

$$\mathrm{Var}(X_t) = \sigma^2\sum_{r=0}^{\infty}\sum_{s=0}^{\infty}\sum_{n=0}^{\infty}\psi_r^2\alpha_s^2\pi_n^2.$$

The variance of the process will converge if $\sum_{r=0}^{\infty}\psi_r^2 < \infty$, $\sum_{r=0}^{\infty}\alpha_s^2 < \infty$ and $\sum_{r=0}^{\infty}\pi_n^2 < \infty$. Now according to the assumption all roots of $\Phi(B)=0$ and $\Theta(B)=0$ lie outside the unit circle which implies $\sum_{r=0}^{\infty}|\psi_r| < \infty$ and for large s using Stirling's approximation

$$\frac{\Gamma(s-l+d_0)}{\Gamma(s-l+1)}\frac{\Gamma(l+d_{k+1})}{\Gamma(l+1)} \sim l^{d_{k+1}-1}(s-l)^{d_0-1}, \tag{4.8}$$

which implies $\sum_{r=0}^{\infty}\alpha_s^2 < \infty$ for $d_0, d_{k+1} \notin \mathbb{Z}$. Further, for large n the Gegenbauer polynomials can be approximated as defined in (4.2). Thus for large $r_1, r_2, \ldots, r_k$ in (4.6) the series sum $\sum_{n=0}^{\infty}|\pi_n|$ is finite for $d_0, d_{k+1}, d_j \notin \mathbb{Z}$, $\lambda > 0$ and $|u_j| \le 1$ for $j = 1, \ldots, k$, which further implies that $\mathrm{Var}(X_t) < \infty$. □

Remark 4.2.3. *In (1.10), the characteristic polynomials $(1-z)^{d_0}$ and $(1-2uz+z^2)$ exhibit a unit root when $d_0 = 1$. However, the introduction of tempering in the tempered fractional ARUMA process circumvents the issue of the unit root by*

incorporating the term $e^{-\lambda}$ within the characteristic polynomial $(1-e^{-\lambda}z)^{d_0}$ as given in (4.1).

Theorem 4.2.2. *Under the assumptions of theorem 4.2.1, the spectral density for the tempered fractional ARUMA$(p, d_0, \ldots, d_{k+1}, \lambda, u_1, \ldots, u_k, q)$ process takes the following form:*

$$f_x(\omega) = \frac{\sigma^2}{2\pi}\frac{|\Theta(z)|^2}{|\Phi(z)|^2}(1+e^{-2\lambda}-2e^{-\lambda}\cos(\omega))^{-d_0}\prod_{j=1}^{k}(A_j - B_j\cos(\omega)+C\cos^2(\omega))^{-d_j} \times (1+e^{-2\lambda}+2e^{-\lambda}\cos(\omega))^{-d_{k+1}}, \tag{4.9}$$

where $z = e^{-\iota\omega}$, $\omega \in (-\pi, \pi)$ and $A_j = (1+4u_j^2e^{-2\lambda}-2e^{-2\lambda}+e^{-4\lambda})$, $B_j = 4u_je^{-\lambda}(1+e^{-2\lambda})$, $C = 4e^{-2\lambda}$.

Proof. Rewrite (4.1) as follows:

$$X_t = \Psi(B)\epsilon_t,$$

where $\Psi(B) = \frac{\Theta(B)}{\Phi(B)}(1-e^{-\lambda}B)^{-d_0}\prod_{j=1}^{k}(1-2u_je^{-\lambda}B+e^{-2\lambda}B^2)^{-d_j}(1+e^{-\lambda}B)^{-d_{k+1}}$. Then using the definition of spectral density of linear process, we have:

$$f_x(\omega) = |\Psi(z)|^2 f_\epsilon(\omega), \tag{4.10}$$

where $z = e^{-\iota\omega}$ and $f_\epsilon(\omega)$ is spectral density of the innovation term. The spectral density of the innovation process ϵ_t is $\sigma^2/2\pi$. Then (4.10) becomes,

$$f_x(\omega) = \frac{\sigma^2}{2\pi}|\Psi(z)|^2 = \frac{\sigma^2}{2\pi}\frac{|\Theta(z)|^2}{|\Phi(z)|^2}\frac{|(1-e^{-\lambda-\iota\omega})|^2}{|(1+e^{-\lambda-\iota\omega})|^{-2}}\prod_{j=1}^{k}\left|1-2u_je^{-\lambda-\iota\omega}+e^{-2\lambda-2\iota\omega}\right|^{-2d_j}.$$

Here, $\left|1-2u_je^{-\lambda-\iota\omega}+e^{-2\lambda-2\iota\omega}\right|^{-2d_j} = (A_j - B_j\cos(\omega)+C\cos^2(\omega))^{-d_j}$ and $A_j = (1+4u_j^2e^{-2\lambda}-2e^{-2\lambda}+e^{-4\lambda})$, $B_j = 4u_je^{-\lambda}(1+e^{-2\lambda})$, $C = 4e^{-2\lambda}$. The spectral density takes the following form:

$$f_x(\omega) = \frac{\sigma^2}{2\pi}\frac{|\Theta(z)|^2}{|\Phi(z)|^2}\frac{(1+e^{-2\lambda}-2e^{-\lambda}\cos(\omega))^{-d_0}}{(1+e^{-2\lambda}+2e^{-\lambda}\cos(\omega))^{-d_{k+1}}}\prod_{j=1}^{k}(A_j - B_j\cos(\omega)+C\cos^2(\omega))^{-d_j}.$$

□

Remark 4.2.4. *In the spectral density defined in (4.9) let us assume that $U(\omega) = \prod_{j=1}^{k}(A_j - B_j\cos(\omega)+C\cos^2(\omega))$. Let $k = 1$, then observing the behavior of $U(w)$ for different values of λ it can be easily demonstrated that for $\lambda > 0$, $U(\omega) > 0$ and for $\lambda = 0$, which is the case of spectral density of seasonal fractional ARUMA process,*

$U(\omega) = 0$ at $\omega = \cos^{-1}(u)$ (see [19]) and the spectral density becomes unbounded at these points. The following figure 4.1 observes the behavior of $U(\omega)$ for different values of λ.

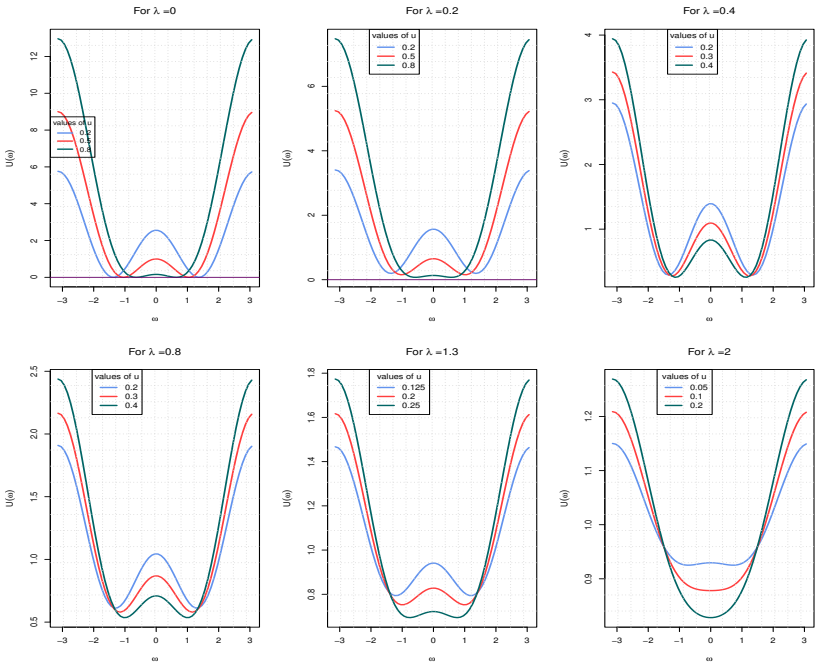

Figure 4.1: Plot of the function $U(\omega)$ for different values of $\lambda \in \{0, 0.3, 0.4, 0.8, 1.3, 2\}$ and $0 \leq u \leq 1$.

Similarly, letting $U'(\omega) = (1 + e^{-2\lambda} - 2e^{-\lambda}\cos(\omega))$ in (4.9), the spectral density becomes unbounded at $w = 0$ for $\lambda = 0$. For $\lambda > 0$, the spectral density is bounded everywhere in $\omega \in (-\pi, \pi)$. Under the assumptions of stationarity and invertibility, the introduced tempered fractional ARUMA process guarantees that the spectral density of the process maintains its bounded characteristics.

4.3 Parameter Estimation

In our study, we employ the Whittle likelihood method, discussed in Chapter 1, to estimate the parameters of interest. This method, introduced by [94], involves minimizing a theoretical distance measure to obtain reliable parameter estimates. For applications of the Whittle likelihood method in parameter estimations of ARTFIMA process and Humbert generalized ARMA process see [11,76]. The performance of the proposed methods is assessed on a simulated time series. Encouragingly, the results obtained from these simulations show promising outcomes, indicating the potential effectiveness of the Whittle likelihood method in accurately estimating the parameters of interest. In the next section, we investigate the theoretical aspects of our approach. This includes studying the asymptotic

normality and consistency properties of the estimated parameters. Understanding the asymptotic behavior of the estimates is crucial for assessing their reliability and establishing the statistical properties of the proposed method. We recall the Whittle likelihood method from Chapter 1, which is a periodogram based technique for estimation. Consider a set of harmonic frequencies denoted as ω_j, where $j = 0, 1, \ldots, \lfloor n/2 \rfloor$, and we recall the empirical spectral density of the process, which is defined as:

$$I(\omega_j) = \frac{1}{2\pi}\{R(0) + \sum_{s=1}^{n-1} R(s)\cos(s\omega_j)\},\ \omega_j = \frac{2\pi j}{n},\ j = 0, 1, \ldots, \lfloor n/2 \rfloor, \tag{4.11}$$

where $R(s) = \frac{1}{n}\sum_{i=1}^{n-s}(X_i - \bar{X})(X_{i+s} - \bar{X})$, $s = 0, 1, \ldots, (n-1)$, is the sample autocovariance function with sample mean $\bar{X}$. We recall the Whittle likelihood function from Chapter 1, denoted by $l_w(\theta)$, is defined as follows:

$$l_w(\theta) = \sum_{j=1}^{n} \left\{ \frac{I(\omega_j)}{f_x(\omega_j)} + \log(f_x(\omega_j)) \right\},$$

where in the context of this discussion θ stands for a vector that encompasses unknown parameters, which can be denoted as $\theta = (d_0, d_1, \cdots, d_{k+1}, \lambda, u_1, u_2, \cdots, u_k)$. Let $\Omega = \{d_0, d_1, \cdots, d_{k+1}, \lambda, u_1, u_2, \cdots u_k : \lambda > 0, d_0, d_{k+1}, d_j \notin \mathbb{Z}, |u_j| \leq 1, j = 1, \cdots, k\}$ and $\Omega_0 \subset \Omega$ is compact set. Also, $\theta = (d_0, d_1, \cdots, d_{k+1}, \lambda, u_1, u_2, \cdots, u_k) \in \Omega_0$. Moreover, $f_x(\omega_j)$ is the spectral density defined in (4.9), (see [47]). Then estimates are achieved by minimizing the likelihood function $l_w(\theta)$ with respect to θ, that is

$$\hat{\theta}_n = \underset{\theta}{\operatorname{argmin}}\ l_w(\theta),\ \theta \in \Omega_0.$$

The likelihood method is the minimum contrast estimator, which will be further applied for the class of fractional ARUMA processes using ideas from work done in [5,6,23,24,66].

Theorem 4.3.1. *The Whittle likelihood estimator is consistent under the assumptions of Theorem 4.2.1. This implies* $\lim_{n\to\infty} \hat{\theta}_n = \theta$ *almost surely.*

Proof. To prove the consistency of the Whittle likelihood estimator, we can rely on Hannan's result (see Theorem 1.3.1) using the assumption that the parameter vector θ belongs to a compact parametric space Ω_0 and the spectral density defined

in (4.9) is written as $f_x(\omega) = \frac{\sigma^2}{2\pi}K(\omega)$, where

$$K(\omega) = \frac{|\Theta(z)|^2}{|\Phi(z)|^2}\frac{(1+e^{-2\lambda}-2e^{-\lambda}\cos(\omega))^{-d_0}}{(1+e^{-2\lambda}+2e^{-\lambda}\cos(\omega))^{d_{k+1}}}\prod_{j=1}^{k}(A_j - B_j\cos(\omega)+C\cos^2(\omega))^{-d_j}. \tag{4.12}$$

We need to verify the following conditions to prove the result

(a) The time series as represented in (4.1) has a moving average representation as $X_t = \sum_{z=0}^{\infty}\tau_z\epsilon_{t-z}$, $\sum_{z=0}^{\infty}\tau_z^2 < \infty$ and $\tau_0 = 1$.

(b) $\frac{1}{K(\omega)+a}$ is a continuous function for $\omega \in (-\pi,\pi)$ for all $a > 0$.

(c) The parameter vector $\theta \in \Omega_0$ define the spectral density uniquely.

To prove the condition (a), we can proceed as follows. We can write

$$\frac{\Theta(B)}{\Phi(B)}\left(1-e^{-\lambda}B\right)^{-d_0}\left(1+e^{-\lambda}B\right)^{-d_{k+1}} = \sum_{r=0}^{\infty}\psi_r B^r\sum_{s=0}^{\infty}\alpha_s B^s = \sum_{m=0}^{\infty}a_m B^m, \tag{4.13}$$

where $a_m = \sum_{t=0}^{m}\psi_{m-t}\alpha_t$ and α_t takes the form defined in (4.5) and $\alpha_0 = 1$. To demonstrate that $\sum_{m=0}^{\infty}a_m^2 < \infty$ we can show that $\sum_{m=0}^{\infty}|a_m| < \infty$ as follows:

$$\sum_{m=0}^{\infty}|a_m| \le \sum_{m=0}^{\infty}\sum_{t=0}^{m}|\psi_{m-t}|\,|\alpha_t| = \sum_{t=0}^{\infty}\sum_{m=t}^{\infty}|\psi_{m-t}|\,|\alpha_t| = \sum_{t=0}^{\infty}\sum_{\omega=0}^{\infty}|\psi_\omega|\,|\alpha_t|. \tag{4.14}$$

Now, we know that the $\Theta(B)$ and $\Phi(B)$ are stationary autoregressive and invertible moving average operators, respectively and $\frac{\Theta(z)}{\Phi(z)} = \sum_{w=0}^{\infty}\psi_w z^w$, where $\sum_{w=0}^{\infty}|\psi_w| < \infty$ and $\psi_0 = 1$, for $|z| \le 1+\epsilon$. This implies $|\psi_w| < C(1+\epsilon)^{-w}$ for some constant C. Also, in theorem 4.2.1, it is proved that $\sum_{t=0}^{\infty}|\alpha_t|$ is finite for $\lambda > 0$ and $d_0, d_{k+1} \notin \mathbb{Z}$. This, in turn, implies that $\sum_{m=0}^{\infty}|a_m| < \infty$ and $a_0 = 1$. Therefore, we conclude that $\sum_{m=0}^{\infty}a_m^2 < \infty$. Further $\prod_{j=1}^{m}\left(1-2u_je^{-\lambda}b+e^{-2\lambda}B^2\right)^{-d_j} = \sum_{n=0}^{\infty}\pi_n B^n$, where π_n is given by (4.6) and

$$\begin{aligned}&\left(\frac{\Theta(B)}{\Phi(B)}\right)(1-e^{-\lambda}B)^{-d_0}\prod_{j=1}^{k}(1-2u_je^{-\lambda}B+e^{-2\lambda}B^2)^{-d_j}(1+e^{-\lambda}B)^{-d_{k+1}}\\ &= \sum_{m=0}^{\infty}a_mB^m\sum_{n=0}^{\infty}\pi_nB^n = \sum_{z=0}^{\infty}\tau_zB^z,\end{aligned} \tag{4.15}$$

where $\tau_z = \sum_{\nu=0}^{z}a_{z-\nu}\pi_s$. It can be demonstrated that $\sum_{z=0}^{\infty}|\tau_z| \le$ as follows:

$$\sum_{z=0}^{\infty}|\tau_z| \le \sum_{z=0}^{\infty}\sum_{v=0}^{z}|a_{z-v}|\,|\pi_v| = \sum_{v=0}^{\infty}\sum_{z=v}^{\infty}|a_{z-v}|\,|\pi_v| = \sum_{v=0}^{\infty}\sum_{v'=0}^{\infty}|a_{v'}|\,|\pi_v|. \tag{4.16}$$

Now, we know that $\frac{\theta(z)}{\Phi(z)}(1-e^{-\lambda}z)^{-d_0}(1+e^{-\lambda}z)^{-d_{k+1}} = \sum_{m=0}^{\infty} a_m z^m$, where $\sum_{m=0}^{\infty}|a_m| < \infty$ for $|z| < (1+\epsilon)$. This implies $|a_m| < C(1+\epsilon)^{-m}$ for some constant C and in theorem 4.2.1 it is proved that $\sum_{n=0}^{\infty}|\pi_n|$ is finite, which implies $\sum_{z=0}^{\infty}|\tau_z| < \infty$ implying $\sum_{z=0}^{\infty}\tau_z^2 < \infty$ and $\tau_0 = 1$. Since, $K(\omega)$ does not have any singularity for $\omega \in (-\pi, \pi)$ and continuous hence the function $\frac{1}{K(\omega)+a}$ is continuous for $a > 0$ and the condition (c) can be easily verified. □

Theorem 4.3.2. *For the tempered fractional ARUMA process, the Whittle likelihood estimators satisfy the asymptotic normality property, that is* $\sqrt{n}(\hat{\theta}_n - \theta) \xrightarrow{d} \mathcal{N}(0, W)$ *as* $n \to \infty$. *Here,* W *represents the variance-covariance matrix, which takes a specific form:*

$$W = \frac{1}{4\pi}\int_{-\pi}^{\pi}\left\{\frac{\partial \log K(\omega)}{\partial\theta}\right\}\left\{\frac{\partial \log K(\omega)}{\partial\theta}\right\}' d\omega$$

and the $(2k+3)\times 1$ *column vector* $\frac{\partial \log K(\omega)}{\partial\theta}$ *represents the derivative of* $\log K(\omega)$ *with respect to all the parameters* $d_0, d_1, \cdots, d_{k+1}, \lambda, u_1, u_2, \cdots u_k$. *On the other hand* $\left\{\frac{\partial \log K(\omega)}{\partial\theta}\right\}'$ *represents the transpose of a* $(2k+3)\times 1$ *column vector.*

Proof. To prove the asymptotic normality of the parameters using the results defined by Hannan (refer to Theorem 1.3.2), it is sufficient to verify the following conditions.

(a) We first examine the condition $K(\omega) > 0$ for all $\omega \in (-\pi, \pi)$ and $\theta \in \Omega_0$. In the decomposition of $K(\omega)$, let us assume $K_1(\omega) = (1+e^{-2\lambda}-2e^{-\lambda}\cos(\omega))^{-d_0}$, $K_2(\omega) = (1+e^{-2\lambda}+2e^{-\lambda}\cos(\omega))^{-d_{k+1}}$ and $K_{3,j}(\omega) = (A_j - B_j\cos(\omega) + C\cos^2(\omega))^{-d_j}$ for $j = 1, \cdots, k$. By looking at the function values $K_1(\omega)$, $K_2(\omega)$ and $K_{3,j}(\omega)$ with the help of their extreme points it can be easily verified that $K_1(\omega) > 0$, $K_2(\omega) > 0$ and $K_{3,j}(\omega) > 0$ implying $K(\omega) > 0$.

(b) The second condition requires verifying that $K(\omega)$ is twice differentiable with respect to the parameters. This verification is straightforward, as the function $K(\omega)$ can be shown to be twice differentiable for these parameters.

(c) Lastly, we note that condition (c) is proved in theorem 4.3.1 and we can establish that the time series defined in Equation (1) can be written as $X_t = \sum_{m=0}^{\infty}\tau_z\epsilon_{t-z}$, where $\sum_{z=0}^{\infty}\tau_z^2 < \infty$ and $\tau_0 = 1$. By satisfying these conditions, we have successfully demonstrated the desired result regarding the asymptotic normality of the parameters.

□

4.4 Simulation Study for Tempered Fractional ARUMA Process

To evaluate the proposed estimation technique, a simulation study is conducted in this section. Synthetic data is generated based on a predetermined set of parameters from the introduced model. For each case single trajectory is used for estimation. These parameters are then estimated using the defined estimation technique and compared with the actual parameters. The simulation based evaluation allows to validate the robustness and efficacy of the parameter estimation techniques under controlled conditions ensuring their reliability in real-world applications. To generate data for the tempered fractional ARUMA process, we begin by simulating independent and identically distributed (i.i.d.) innovations, denoted as $\epsilon_t \sim \mathcal{N}(0, \sigma^2)$ with the help of R programming language. Use the relation between X_t and ϵ_t defined in (4.1) as

$$X_t = \left(\frac{\Theta(B)}{\Phi(B)}\right)(1 - e^{-\lambda}B)^{-d_0} \prod_{j=1}^{k}(1 - 2u_j e^{-\lambda}B + e^{-2\lambda}B^2)^{-d_j}(1 + e^{-\lambda}B)^{-d_{k+1}}\epsilon_t. \tag{4.17}$$

First we generate the series $\eta_t = (1 - e^{-\lambda}B)^{-d_0} \prod_{j=1}^{k}(1 - 2u_j e^{-\lambda}B + e^{-2\lambda}B^2)^{-d_j}(1 + e^{-\lambda}B)^{-d_{k+1}}\epsilon_t$ using the simulated innovation series ϵ_t in (4.17). The generation of the series is done by taking the binomial expansion of $(1 - 2u_j e^{-\lambda}B + e^{-2\lambda}B^2)^{-d_j}$, $(1 - e^{-\lambda}B)^{-d_0}$ and $(1 + e^{-\lambda}B)^{-d_{k+1}}$ up to 4 terms, which is given as follows:

$$\prod_{j=1}^{k}\left(1 - 2u_j e^{-\lambda}B + e^{-2\lambda}B^2\right)^{-d_j} = \prod_{j=1}^{k}\sum_{n=0}^{\infty}\sum_{r=0}^{n}(-1)^r \frac{(d_j)_n}{n!}\binom{n}{r}(2u_j e^{-\lambda})^{n-r}\epsilon_{t-n-2r} \tag{4.18}$$

and $\left(1 - e^{-\lambda}B\right)^{-d_0}\left(1 + e^{-\lambda}B\right)^{-d_{k+1}} = \sum_{s=0}^{\infty}\alpha_s B^s$, where α_s takes the form defined in (4.5). The process in (4.17) is an ARMA process defined as $X_t = \frac{\Theta(B)}{\Phi(B)}\eta_t$ and can be generated using the "arima" library in R for any lag values. We conduct a simulation involving the generation of three series using different parameter combinations. We assume that the innovation ϵ_t follows a normal distribution with mean 0 and variance 1, i.e. $\epsilon_t \sim \mathcal{N}(0, 1)$, $\forall t$. For $k = 1$, we set some initial values for the parameters d_0, d_1, d_2, λ, u_1 and simulate the series X_t for $\theta_1 = 0$ and $\phi_1 = 0.6$ accordingly. The actual and estimated parameters for all the simulated series are presented in Table 4.1.

From the above table, it is evident that the Whittle likelihood technique performs well on the simulated dataset. Further, to evaluate the effectiveness of the Whittle

	Case 1	**Case 2**	**Case 3**
Actual	$d_0 = 0.45, d_1 = 0.35,$ $d_2 = 0.25, \lambda = 0.1,$ $u_1 = 0.2$	$d_0 = 0.5, d_1 = 0.2,$ $d_2 = 0.1, \lambda = 0.4,$ $u_1 = 0.3$	$d_0 = 0.2, d_1 = 0.4,$ $d_2 = 0.45, \lambda = 0.3,$ $u_1 = 0.5$
Estimated	$\hat{d}_0 = 0.42, \hat{d}_1 = 0.37,$ $\hat{d}_2 = 0.235, \hat{\lambda} = 0.08,$ $\hat{u}_1 = 0.22$	$\hat{d}_0 = 0.52, \hat{d}_1 = 0.24,$ $\hat{d}_2 = 0.13, \hat{\lambda} = 0.38,$ $\hat{u}_1 = 0.27$	$\hat{d}_0 = 0.19, \hat{d}_1 = 0.41,$ $\hat{d}_2 = 0.43, \hat{\lambda} = 0.28,$ $\hat{u}_1 = 0.5$

Table 4.1: Actual and estimated parameter values for single trajectory with different choices of parameters using the Whittle likelihood approach.

likelihood technique, which is based on empirical spectral density, a comprehensive analysis is conducted using box plots. These box plots provide insights into the estimation performance of the technique for different parameter settings.
To begin, a simulation is carried out, generating 1000 series, each comprising 1000 observations. These series are simulated assuming two combinations of specific parameter values: $(d_1 = 0.45, d_0 = 0.3, d_2 = 0.2, \lambda = 0.2,\ u_1 = 0.1)$ and $(d_1 = 0.49, d_0 = 0.4, d_2 = 0.35, \lambda = 0.3,\ u_1 = 0.2)$. Subsequently, the estimation is employed to estimate the values of the parameters for each simulated series. The resulting estimated parameters from each simulation are then used to construct the box plots, which visually represent the distribution of the estimated parameter values. These box plots can be observed in Figure 4.2 By examining the box plots

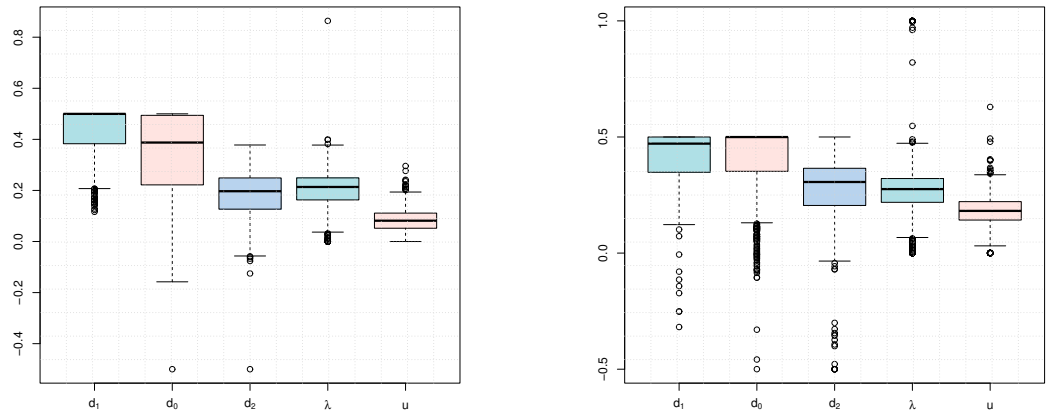

(a) (b)

Figure 4.2: Box plot of parameters using 1000 samples for $d_1 = 0.45, d_0 = 0.3, d_2 = 0.2, \lambda = 0.2$ and $u_1 = 0.1$ (4.2a) and $d_1 = 0.49, d_0 = 0.4, d_2 = 0.35, \lambda = 0.3$ and $u_1 = 0.2$ (4.2b) based on Whittle quasi-likelihood approach

from both simulations, valuable insights can be gained regarding the accuracy and

variability of the estimated parameters. This analysis aids in understanding the behavior of the Whittle likelihood technique and its effectiveness in capturing the underlying characteristics of the time series under different parameter settings.

Chapter 5

Horadam ARMA and Horadam-Pethe ARMA Processes

This chapter explores time series ARMA models characterized by the type 2 Humbert polynomials discussed in Chapter 1, specifically the Horadam ARMA(p, ν, u, q) and Horadam-Pethe ARMA(p, ν, u, q) processes. The main focus is to investigate the autocovariance function and its properties for both of these processes. The chapter utilizes the minimum contrast Whittle likelihood parameter estimation technique, which employs a contrast function involving the actual and empirical spectral densities for both processes. Another technique known as the debiased Whittle likelihood estimation is also used for estimation purposes. The effectiveness of these estimation methods is evaluated using simulated data.

5.1 Introduction

In Chapter 1, we have discussed the importance of fractionally differenced time series for modeling LRD data. The Autoregressive Tempered Fractionally Integrated Moving Average (ARTFIMA) process, derived from ARFIMA, exhibits semi-LRD characteristics with a summable autocovariance function, ensuring stability and reliability. The Gegenbauer process, introduced by Hosking, further extends the long memory modeling capabilities with Gegenbauer ARMA (GARMA) models, utilizing Gegenbauer polynomials. The estimation methods for time series models with their asymptotic properties are extensively studied in the literature. Some of the well-known methods are maximum likelihood estimation, Whittle likelihood estimation, minimum contrast estimation, and so on [5,6,19]. The generalized spectral density based approach was proposed by Hong in [43], which is suitable for both linear and non-linear time series models. The empirical characteristic functions (ECFs) and their derivatives are used in a time series framework for estimation. The ECF based estimation was first proposed by Press in 1972 by providing several methods of estimation for univariate and multivariate stable distributions [70]. Similarly, we use the true spectral density and empirical spectral density to estimate the model parameters by minimizing the contrast function between the

two. The Whittle likelihood is one of the widely used estimation methods which provide computationally efficient likelihood. However, it is known to produce biased parameter estimates for finite samples. Recently, Sykulski et al. proposed modified pseudolikelihoods by reducing the bias in Whittle likelihood, and hence, known as the debiased Whittle likelihood. This method effectively offer substantial reductions in bias and mean-squared error without imposing notable computational cost [86]. In summary, new properties like autocovariance function, infinite autoregressive representation are studied for type 2 Horadam ARMA processes. Additionally, the proposal to use existing debiased Whittle likelihood contrast functions for parameter estimation may represent new contributions to the field. Other aspects, such as the overview of fractionally differenced time series modeling, utilization of the generalized spectral density-based approach, and application of empirical characteristic functions for parameter estimation, are likely drawn from existing literature on time series analysis and modeling methodologies.

In this chapter, we study the particular cases of type 2 Humbert ARMA processes which are defined by using type 2 Humbert polynomials. In Section 5.2, we provide a brief introduction of Horadam and Horadam-Pethe ARMA(p, ν, u, q) processes. We also find the autocovariance function of these processes and study the summability of autocovariance. Section 5.3 contributes to the parameter estimation of Horadam and Horadam-Pethe ARMA(p, ν, u, q) processes using contrast function $D(f_x(\omega), I(\omega))$ with $f_x(\omega)$ as true spectral density and $I(\omega)$ being the empirical spectral density. We also propose to use the debiased Whittle likelihood method to estimate the parameters. The estimation results are analyzed on simulation data for both models. Further, we study the consistency of the estimators.

5.2 Horadam and Horadam-Pethe ARMA(p, ν, u, q) Processes

In this section, we present the Horadam ARMA(p, ν, u, q) process and the Horadam–Pethe ARMA(p, ν, u, q) processes, which are specific cases of the type 2 Humbert ARMA (HARMA$(p.\nu, u, q)$) process. For more in-depth information, one can refer to [11]. The type 2 HARMA process is characterized by its use of the type 2 Humbert polynomials. Here, we recall Def. 1.5 of type 2 Humbert polynomials and type 2 Humbert ARMA process from Chapter 1. The type 2 Humbert polynomials have the following generating function representation:

$$(1 - 2ut + t^m)^{-\nu} = \sum_{n=0}^{\infty} Q_{n,m}^{\nu}(u)t^n \quad \text{for } |t| < 1,\ |\nu| < 1/2,\ \text{and } |u| \leq 1, \tag{5.1}$$

where

$$Q^{\nu}_{n,m}(u) = \sum_{k=0}^{[\frac{n}{m}]} (-1)^k \frac{(\nu)_{(n-(m-1)k)}}{k!(n-mk)!} (2u)^{n-mk},$$

for $\nu_0 = 1$ and $(\nu)_n = \frac{\Gamma(\nu+n)}{\Gamma(\nu)}$.

Definition 5.1 (Type 2 Humbert ARMA(p, ν, u, q) process)**.** The type 2 Humbert ARMA process is defined by using the generating function of type 2 Humbert polynomials in the following manner:

$$\Phi(B)(1 - 2uB + B^m)^{\nu} X_t = \Theta(B)\epsilon_t, \tag{5.2}$$

where ϵ_t is Gaussian white noise with variance σ^2, $0 \leq u \leq 1$, $|\nu| < 1/2$, and B is the lag operator defined as $BX_t = X_{t-1}$. $\Phi(B)$ and $\Theta(B)$ are stationary AR and invertible MA operators with lags p and q, respectively.

The characteristics of the type 2 Humbert ARMA process have been examined in a study in [11], which shows that the process is stationary and invertible, for $|\nu| < 1/2$ and $|u| \leq 1$. The Horadam ARMA(p, ν, u, q) process is derived when m is set to 1 in (5.2).

Definition 5.2 (Horadam ARMA(p, ν, u, q) process)**.** The Horadam ARMA process has the following form:

$$\Phi(B)(1 - 2uB + B)^{\nu} X_t = \Theta(B)\epsilon_t, \tag{5.3}$$

where ϵ_t is Gaussian white noise with variance σ^2, $0 \leq u \leq 1$, $|\nu| < 1/2$, and B is the lag operator. $\Phi(B)$ and $\Theta(B)$ are stationary AR and invertible MA operators with lags p and q, respectively.

Remark 5.2.1. *In [11], it is proved that the spectral density of the Horadam ARMA(p, ν, u, q) process is:*

$$f_x(\omega) = \frac{\sigma^2}{2\pi} \frac{|\Theta(z)|^2}{|\Phi(z)|^2} (2 + 4u^2 - 4u - 4u\cos(\omega) + 2\cos(\omega))^{-\nu}, \; z = e^{-\iota\omega}. \tag{5.4}$$

For the processes' properties and details, see [11].

Now, we discuss another process referred to as the Horadam-Pethe ARMA(p, ν, u, q) process by setting $m = 3$ in (5.2).

Definition 5.3 (Horadam-Pethe ARMA(p, ν, u, q) process)**.** The Horadam-Pethe ARMA process has the following form:

$$\Phi(B)(1 - 2uB + B^3)^{\nu} X_t = \Theta(B)\epsilon_t, \tag{5.5}$$

where $(1-2uB+B^3)^{-\nu} = \sum_{n=0}^{\infty} Q_{n,3}^{\nu}(u)B^n$, ϵ_t is Gaussian white noise with variance σ^2, $0 \leq u \leq 1$, and $|\nu| < 1/2$. $\Phi(B)$ and $\Theta(B)$ are stationary AR and invertible MA operators defined in (1.2) and (1.3), respectively.

Remark 5.2.2. *Again, in [11], it is proved that the spectral density of the Horadam-Pethe ARMA(p, ν, u, q) process is:*

$$f_x(\omega) = \frac{\sigma^2}{2\pi}\frac{|\Theta(z)|^2}{|\Phi(z)|^2}(2+4u^2-4u(\cos(\omega)+\cos(2\omega))+2\cos(3\omega))^{-\nu},\ z = e^{-\iota\omega}.$$

For the processes' properties and more details, see [11].

The focus of this work is to provide the estimation methods for the discussed models using spectral density. In the next results, we provide the autocorrelation function of the Horadam ARMA(p, ν, u, q) and Horadam-Pethe ARMA(p, ν, u, q) process.

Some notations and preliminaries:

We state some relevant results that will be required in subsequent sections. Using the spectral density of the Horadam ARMA(p, ν, u, q) process defined in (5.4) assuming $\Phi(x) = \prod_{j=1}^{p}(1-\rho_j x)$, where $\rho_1, \rho_2, \ldots, \rho_p$ are complex numbers such that $|\rho_j| < 1$ for $j = 1, 2, \ldots, p$, we can write

$$\frac{|\Theta(z)|^2}{|\Phi(z)|^2} = \sum_{l=-q}^{q}\sum_{j=1}^{p}\psi(l)z^{l+p}\zeta_j\left[\frac{\rho_j^{2p}}{1-\rho_j e^{\iota\omega}} - \frac{1}{1-\rho^{-1}e^{\iota\omega}}\right], \tag{5.6}$$

where

$$\psi(l) = \sum_{s=\min[0,l]}^{\max[q,q+l]}\theta_s\theta_{s-l}$$

and

$$\zeta_j = \frac{\sigma^2}{2\pi}\left[\rho_j\prod_{i=1}^{p}(1-\rho_i\rho_j)\prod(\rho_j-\rho_m)\right]^{-1}.$$

For more details, one can refer to [76]. We will also require the following integral formula (see [51]):

$$\int_0^{\pi}\cos^l\omega\cos(k\omega)d\omega = \left[1+(-1)^{k+l}\right]\int_0^{\frac{\pi}{2}}\cos^l\omega\cos(k\omega)d\omega =$$

$$= [1 + (-1)^{k+l}] \begin{cases} s\frac{l!}{(k-l)(k-l+2)\ldots(k+l)}, & \text{for } l < k, \\ \frac{\pi}{2^{l+1}}\binom{l}{y}, & \text{for } k \leq l \text{ and } l-k = 2y, \\ \frac{l!}{(2y+1)!!(2k+2y+1)!!}, & \text{for } k < l \text{ and } l-k = 2y+1, \end{cases} \tag{5.7}$$

$$\text{where } s = \begin{cases} 0, & \text{for } k-l = 2y, \\ 1, & \text{for } k-l = 4y+1, \\ -1, & \text{for } k-l = 4y-1. \end{cases}$$

Also,

$$n!! = \begin{cases} n(n-2)\cdots 5\cdot 3\cdot 1, & \text{if } n > 0, \text{ odd}, \\ n(n-2)\cdots 6\cdot 4\cdot 2, & \text{if } n > 0, \text{ even}, \\ 1, & \text{if } n = 0, -1. \end{cases}$$

Theorem 5.2.1. *For the Horadam ARMA(p, ν, u, q) process, the autocovariance function is given by:*

$$\gamma(h) = \sum_{l=-q}^{q}\sum_{j=1}^{p}\psi(l)\zeta_j\left[\rho^{2p}\sum_{m=0}^{\infty}\rho^m\gamma_w(h-m)d\omega + \sum_{n=1}^{\infty}\rho^n\gamma_w(h+n)\right],$$

where

$$\gamma_w(k) = \frac{\sigma^2}{2\pi}\sum_{n=0}^{\infty}\frac{(\nu)_n}{n!}\frac{(2-4u)^n}{(2+4u^2-4u)^{n+\nu}}\int_{-\pi}^{\pi}\cos(k\omega)\cos^n(\omega)d\omega$$

and the integral $\int_{-\pi}^{\pi}\cos(k\omega)\cos^n(\omega)d\omega$ is defined in (5.7).

Proof. Using (5.4) and (5.6), the spectral density of Horadam ARMA process takes the following form:

$$f_x(\omega) = \frac{\sigma^2}{2\pi}\sum_{l=-q}^{q}\sum_{j=1}^{p}\psi(l)z^{p+l}\zeta_j\left[\frac{\rho_j^{2p}}{1-\rho_j e^{\iota\omega}} - \frac{1}{1-\rho_j^{-1}e^{\iota\omega}}\right] \tag{5.8}$$

$$\times (2 + 4u^2 - 4u - 4u\cos(\omega) + 2\cos(\omega))^{-\nu}. \tag{5.9}$$

The autocovariance function, denoted as $\gamma(h)$, of a stochastic process X_t can be computed by performing the inverse Fourier transform of its spectral density $f_x(\omega)$ using the following relationship:

$$\gamma(h) = \int_{-\pi}^{\pi} f_x(\omega)e^{\iota\omega h}d\omega.$$

Using the spectral density defined in (5.8), the $\gamma(h)$ can be calculated as:

$$\gamma(h) = \frac{\sigma^2}{2\pi}\int_{-\pi}^{\pi}\left[\sum_{l=-q}^{q}\sum_{j=1}^{p}\psi(l)z^{p+l}\zeta_j\left[\frac{\rho_j^{2p}}{1-\rho_j e^{\iota\omega}} - \frac{1}{1-\rho_j^{-1}e^{\iota\omega}}\right] \times (2+4u^2-4u-4u\cos(\omega)+2\cos(\omega))^{-\nu}\right]e^{\iota\omega h}d\omega.$$

Alternatively, we can write

$$\gamma(h) = \frac{\sigma^2}{2\pi}\int_{-\pi}^{\pi}\left[\sum_{l=-q}^{q}\sum_{j=1}^{p}\psi(l)\zeta_j z^{p+l}\left(\rho^{2p}\sum_{m=0}^{\infty}(\rho e^{-\iota\omega})^m + \sum_{n=1}^{\infty}(\rho e^{\iota\omega})^n\right) \times (2+4u^2-4u-4u\cos(\omega)+2\cos(\omega))^{-\nu}\right]e^{\iota\omega h}.$$

Now, let us assume the process $W_t = (1-2uB+B)^{-\nu}\epsilon_t$. Then, the spectral density of the process W_t is

$$f_w(\omega) = \frac{\sigma^2}{2\pi}(2+4u^2-4u-4u\cos(\omega)+2\cos(\omega))^{-\nu}. \tag{5.10}$$

Then, $\gamma(h)$ takes the following form:

$$\begin{aligned}\gamma(h) &= \frac{\sigma^2}{2\pi}\sum_{l=-q}^{q}\sum_{j=1}^{p}\psi(l)\zeta_j\frac{2\pi}{\sigma^2}\left[\rho^{2p}\sum_{m=0}^{\infty}\rho^m\int_{-\pi}^{\pi}f_w(\omega)e^{\iota\omega(h-m)}d\omega + \sum_{n=1}^{\infty}\rho^n\int_{-\pi}^{\pi}f_w(\omega)e^{\iota\omega(h+n)}d\omega\right] \\ &= \sum_{l=-q}^{q}\sum_{j=1}^{p}\psi(l)\zeta_j\left[\rho^{2p}\sum_{m=0}^{\infty}\rho^m\gamma_w(h-m)d\omega + \sum_{n=1}^{\infty}\rho^n\gamma_w(h+n)\right]. \end{aligned}\tag{5.11}$$

In the above equation, we can calculate $\gamma_w(h-m)$ and $\gamma_w(h+n)$ by taking the inverse Fourier transform of the spectral density of the process W_t as follows:

$$\gamma_w(k) = \int_{-\pi}^{\pi}\cos(k\omega)f_w(\omega)d\omega = \frac{\sigma^2}{2\pi}\int_{-\pi}^{\pi}\cos(k\omega)(2+4u^2-4u-4u\cos(\omega)+2\cos(\omega))^{-\nu}d\omega. \tag{5.12}$$

We can write $(2+4u^2-4u-4u\cos(\omega)+2\cos(\omega))^{-\nu} = (a+b\cos(\omega))^{-\nu}$, where $a = (2+4u^2-4u)$ and $b = (2-4u)$. Now, above integration takes the following form:

$$\begin{aligned}\gamma_w(k) &= \frac{\sigma^2}{2\pi}\int_{-\pi}^{\pi}\cos(k\omega)(a+b\cos(\omega))^{-\nu}d\omega \\ &= \frac{\sigma^2 a^{-\nu}}{2\pi}\int_{-\pi}^{\pi}\cos(k\omega)(1+b/a\cos(\omega))^{-\nu}d\omega\end{aligned}$$

$$= \frac{\sigma^2 a^{-\nu}}{2\pi} \sum_{n=0}^{\infty} \frac{(\nu)_n}{n!} \frac{(2-4u)^n}{(2+4u^2-4u)^n} \int_{-\pi}^{\pi} \cos(k\omega) \cos^n(\omega) d\omega.$$

Substitute the value of $\gamma_w(k)$, for $k = h - m$ and $k = h + n$ in (5.11) and using the integral defined in (5.7), the desired result is obtained. □

Theorem 5.2.2. *The autocovariance function for the particular cases of type 2 HARMA process is discussed as follows:*
(a) The autocovariance function for Horadam ARMA$(0, \nu, u, 0)$ *process is given by:*

$$\gamma_w(k) = \frac{\sigma^2}{2\pi} \sum_{n=0}^{\infty} Q^{\nu}_{n,1}(u) Q^{\nu}_{n+k,1}(u),$$

where $Q^{\nu}_{n,1}(u)$ *is defined in* (5.1) *with* $m = 1$.
(b) The autocovariance function for Horadam-Pethe ARMA$(0, \nu, u, 0)$ *process is given by:*

$$\gamma_w(k) = \frac{\sigma^2}{2\pi} \sum_{n=0}^{\infty} Q^{\nu}_{n,3}(u) Q^{\nu}_{n+k,3}(u),$$

where $Q^{\nu}_{n,3}(u)$ *is defined in* (5.1) *with* $m = 3$.

Proof. (a): The Horadam ARMA $(0, \nu, u, 0)$ process is defined as follows:

$$W_t = (1 - 2uB + B)^{-\nu} \epsilon_t. \tag{5.13}$$

Rewrite (5.13) as follows:

$$X_t = \Psi(B)\epsilon_t, \text{ where } \Psi(B) = (1 - 2uB + B)^{-\nu}.$$

Then, using the definition of spectral density of linear process, we have:

$$f_w(\omega) = \frac{\sigma^2}{2\pi} |(1 - 2ue^{-\iota\omega} + e^{-\iota\omega})|^{-2\nu}.$$

For the process W_t, the autocovariance function $\gamma_w(k)$ can be computed by taking the inverse Fourier transform of spectral density as follows:

$$\begin{aligned}
\gamma_w(k) &= \int_{-\pi}^{\pi} \cos(k\omega) f_w(\omega) d\omega \\
&= \frac{\sigma^2}{2\pi} \int_{-\pi}^{\pi} \cos(k\omega) |(1 - 2ue^{-\iota\omega} + e^{-\iota\omega})|^{-2\nu} d\omega \\
&= \frac{\sigma^2}{2\pi} \int_{-\pi}^{\pi} \cos(k\omega) \left| \sum_{n=0}^{\infty} Q^{\nu}_{n,1}(u) (e^{-\iota\omega})^n \right|^2 d\omega.
\end{aligned}$$

Let $Q^{\nu}_{n,1}(u) = a_n$, then

$$\left|\sum_{n=0}^{\infty} Q^{\nu}_{n,1}(u)(e^{-\iota\omega})^n\right|^2 = \sum_{n=0}^{\infty} a_n^2 e^{-2n\lambda} + 2\sum_{r=1}^{\infty}\sum_{n=0}^{\infty} a_n a_{n+r}\cos(\omega r).$$

Using the above relation, we can show

$$\begin{aligned}\gamma_w(k) &= \frac{\sigma^2}{\pi}\int_{-\pi}^{\pi}\cos(k\omega)\sum_{r=1}^{\infty}\sum_{n=0}^{\infty} a_n a_{n+r}\cos(\omega r)d\omega \\ &= \frac{\sigma^2}{\pi}\sum_{r=1}^{\infty}\sum_{n=0}^{\infty} a_n a_{n+r}\int_{-\pi}^{\pi}\cos(k\omega)\cos(\omega r)d\omega = \sigma^2\sum_{n=0}^{\infty} Q_{n,1}Q_{(n+k),1}. \qquad (5.14)\end{aligned}$$

(b) The Horadam-Pethe ARMA $(0, \nu, u, 0)$ process is defined as follows:

$$W_t = (1 - 2uB + B^3)^{-\nu}\epsilon_t. \qquad (5.15)$$

Similar to case (a), rewrite (5.15) as follows:

$$X_t = \Psi(B)\epsilon_t,$$

where $\Psi(B) = (1 - 2uB + B^3)^{-\nu}$ and we have spectral density as follows:

$$f_w(\omega) = \frac{\sigma^2}{2\pi}|(1 - 2ue^{-\iota\omega} + e^{-3\iota\omega})|^{-2\nu}.$$

Similar to the above case for the process W_t, we can compute the autocovariance function $\gamma_w(k)$, which comes out to be

$$\begin{aligned}\gamma_w(k) &= \frac{\sigma^2}{2\pi}\int_{-\pi}^{\pi}\cos(k\omega)\left|\sum_{n=0}^{\infty} Q^{\nu}_{n,3}(u)(e^{-3\iota\omega})^n\right|^2 d\omega \\ &= \sum_{n=0}^{\infty}(Q^{\nu}_{n,3}(u))^2(Q^{\nu}_{n+r,3}(u))^2 e^{-2n\lambda}\int_{-\pi}^{\pi}\cos(k\omega)\cos(\omega r)d\omega = \sigma^2\sum_{n=0}^{\infty} Q_{n,3}Q_{(n+k),3}.\end{aligned}$$

□

Theorem 5.2.3. *For Horadam ARMA$(0, \nu, u, 0)$ process with $|\nu| < 1/2$ and $0 < u < 1$, $\sum_{k=0}^{\infty}|\gamma_w(k)| < \infty$.*

Proof. For Horadam polynomials, using the relation $Q^{\nu}_n(u) = \dfrac{(\nu)_n(2u-1)^n}{n!}$, we obtain:

$$\gamma_w(k) = \sigma^2\sum_{n=0}^{\infty} Q^{\nu}_n(u)Q^{\nu}_{n+k}(u)$$

$$
\begin{aligned}
&= \sigma^2 \sum_{n=0}^{\infty} \frac{(\nu)_n (2u-1)^n}{n!} \frac{(\nu)_{n+k} (2u-1)^{(n+k)}}{(n+k)!} \\
&= \sigma^2 \sum_{n=0}^{\infty} \frac{\Gamma(\nu+n)(2u-1)^n}{\Gamma(\nu)\Gamma(n+1)} \frac{\Gamma(\nu+n+h)(2u-1)^{(n+k)}}{\Gamma(\nu)\Gamma(n+k+1)} \\
&= \sigma^2 \sum_{n=0}^{\infty} \frac{\Gamma(\nu+n)}{\Gamma(\nu)\Gamma(n+1)} \frac{\Gamma(\nu+n+k)(2u-1)^{(2n+k)}}{\Gamma(\nu)\Gamma(n+k+1)}.
\end{aligned}
$$

For large n, $\frac{\Gamma(\nu+n)}{\Gamma(\nu)\Gamma(n+1)} \sim n^{\nu-1}$ and $\frac{\Gamma(\nu+n+k)}{\Gamma(\nu)\Gamma(n+k+1)} \sim (n+k)^{\nu-1}$. Thus,

$$
\sum_{h=0}^{\infty} |\gamma_w(k)| \sim \sigma^2 \sum_{n=0}^{\infty} |n^{\nu-1}(n+k)^{\nu-1}||(2u-1)^{(2n+k)}|. \tag{5.16}
$$

We consider the following cases:

$$
|n^{\nu-1}(n+k)^{\nu-1}||(2u-1)^{(2n+k)}| \sim \begin{cases} \sum_{n=0}^{\infty} |n^{2\nu-2}||(2u-1)^{2n}| & \text{if } n \to \infty \text{ and } k \text{ is finite,} \\ \sum_{k=0}^{\infty} |C_1 k^{\nu-1}||(2u-1)^{k}| & \text{if } k \to \infty \text{ and } n \text{ is finite,} \\ \sum_{n=0}^{\infty} |C_2 n^{2\nu-2}||(2u-1)^{3n}| & \text{if } k \to \infty \text{ and } n \to \infty. \end{cases}
$$

From all the cases, we get $\sum_{k=0}^{\infty} |\gamma(k)| < \infty$, for $0 < u < 1$. □

Theorem 5.2.4. *For the Horadam-Pethe ARMA(p, ν, u, q) process, the autocovariance function is given by:*

$$
\gamma(h) = \sum_{l=-q}^{q} \sum_{j=1}^{p} \psi(l)\zeta_j \left[\rho^{2p} \sum_{m=0}^{\infty} \rho^m \gamma_w(h-m) d\omega + \sum_{n=1}^{\infty} \rho^n \gamma_w(h+n) \right],
$$

where $\gamma_w(k) = \frac{\sigma^2}{2\pi} \sum_{n=0}^{\infty} \sum_{r=0}^{n} \sum_{s=0}^{r} C \frac{(\nu)_n}{n!} \binom{n}{r} \binom{r}{s} \int_{-\pi}^{\pi} \cos(k\omega) \cos(\omega)^{n+r+s} d\omega$ *and constant* $C = \frac{8^r (4u+6)^{n-r} (u)^{r-k}}{(4u^2+4u+2)^n}$.

Proof. Using (5.5) and (5.6), the spectral density of Horadam-Pethe ARMA process X_t takes the following form:

$$
\begin{aligned}
f_x(\omega) = \frac{\sigma^2}{2\pi} \sum_{l=-q}^{q} \sum_{j=1}^{p} \psi(l) z^{p+l} \zeta_j \left[\frac{\rho_j^{2p}}{1-\rho_j e^{\iota\omega}} - \frac{1}{1-\rho^{-1} e^{\iota\omega}} \right] \\
\times (2 + 4u^2 - 4u(\cos(\omega) + \cos(2\omega)) + 2\cos(3\omega))^{-\nu}.
\end{aligned}
$$

The autocovariance of the process is computed using the inverse Fourier transform

of the spectral density as follows:

$$\begin{aligned}\gamma(h) &= \int_{-\pi}^{\pi} f_x(\omega)e^{\iota\omega h}d\omega \\ &= \frac{\sigma^2}{2\pi}\int_{-\pi}^{\pi}\left[\sum_{l=-q}^{q}\sum_{j=1}^{p}\psi(l)z^{p+l}\zeta_j\left(\rho^{2p}\sum_{m=0}^{\infty}(\rho e^{-\iota\omega})^m+\sum_{n=1}^{\infty}(\rho e^{\iota\omega})^n\right)(2+4u^2-4u(\cos(\omega)\right. \\ &\quad \left.+\cos(2\omega))+2\cos 3\omega)^{-\nu}\right]e^{\iota\omega h}d\omega \\ &= \frac{\sigma^2}{2\pi}\sum_{l=-q}^{q}\sum_{j=1}^{p}\psi(l)\zeta_j\left[\rho^{2p}\sum_{m=0}^{\infty}\rho^m\int_{-\pi}^{\pi}e^{\iota\omega(h-m)}(2+4u^2-4u(\cos(\omega)+\cos(2\omega))\right. \\ &\quad \left.+2\cos(3\omega))^{-\nu}d\omega+\sum_{n=1}^{\infty}\rho^n\int_{-\pi}^{\pi}e^{\iota\omega(n+h)}(2+4u^2-4u(\cos(\omega)+\cos(2\omega))+2\cos(3\omega))^{-\nu}d\omega\right].\end{aligned}$$

Assume the process, $W_t = (1-2uB+B^3)^{-\nu}\varepsilon_t$. Then, the spectral density of W_t will be

$$f_w(\omega) = \frac{\sigma^2}{2\pi}(2+4u^2-4u(\cos(\omega)+\cos(2\omega))+2\cos 3\omega)^{-\nu}.$$

We compute the autocovariance of W_t as follows:

$$\begin{aligned}\gamma_w(k) &= \int_{-\pi}^{\pi}\frac{\sigma^2}{2\pi}\cos(k\omega)(2+4u^2-4u(\cos(\omega)+\cos(2\omega))+2\cos 3\omega)^{-\nu}d\omega \\ &= \frac{\sigma^2}{2\pi}\int_{-\pi}^{\pi}\cos(k\omega)(a+b\cos(\omega)+c\cos^2(\omega)+8\cos^3(\omega))^{-\nu}d\omega,\end{aligned}$$

where $a=(2+4u+4u^2), b=(-6-4u),$ and $c=-8u$. Now, we write the above equation as follows:

$$\gamma_w(k) = \frac{\sigma^2}{2\pi}\int_{-\pi}^{\pi}\cos(k\omega)a^{-\nu}(1+b_1\cos(\omega)+b_2\cos^2(\omega)+b_3\cos^3(\omega))^{-\nu}\,d\omega,$$

where $b_1 = b/a$, $b_2 = c/a$, and $b_3 = 8/a$. Since, $|(b_1\cos(\omega)+b_2\cos^2(\omega)+b_3\cos^3(\omega))|<1$, we use the binomial expansion and obtain:

$$=\frac{\sigma^2}{2\pi}\sum_{n=0}^{\infty}\sum_{r=0}^{n}\sum_{s=0}^{r}(-1)^n(b_1)^{n-r}(b_2^{r-s})(b_3)^s\frac{(\nu)_n}{n!}\binom{n}{r}\binom{r}{s}\int_{-\pi}^{\pi}\cos(k\omega)\cos(w)^{n+r+s}d\omega.$$

Now, $\gamma(h)$ can be written as:

$$\begin{aligned}\gamma(h) &= \sum_{l=-q}^{q}\sum_{j=1}^{p}\psi(l)\zeta_j\left[\rho^{2p}\sum_{m=0}^{\infty}\rho^m\int_{-\pi}^{\pi}f_w(\omega)e^{\iota\omega(h-m)}d\omega+\sum_{n=1}^{\infty}\rho^n\int_{-\pi}^{\pi}f_w(\omega)e^{\iota\omega(h+n)}d\omega\right] \\ &= \sum_{l=-q}^{q}\sum_{j=1}^{p}\psi(l)\zeta_j\left[\rho^{2p}\sum_{m=0}^{\infty}\rho^m\gamma_w(h-m)+\sum_{n=1}^{\infty}\rho^n\gamma_w(h+n)\right],\end{aligned}$$

where $\gamma_w(k) = \frac{\sigma^2}{2\pi}\sum_{n=0}^{\infty}\sum_{r=0}^{n}\sum_{s=0}^{r} C\frac{(\nu)_n}{n!}\binom{n}{r}\binom{r}{s}\int_{-\pi}^{\pi}\cos(k\omega)\cos(\omega)^{n+r+s}d\omega$ and constant

$$C = \frac{(-1)^{n-s}8^r(4u+6)^{n-r}(u)^{r-s}}{(4u^2+4u+2)^n}.$$

Substitute the value of $\gamma_w(k)$, for $k = h-m$ and $k = h+n$ in the above equation and use the integral defined in (5.7) to get the desired result. □

Theorem 5.2.5. *For the Horadam and Horadam-Pethe ARMA(p,ν,u,q) process, the equivalent AR(∞) has the form:*

(a) For Horadam ARMA(p,ν,u,q), $\epsilon_t = \sum_{s=0}^{\infty} a_s X_{t-s}$, where $a_s = \sum_{m=0}^{s}\psi_{s-m}\beta_m$ and

$$\beta_m = \sum_{k=0}^{m}\frac{\Gamma(-\nu+m)}{\Gamma(-\nu)\Gamma(m+1)}(-1)^k\binom{m}{k}(2u)^{m-k}.$$

(b) For Horadam-Pethe ARMA(p,ν,u,q), $\epsilon_t = \sum_{s=0}^{\infty} a_s X_{t-s}$, where $a_s = \sum_{m=0}^{s}\psi_{s-m}\zeta_m$ and

$$\zeta_m = \frac{\Gamma(-\nu+m)(2u)^m}{\Gamma(-\nu)\Gamma(m+1)} - \frac{\Gamma(-\nu+m-2)(2u)^{m-3}}{\Gamma(-\nu)\Gamma(m-1)}.$$

Proof. (a): We rewrite the Horadam ARMA(p,ν,u,q) defined in (5.3) as:

$$\begin{aligned}
\epsilon_t &= \frac{\Phi(z)}{\Theta(z)}(1-2uB+B)^{\nu}X_t \\
&= \frac{\Phi(z)}{\Theta(z)}(1-(2uB-B))^{\nu}X_t \\
&= \frac{\Phi(z)}{\Theta(z)}(1-B(2u-1))^{\nu}X_t \\
&= \Big(\sum_{m=0}^{\infty}\psi_m B^m\Big)\sum_{j=0}^{\infty}\frac{\Gamma(-\nu+j)}{\Gamma(-\nu)\Gamma(j+1)}B^j(2u-1)^jX_t \\
&= \Big(\sum_{m=0}^{\infty}\psi_m B^m\Big)\sum_{j=0}^{\infty}\frac{\Gamma(-\nu+j)}{\Gamma(-\nu)\Gamma(j+1)}\sum_{k=0}^{j}(-1)^k\binom{j}{k}(2u)^{j-k}X_{t-j}.
\end{aligned}$$

We get, $\epsilon_t = \sum_{s=0}^{\infty} a_s X_{t-s}$, where $a_s = \sum_{m=0}^{s}\psi_{s-m}\beta_m$ and

$$\beta_m = \sum_{k=0}^{m}\frac{\Gamma(-\nu+m)}{\Gamma(-\nu)\Gamma(m+1)}(-1)^k\binom{m}{k}(2u)^{m-k}.$$

We also need to show that $\sum_{s=0}^{\infty}|a_s| < \infty$, where $a_s = \sum_{m=0}^{s}\psi_{s-m}\beta_m$. We rewrite above as:

$$\epsilon_t = \Big(\sum_{m=0}^{\infty}\psi_m B^m\Big)\sum_{j=0}^{\infty}\frac{\Gamma(-\nu+j)}{\Gamma(-\nu)\Gamma(j+1)}(2u-1)^j B^j X_t \tag{5.17}$$

$$= \Big(\sum_{m=0}^{\infty}\psi_m B^m\Big)\Big(\sum_{m=0}^{\infty}\rho_m B^m\Big)X_t, \tag{5.18}$$

where $\rho_m = \sum_{m=0}^{\infty}\frac{\Gamma(-\nu+m)}{\Gamma(-\nu)\Gamma(m+1)}(2u-1)^m$.

The operators $\Theta(B)$ and $\Phi(B)$ can be characterized as stationary autoregressive and invertible moving average operators, respectively. The corresponding polynomial representations $\frac{\Theta(z)}{\Phi(z)} = \sum_{j=0}^{\infty}\psi_j z^j$, where the series $\sum_{j=0}^{\infty}|\psi_j| < \infty$, for $|z| \leq 1+\epsilon$. We deduce that the absolute values of the coefficients ψ_j decrease exponentially with increasing j, bounded by the inequality $|\psi_j| < C(1+\epsilon)^{-j}$, where C represents a constant. Also, in (5.17) using Stirling's approximation for large m, ρ_m is approximated as follows:

$$\frac{\Gamma(-\nu+m)}{\Gamma(-\nu)\Gamma(m+1)}(2u-1)^m \sim (m)^{-(\nu+1)}(2u-1)^m,$$

which indicates that $\sum_{m=0}^{\infty}|\rho_m| < \infty$, for $0 < u < 1$ and $\nu > 0$. Further,

$$\sum_{s=0}^{\infty}|a_s| \leq \sum_{s=0}^{\infty}\sum_{m=0}^{s}|\psi_{s-m}\rho_m|$$

$$\leq \sum_{m=0}^{\infty}\sum_{m=s}^{\infty}|\psi_{s-m}||\rho_m| = \sum_{m=0}^{\infty}\sum_{r=0}^{\infty}|\psi_r||\rho_m|.$$

Since, we have proved that $\sum_{m=0}^{\infty}|\rho_m|$ is finite, we get $\sum_{s=0}^{\infty}|a_s| < \infty$.

(b): We rewrite the Horadam-Pethe ARMA(p,ν,u,q) defined in (5.5) as:

$$\epsilon_t = \frac{\Phi(z)}{\Theta(z)}(1-2uB+B^3)^\nu X_t \ = (1-B(2u-B^2))^\nu X_t$$

$$= \frac{\Phi(z)}{\Theta(z)}\sum_{j=0}^{\infty}\frac{\Gamma(j-\nu)}{\Gamma(-\nu)\Gamma(j+1)}(2u-B^2)^j B^j X_t$$

$$= \Big(\sum_{m=0}^{\infty}\psi_m B^m\Big)\sum_{j=0}^{\infty}\frac{\Gamma(j-\nu)}{\Gamma(-\nu)\Gamma(j+1)}\sum_{k=0}^{j}(-1)^k\binom{j}{k}(2u)^{j-k}X_{t-j-2k}.$$

The above series can be written as:

$$\epsilon_t = \Big(\sum_{m=0}^{\infty} \psi_m B^m\Big)\Big(\sum_{i=0}^{\infty} \zeta_i B^i\Big) X_t, \text{ where } \zeta_i = \frac{\Gamma(-\nu+i)(2u)^i}{\Gamma(-\nu)\Gamma(i+1)} - \frac{\Gamma(-\nu+i-2)(2u)^{i-3}}{\Gamma(-\nu)\Gamma(i-1)}.$$

Again we write, $\epsilon_t = \sum_{s=0}^{\infty} a_s X_{t-s}$, where $a_s = \sum_{m=0}^{s} \psi_{s-m}\zeta_m$. The proof of $\sum_{s=0}^{\infty} |a_s| < \infty$ is similar as done above.

□

Theorem 5.2.6. *For Horadam ARMA$(0, \nu, u, 0)$ process $\{X_t\}$, let $\bar{X}_n = \frac{1}{n}\sum_{t=1}^{n} X_t$. Then, for $|u| < 1$ the* $\mathrm{Var}(\bar{X}_n)$ *is given as follows:*

$$\mathrm{Var}(\bar{X}_n) = \sum_{r=0}^{\infty}(-1)^r \frac{(\nu)_r \sigma^2 q^r}{\pi p^{r+\nu} n^2 r!}\left[\frac{r\pi(2n)!}{2^{2n}(n!)^2(2r-1)} + \frac{(r^2-n^2)\,(-1)^n \pi}{r(1+2r)(1-2r)2^{2r}\mathcal{B}(1+n+r, 1-n+r)}\right].$$

Proof. The spectral density of Horadam ARMA$(0, \nu, u, 0)$ can be written using (5.10) as:

$$f(\omega) = \frac{\sigma^2}{2\pi}(a + b\cos(\omega))^{-\nu},$$

where $a = (2 + 4u^2 - 4u)$ and $b = (2 - 4u)$. Using (3.4c) in [3], we get

$$\begin{aligned}
\mathrm{E}\left[\bar{X}_n^2\right] &= \int_{-\pi}^{\pi} \left|\frac{1}{n}\sum_{t=1}^{n} e^{it\omega}\right|^2 f(\omega)d\omega \\
&= \frac{\sigma^2}{2\pi}\int_{-\pi}^{\pi} \frac{\sin^2(n\omega/2)}{n^2\left(\sin^2(\omega/2)\right)}(a + b\cos(\omega))^{-\nu} d\omega \\
&= \frac{\sigma^2}{2\pi}\int_{-\pi}^{\pi} \frac{\sin^2\left(\frac{n\omega}{2}\right)}{n^2\sin^2\left(\frac{\omega}{2}\right)}\left(c + d\sin^2(\omega/2)\right)^{-\nu} d\omega \text{ where } c = a + b \text{ and } d = -2b \\
&= \frac{\sigma^2 c^{-\nu}}{2\pi n^2}\int_{-\pi}^{\pi} \frac{\sin^2\left(\frac{n\omega}{2}\right)}{\sin^2\left(\frac{\omega}{2}\right)} \sum_{r=0}^{\infty}(-1)^r \frac{(\nu)_r}{r!}\left(\frac{d}{c}\sin^2(\omega/2)\right)^r d\omega \\
&= \sum_{r=0}^{\infty}(-1)^r \frac{(\nu)_r \sigma^2 d^r}{\pi c^{r+\nu} n^2 r!}\int_0^{\pi} \sin^2(nx)\sin^{-2+2r}(x)dx.
\end{aligned}$$

The integral of $\int_0^{\pi} \sin^2(nx)\sin^{-2+2r}(x)dx$ can be calculated using Theorem 6.6

defined in [4] which is given as follows:

$$\int_0^{\pi} \sin^2(nx)\sin^{-2-a}(x)dx = \frac{1}{2}(1+a)^{-1}a\int \sin^{-a}xdx - \frac{1}{2}(1+a)^{-1}a\int \sin^{-a}x\cos 2nxdx$$
$$-(1+a)^{-1}\cos x\sin^{-1-a}x\sin^2 nx + (1+a)^{-1}nK_n(a),$$

where taking $a=-2r$, we have:

$$K_n(-2r) = \frac{(-1)^n\pi n}{(-1-2r)2^{2r}(2r)\mathcal{B}(1+n+r,1-n+r)},$$

$$\int_0^{\pi}\sin^{2r}(x)dx = \frac{\pi}{2^{2n}}\frac{(2n)!}{(n!)^2},$$

and

$$\int_0^{\pi}\sin^{2r}(x)\cos(2nx)dx = \frac{(-1)^n\pi}{2^{2r}(1+2r)\mathcal{B}(1+n+r,1-n+r)}.$$

The integral is given as follows:

$$\int_0^{\pi}\sin^2(nx)\sin^{-2+2r}(x)dx = \frac{r\pi(2n)!}{2^{2n}(n!)^2(2r-1)} + \frac{(r^2-n^2)(-1)^n\pi}{r(1+2r)(1-2r)2^{2r}\mathcal{B}(1+n+r,1-n+r)}.$$

□

Theorem 5.2.7. *For Horadam-Pethe ARMA$(0,\nu,u,0)$ process, let $\bar{X}_n = \frac{1}{n}\sum_{t=1}^{n}X_t$. Then, for $|u|<1$, the $\mathrm{Var}(\bar{X}_n)$ is given as follows:*

$$\mathrm{Var}(\bar{X}_n) = \sum_{r=0}^{\infty}(-1)^r\frac{(\nu)_r\sigma^2q^r}{\pi p^{r+\nu}n^2r!}\left[\frac{r\pi(2n)!}{2^{2n}(n!)^2(2r-1)}\right.$$
$$\left. + \frac{(r^2-n^2)(-1)^n\pi}{r(1+2r)(1-2r)2^{2r}\mathcal{B}(1+n+r,1-n+r)}\right].$$

Proof. Using the same approach defined in Theorem 5.2.6, the following relation is used to establish the result:

$$\mathrm{E}\left[\bar{X}_n^2\right] = \frac{a^{-\nu}\sigma^2}{2\pi n^2}\int_{-\pi}^{\pi}\frac{\sin^2(n\omega/2)}{(\sin^2(\omega/2))}(1+b_1\cos(\omega)+b_2\cos^2(\omega)+b_3\cos^3(\omega))^{-\nu}d\omega$$
$$= \frac{a^{-\nu}\sigma^2}{2\pi n^2}\sum_{k=0}^{\infty}\sum_{r=0}^{k}\int_{-\pi}^{\pi}(-1)^k\frac{\sin^2\left(\frac{n\omega}{2}\right)}{\sin^2\left(\frac{\omega}{2}\right)}\frac{(\nu)_k}{k!}\binom{k}{r}(b_2\cos^2(\omega)+b_3\cos^3(\omega))^r(b_1\cos(\omega))^{k-r}$$
$$= \frac{a^{-\nu}\sigma^2}{2\pi n^2}\sum_{k=0}^{\infty}\sum_{r=0}^{k}\int_{-\pi}^{\pi}(-1)^k\frac{\sin^2\left(\frac{n\omega}{2}\right)}{\sin^2\left(\frac{\omega}{2}\right)}\frac{(\nu)_k}{k!}\binom{k}{r}(b_2\cos^2(\omega))^r(b_1\cos(\omega))^{k-r}$$

$$\times \left(1+\frac{b_3}{b_2}\cos(\omega)\right)^r$$

$$= \frac{a^{-\nu}\sigma^2}{2\pi n^2}\sum_{k=0}^{\infty}\sum_{r=0}^{k}\sum_{s=0}^{r}(-1)^k\frac{(q')^s(\nu)_k}{k!}\binom{k}{r}\binom{r}{s}(p')^{r-s}\int_0^{\pi}\frac{\sin^2(nx)}{\sin^2(x)}\sin^{2s}(x))dx,$$

where $p'=1+\dfrac{b_3}{b_2}$ and $q'=\dfrac{-2b_3}{b_2}$.

The integral of $\int_0^{\pi}\frac{\sin^2(nx)}{\sin^2(x)}\sin^{2s}(x)dx$ is given in Theorem 5.2.6. □

5.3 Parameter Estimation

The minimum contrast Whittle likelihood approach:
In this section, we discuss the estimation methods based on the contrast function defined by Whittle [94]. For Horadam ARMA(p,ν,u,q) and Horadam-Pethe ARMA(p,ν,u,q) processes, the estimation based on the minimum contrast Whittle likelihood is discussed by Sabzikar et al. [77], where they use the true spectral density $f_x(\omega)$ and empirical spectral density $I(\omega)$ to construct the contrast function $D(f_x(\omega),I(\omega))$. This function acts as a measure of dissimilarity or proximity between the true and empirical spectral densities. Let us recall the empirical spectral density of the process from Chapter 1, which is given as follows:

$$I(\omega_j)=\frac{1}{2\pi}\left\{R(0)+\sum_{s=1}^{n-1}R(s)\cos(s\omega_j)\right\},$$

where $R(s)=\frac{1}{n}\sum_{i=1}^{n-s}(X_i-\bar{X})(X_{i+s}-\bar{X})$, $s=0,1,\ldots,(n-1)$ is the sample autocovariance function with sample mean $\bar{X}$, and $\omega_j=2\pi j/n$, $j=0,1,\ldots,\lfloor n/2\rfloor$. Let us assume $\Omega=\{\nu,\ u:|\nu|<1/2,\ 0\le u\le 1\}$, and $\Omega_0\subset\Omega$ is a compact set, then the criteria to measure the nearness of $f_x(\omega)$ and $I(\omega)$ is defined in 1.3, which is as follows:

$$D(f_x(\omega),I(\omega))=\int_{-\pi}^{\pi}K(I(\omega)/f_x(\omega))\,d\omega.$$

The contrast function defined by Sabzikar et al. [77] has the following representation:

$$l_\omega(\theta)=\frac{1}{2\sigma^2}D(f_x(\omega),I(\omega))+\log\sigma, \tag{5.19}$$

where σ^2 is variance of innovation term and θ=(ν,u) is a vector of true parameters value. The minimum contrast estimator $(\hat{\theta}_n)$, for the process is defined by minimizing the contrast function $l_\omega(\theta)$ as follows:

$$\hat{\theta}=\operatorname{argmin}(l_w(\theta),\theta\in\Omega_0). \tag{5.20}$$

The debiased Whittle likelihood:

We propose to use the debiased Whittle likelihood method, which is an improved computationally efficient method based on spectral density. Recently, the method is introduced by Sykulski et.al [85] with the aim of reducing the bias in the Whittle likelihood method. The Whittle likelihood method introduced by P. Whittle [93] estimates the model parameters by maximizing the following likelihood function defined with parametric spectral density $f_x(\omega)$ and empirical spectral density $I(\omega)$:

$$l_w(\theta) = \text{argmin}\Big(\sum_{\omega}\Big\{\log(f_x(\omega,\theta)) + \frac{I(\omega)}{f_x(\omega,\theta)}\Big\}, \theta \in \Omega_0\Big),$$

where $I(\omega)$ is the periodogram. Recall from Chapter 1, the pseudolikelihood function defined by Sykulski [85] has the following form:

$$l_d(\theta) = \sum_{\omega}\Big\{\log(\bar{f}_n(\omega;\theta)) + \frac{I(\omega)}{\bar{f}_n(\omega;\theta)}\Big\},$$

where

$$\bar{f}_n(\omega;\theta) = \int_{-\pi}^{\pi} f(\omega';\theta)\mathcal{F}_n(\omega-\omega')d\omega'$$

is the expected periodogram, here,

$$\mathcal{F}_n(\omega) \equiv \frac{2\pi n \sin^2(n\omega/2)}{\sin^2(\omega/2)}$$

and $I(\omega)$ is the periodogram. The estimates are obtained by maximizing the function $l_d(\theta)$ as:

$$\hat{\theta}_n = \text{argmax}(l_d(\theta), \theta \in \Omega_0). \tag{5.21}$$

We optimize $l_d(\theta)$ using the numerical scheme and the Simpson integral is used to compute the integral in the pseudo likelihood function. Also, from [85] it is evident that the debiased estimator is computationally efficient and provides consistent estimates. In the next section, we perform an extensive simulation study to assess the methods of estimation for the discussed models.

Theorem 5.3.1. *For Horadam ARMA(p,ν,u,q) and Horadam-Pethe ARMA(p,ν,u,q) process, let us assume $S = \{\nu,\ u : |\nu| < 1/2,\ 0 < u < 1\}$, and $S_0 \subset S$ is a compact set such that the parametric space $\theta = (u,\nu) \in S_0$. Then, the estimator*

$$\hat{\theta} = argmax(l_d(\theta), \theta \in S_0)$$

satisfies $\hat{\theta} \xrightarrow{P} \theta$.

Proof. The consistency of the debiased Whittle likelihood can be proved by using the conditions defined in [85] (see Prop. 1.3.1), which are as follows:

(a) The parameter set $\Theta \in \mathrm{R}^p$ is compact with a non-null interior, and the true length p parameter vector θ lies in the interior of Θ.

(b) For all $\theta \in \Theta$, and $\omega \in [-\pi, \pi]$, the spectral density of the sequence $\{X_t\}$ is bounded below by $f(\omega;\theta) \geq f_{min} > 0$, and bounded above by $f(\omega;\theta) \leq f_{max}$.

(c) If $\theta \neq \tilde{\theta}$, then there is a space of non-zero measure such that for all ω in this space $f(\omega;\theta) \neq f(\omega;\tilde{\theta})$.

(d) The $f(\omega;\theta)$ is continuous in θ and Riemann integrable in ω.

(e) The expected periodogram $\bar{f}_n(\omega : \theta)$, as defined in (θ), has two continuous derivatives in θ which are bounded above in magnitude uniformly for all n, where the first derivative in θ also has $\Theta(n)$ frequencies in Ω ihat are non-zeno.

Here, we have assumed that the parametric space $\theta = (u, \nu) \in S_0$, which is compact and over this parametric space the function is continuous. A continuous function on a compact metric space is bounded, which clearly satisfies Conditions (a) and (b). The continuous function $f(\omega : \theta)$ over the compact parametric space is Riemann integrable. For Condition (c), we assume that $\theta_1 \neq \theta_2$ and let $f(\omega, \theta_1) = f(\omega, \theta_2)$. The spectral density can be written as:

$$\frac{1}{(2 + 4u_1^2 - 4u_1 - 4u_1 \cos\omega + 2\cos\omega)^{\nu_1}} = \frac{1}{(2 + 4u_2^2 - 4u_2 - 4u_2 \cos\omega + 2\cos\omega)^{\nu_2}}.$$

But by the properties of exponents, we get that $\nu_1 = \nu_2$, which is a contradiction to our assumption that $\theta_1 \neq \theta_2$. Hence, Condition (c) is proved. Similarly, we can prove these conditions for the Horadam-Pethe ARMA(p, ν, u, q) process also.

□

5.4 Simulation Steps

To rigorously evaluate the performance of our estimation procedure, we executed an extensive and systematic simulation study. Simulation studies provide a controlled environment for testing and benchmarking estimation methods. By generating synthetic data with known properties, we can assess how well our estimation

procedure recovers the true model parameters. We can vary parameters, sample sizes, and other factors to assess the robustness and reliability of our procedure. We can compare the estimated parameters with the known true parameters to ensure that our method produces accurate results. Our primary objective was to model the Horadam and Horadam-Pethe ARMA(p, ν, u, q) processes using simulated data. The simulation process involved the following key steps:

- **Generation of Innovation Data:** Our simulation methodology commenced with the generation of innovation data, where each ϵ_t was drawn from a normal distribution with mean μ and variance σ^2. Specifically, we simulated an error series with a standard normal distribution $N(0, 2)$ using the programming language R.

- **Model Formulation:** To simulate the Horadam ARMA(p, ν, u, q) processes, we employed the relation defined in (5.3). This equation was then reformulated as follows:

$$X_t = \frac{\Theta(B)}{\Phi(B)}(1 - 2uB + B)^{-\nu}\epsilon_t.$$

  Now, using the binomial expansion of $(1 - 2uB + B)^{-\nu}$ and truncating the series up to $4th$ term, the series $\eta_t = (1 - 2uB + B)^{-\nu}\epsilon_t$ is generated and the process takes the following form:

$$X_t = \frac{\Theta(B)}{\Phi(B)}\eta_t.$$

- **ARMA Representation:** The above representation transformed the original problem into an ARMA process with the innovation term η_t. Notably, this ARMA process could be conveniently simulated using the"arima" library in R, making it amenable to further analysis and assessment of our estimation procedure.

Minimum contrast Whittle likelihood estimation results:
By considering distinct sets of initial parameters, we generated different time series. For each case single trajectory is used for estimation. Subsequently, we applied our simulation procedure to create two distinct series for Horadam ARMA process, following the previously described methodology. The outcomes of parameter estimation, employing the minimum contrast Whittle likelihood approach, are summarized in the Table 5.1:
The information in Table 5.1 clearly demonstrates that the estimated parameters closely match the actual values. This observation indicates that our estimation

	Case 1	**Case 2**	**Case 3**
Actual	$u = 0.15, \nu = 0.3$	$u = 0.1, \nu = 0.4$	$u = 0.25, \nu = 0.35$
Estimared	$\hat{u} = 0.16, \hat{\nu} = 0.28$	$\hat{u} = 0.13, \hat{\nu} = 0.37$	$\hat{u} = 0.18, \hat{\nu} = 0.27$

Table 5.1: Actual and estimated parameter values for single trajectory with different choices of parameters based on the minimum contrast Whittle likelihood approach.

technique performs well when applied to synthetic datasets. Also, in our analysis, we delve into the examination of violin plots generated from a dataset comprising 1000 simulations. Violin plots offer a tool that combines elements of both box plots and kernel density estimation (KDE). These plots not only display key summary statistics, such as medians and quartiles (akin to box plots) but also provide a continuous representation of the data's probability density through the incorporation of KDE. However, the true power of the violin plot lies in its "violin" shape, which mirrors a KDE curve on either side of the box plot. This curve represents the probability density of the data across its range, allowing us to visualize not only central tendencies but also the distribution's modes, peaks, and density variations. These simulations are executed using the method described earlier and are based on two distinct sets of parameters for Horadam ARMA process: one with $u = 0.15, \nu = 0.3$ and the other with $u = 0.4, \nu = 0.1$. We construct violin plots to gain insights into the characteristics of this dataset and better understand the behaviour of the system under the specified parameter conditions. For each iteration, 500 observations are generated and recorded, resulting in a substantial dataset. Consequently, wider sections of the violin indicate regions of higher data density, whereas narrower sections represent areas of lower density. Any asymmetry in the violin may also be indicative of skewness in the data distribution. The violin plots corresponding to each parameter combination are given in Fig. 5.1.

Debiased Whittle likelihood results

We consider the same set of simulated data for Horadam ARMA process and apply the debiased Whittle likelihood method to estimate the parameters. The estimated parameters are shown in Table 5.2. Again, we construct the violin plots for two

	Case 1	**Case 2**	**Case 3**
Actual	$u = 0.15, \nu = 0.4$	$u = 0.1, \nu = 0.3$	$u = 0.2, \nu = 0.48$
Estimated	$\hat{u} = 0.16, \hat{\nu} = 0.45$	$\hat{u} = 0.08, \hat{\nu} = 0.25$	$\hat{u} = 0.22, \hat{\nu} = 0.5$

Table 5.2: Actual and estimated parameter values for single trajectory with different choices of parameters based on the debiased Whittle likelihood approach.

different sets of parameter combinations, that is, $u = 0.1$, $\nu = 0.4$ and the other with $u = 0.2$, $\nu = 0.3$. The plots are given in Fig. 5.2, which clearly indicates that

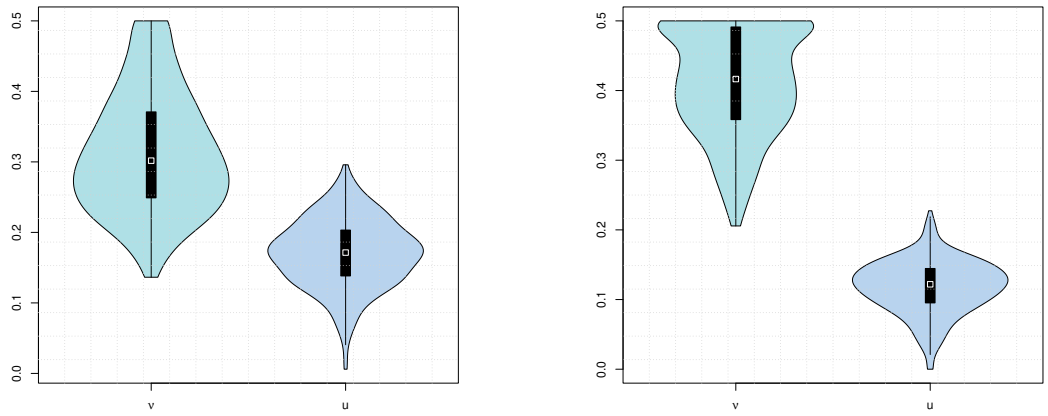

(a) (b)

Figure 5.1: Violin plot of parameters using 500 samples for $\nu = 0.3$, $u = 0.15$ (left panel), and for $\nu = 0.4$, $u = 0.1$ (right panel) based on minimum contrast Whittle likelihood approach.

the debiased Whittle likelihood works well for the simulated dataset.

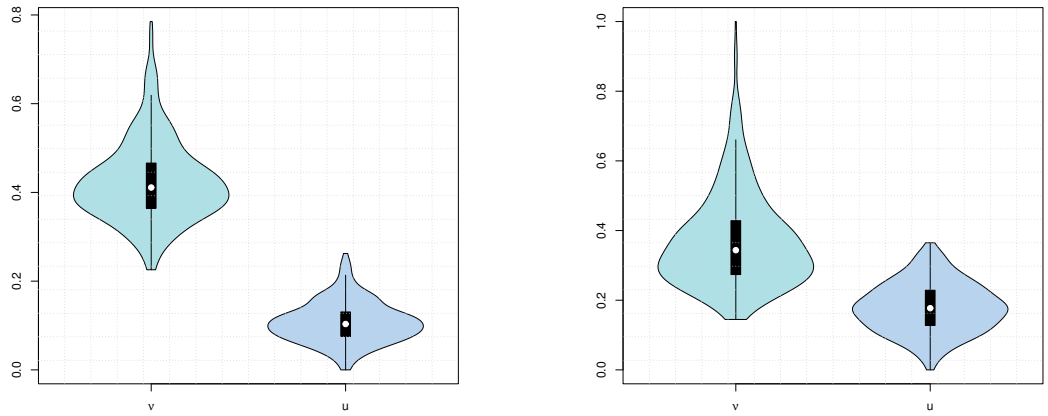

(a) (b)

Figure 5.2: Violin plot of parameters using 500 samples for $\nu = 0.4$, $u = 0.1$ (left panel), and for $\nu = 0.3$, $u = 0.2$ (right panel) based on the debiased Whittle likelihood approach.

Chapter 6

Conclusions and Future Work

The thesis is focused on some generalizations of classical and long memory time series processes. In conclusion, this thesis has navigated through various realms of time series modeling, by introducing generalized models which in some situations can better capture the complexities inherent in real-world data due to the model flexibility. The initial chapters delved into the historical evolution of time series models, starting from the foundational works of Yule, Slutsky, and Wold, paving the way for Box and Jenkins' ARIMA model, which facilitated the modeling of non-stationary data.

The journey continued through the concepts of long memory data and the introduction of fractional differencing by Hosking, expanding our understanding of non-stationary series exhibiting long-range dependence behaviors. Further chapters explored newer extensions in time series models. The introduction of ARTFIMA and tempered processes represented crucial advancements, offering models capable of addressing covariance function summability and spectral density convergence issues, vital for handling datasets previously unmanageable with traditional ARFIMA models. The GARTFIMA and Humbert polynomial based ARMA models were also introduced, focusing on their autocovariance properties and spectral density based parameter estimation techniques, broadening the spectrum of models available for time series analysis. The empirical evaluation showcased the potential of tempered stable autoregressive models in effectively capturing semi heavy-tailed behavior observed in real-world datasets. The novel extensions, such as the tempered fractional ARUMA process and the utilization of the type 2 Humbert polynomials, signify innovative strides towards more flexible, adaptive, and robust time series modeling. Estimation techniques like Whittle likelihood estimation and empirical spectral density comparison have shown promise in accurately estimating parameters, as validated through thorough evaluations with simulated data.

The research presented in this thesis is poised to contribute to various fields reliant on time series analysis, including economics, finance, geophysics, and others. In conclusion, the introduced models and estimation techniques showcased their potential in time series modeling, offering enhanced flexibility, reliability, and applicability to real-world datasets. The contributions made in this thesis lay the foundation for future explorations and advancements in the ever-evolving field of

time series analysis.

However, the introduced models work on the assumption of constant volatility and cannot model heteroscedastic datasets having persistence in the conditional variance of innovation term. There is some work in the literature extending the classical time series processes to the GARCH process to model persistence in data. In the future, we will try to extend the notion of the GARTFIMA, type 1, and type 2 HARMA processes to the GARCH process to capture the volatility in data. We are interested in investigating the application of machine learning techniques for parameter estimations in order to obtain more robust estimates for the generalized processes under discussion. Notably, numerous researchers have delved into this field, and for additional insights, interested individuals can refer to the following articles: [2,61,92]. These sources provide in-depth exploration and analysis of the topic.

References

[1] B. Abraham and N. Balakrishna. Inverse gaussian autoregressive models. *J. Time Series Anal*, 20(6):605–618, 1999.

[2] A. Alexandrov, K. Benidis, M. Bohlke-Schneider, V. Flunkert, J. Gasthaus, T. Januschowski, D. C. Maddix, S. Rangapuram, D. Salinas, J. Schulz, et al. Gluonts: Probabilistic and neural time series modeling in python. *J Mach Learn Res*, 21(1):4629–4634, 2020.

[3] J. Anděl. *Statistische Analyse von Zeitreihen*, volume 1. Akademie-Verlag, 1984.

[4] J. Anděl. Long memory time series models. *Kybernetika*, 22(2):105–123, 1986.

[5] V. Anh, N. N. Leonenko, and L. Sakhno. On a class of minimum contrast estimators for fractional stochastic processes and fields. *J. Statist. Plann. Inference.*, 123(1):161–185, 2004.

[6] V. Anh, N. N. Leonenko, and L. Sakhno. Minimum contrast estimation of random processes based on information of second and third orders. *J. Statist. Plann. Inference.*, 137(4):1302–1331, 2007.

[7] D. Applebaum. *Lévy Processes and Stochastic Calculus*. Cambridge University Press, Cambridge, 2004.

[8] B. Baeumer and M. Meerschaert. Tempered stable lévy motion and transient super-diffusion. *J. Comput. Appl. Math*, 233:2438–2448, 2010.

[9] N. Balakrishna and K. Shiji. Extreme value autoregressive model and its applications. *J. Stat. Theory Pract.*, 8(3):460–481, 2014.

[10] J. Beran. *Statistics for Long-Memory Processes*. Cambridge University Press, Cambridge, 1994.

[11] N. Bhootna, M. S. Dhull, A. Kumar, and N. Leonenko. Humbert generalized fractional differenced arma processes. *Commun. Nonlinear Sci. Numer. Simul.*, 125:107412, 2023.

[12] N. Bhootna and A. Kumar. Tempered stable autoregressive models. *Commun. Stat. - Theory Methods*, 53(2):1–21, 2024.

[13] S. Bisgaard and M. Kulahci. *Time series analysis and forecasting by example*. John Wiley & Sons, 2011.

[14] F. Bliemel. Theil's forecast accuracy coefficient: A clarification. *J. Mark. Res*, 10(4):444-447, 1973.

[15] B. Boashash. *Time-frequency signal analysis and processing: a comprehensive reference*. Academic press, 2015.

[16] G. E. Box, G. M. Jenkins, G. C. Reinsel, and G. M. Ljung. *Time series analysis: forecasting and control*. John Wiley & Sons, 2015.

[17] G. E. P. Box and G. M. Jenkins. *Time series analysis : forecasting and control*. Holden-Day, San Francisco, 1976.

[18] P. J. Brockwell and R. A. Davis. *Time series: theory and methods*. Springer science & business media, 1991.

[19] C.-F. Chung. Estimating a generalized long memory process. *J. Econom*, 73:237–259, 1996.

[20] R. Dahlhaus. Empirical spectral processes and their applications to time series analysis. *Stochastic Process. Appl.*, 30(1):69–83, 1988.

[21] T. Del Barrio Castro and H. Rachinger. Aggregation of seasonal long-memory processes. *Econom. Stat.*, 17:95–106, 2021.

[22] L. Dewald and P. Lewis. A new laplace second-order autoregressive time series model-(nlar(2)). *IEEE Trans. Inf. Theory*, 31:645–51, 1985.

[23] G. Dissanayake, M. Peiris, and T. Proietti. Fractionally differenced gegenbauer processes with long memory: A review. *Statist. Sci.*, 33:413–426, 2018.

[24] R. M. Espejo, N. N. Leonenko, and M. D. Ruiz-Medina. Gegenbauer random fields. *Random Oper. Stochastic Equations*, 22(1):1–16, 2014.

[25] W. Feller. *Introduction to Probability Theory and its Applications*, volume II. John Wiley, New York, 2 edition, 1971.

[26] R. Fox and M. S. Taqqu. Large-sample properties of parameter estimates for strongly dependent stationary gaussian time series. *Ann. Statist.*, 14(2):517–532, 1986.

[27] Z. Fu, G. Liu, and L. Guo. Sequential quadratic programming method for nonlinear least squares estimation and its application. *Math Probl. Eng*, page 1–8, 2019.

[28] T. Gamelin. *Complex analysis*. Springer, New York, 2001.

[29] J. Gao. Modelling long-range-dependent gaussian processes with application in continuous-time financial models. *J. Appl. Probability*, 41(2):467–482, 2004.

[30] J. Gao, V. Anh, C. Heyde, and Q. Tieng. Parameter estimation of stochastic processes with long-range dependence and intermittency. *J. Time Series Anal.*, 22(5):517–535, 2001.

[31] D. Gaver and P. Lewis. First order autoregressive gamma sequences and point processes. *Adv Appl. Probab.*, 12(03):727–745, 1980.

[32] L. Giraitis, J. Hidalgo, and P. Robinson. Gaussian estimation of parametric spectral density with unknown pole. *Ann. Statist*, 29(4):987–1023, 2001.

[33] L. Giraitis, H. L. Koul, and D. Surgailis. *Large sample inference for long memory processes*. World Scientific, 2012.

[34] L. Giraitis and R. Leipus. A generalized fractionally differencing approach in long-memory modeling. *Lith. Math. J.*, 35(1):53–65, 1995.

[35] H. Gould. Inverse series relations and other expansions involving humbert polynomials. *Duke Math. J*, 32(4):697–711, 1965.

[36] M. Grabchak. *Tempered Stable Distributions: Stochastic Models for Multiscale Processes*. Springer, New York, 2016.

[37] J. P. Grainger, A. M. Sykulski, P. Jonathan, and K. Ewans. Estimating the parameters of ocean wave spectra. *Ocean Eng.*, 229:108934, 2021.

[38] H. Gray, N. Zhang, and W. Woodward. On generalized fractional processes. *J. Time Series Anal*, 10:233–257, 1989.

[39] G. Grunwald, R. Hyndman, and L. Tedesco. *A unified view of linear AR(1) models*. D.P. Monash University, Clayton, 1996.

[40] N. Gupta, A. Kumar, and N. Leonenko. Tempered fractional poisson processes and fractional equations with z-transform. *Stochastic Anal. Appl.*, 38(5):939–957, 2020.

[41] E. J. Hannan. The asymptotic theory of linear time-series models. *J. Appl. Probab.*, 10(1):130–145, 1973.

[42] C. C. Heyde and R. Gay. Smoothed periodogram asymptotics and estimation for processes and fields with possible long-range dependence. *Stochastic Processes Appl.*, 45(1):169–182, 1993.

[43] Y. Hong. Hypothesis testing in time series via the empirical characteristic function: A generalized spectral density approach. *J. Am. Stat. Assoc.*, 94(448):1201–1220, 1999.

[44] A. Horadam. Gegenbauer polynomials revisited. *Fibonacci Quart*, 23(4):294–299, 1985.

[45] A. Horadam and S. Pethe. Polynomials associated with gegenbauer polynomials. *Fibonacci Quart*, 19(5):393–398, 1981.

[46] J. Hosking. Fractional differencing. *Biometrika*, 68:165–176, 1981.

[47] Y. Hosoya. The quasi-likelihood approach to statistical inference on multiple time-series with long-range dependence. *J. Econometrics.*, 73(1):217–236, 1996.

[48] P. Humbert. Some extensions of pincherle's polynomials. *Proc. Edinburgh Math. Soc*, 39(1):21–24, 1920.

[49] R. Hunt, S. Peiris, and N. Weber. Estimation methods for stationary gegenbauer processes. *Statist. Papers*, 63(6):1707–1741, 2022.

[50] A. V. Ivanov, N. N. Leonenko, M. D. Ruiz-Medina, and I. N. Savich. Limit theorems for weighted nonlinear transformations of gaussian stationary processes with singular spectra. *Ann. Probab.*, 41(2):1088–1114, 2013.

[51] G. Izrail'S and I. M. Ryžik. *Table of integrals, series, and products*. Acad. Press, 1996.

[52] C. Katris and M. Kavussanos. Time series forecasting methods for the Baltic dry index. *J. Forecast*, 40:1540–1565, 2021.

[53] L. Klimko and P. Nelson. On conditional least squares estimation for stochastic processes,. *Ann Statist.*, 6(3):629–642, 1978.

[54] P. S. Kokoszka and M. S. Taqqu. Parameter estimation for infinite variance fractional arima. *Ann. Statist.*, 24(5):1880–1913, 1996.

[55] A. Kumar and P. Vellaisamy. Inverse tempered stable subordinator. *Statist. Probab. Lett.*, 103:134–141, 2011.

[56] A. Kumar and P. Vellaisamy. Inverse tempered stable subordinators. *Statist Probab. Lett*, 103:134–141, 2014.

[57] S. Lahmiri and S. Bekiros. The effect of COVID-19 on long memory in returns and volatility of cryptocurrency and stock markets. *Chaos Solit. Fractals*, 151:111221, 2021.

[58] A. J. Lawrance and P. A. W. Lewis. The exponential autoregressive-moving average earma(p,q) process. *J. R. Statist. Soc. B.*, 42:150–161, 1980.

[59] N. N. Leonenko and L. M. Sakhno. On the whittle estimators for some classes of continuous-parameter random processes and fields. *Stat. Probab. Lett..*, 76(8):781–795, 2006.

[60] G. Li. Estimation of parameters in aruma models. *Acta Math. Appl. Sinica.*, 6(2):173–192, 1990.

[61] B. Lim and S. Zohren. Time-series forecasting with deep learning: a survey. *Philos. Trans. Roy. Soc. A*, 379(2194):20200209, 2021.

[62] Y. B. Mainassara, Y. Esstafa, and B. Saussereau. Estimating FARIMA models with uncorrelated but non-independent error terms. *Stat. Inference Stoch. Process*, 24:549–608, 2021.

[63] M. M. Meerschaert, E. Nane, and P. Vellaisamy. Transient anamolous subdiffusions on bounded domains. *Proc. Amer. Math. Soc.*, 141:699–710, 2013.

[64] M. M. Meerschaert, F. Sabzikar, M. S. Phanikumar, and A. Zeleke. Tempered fractional time series model for turbulence in geophysical flows. *J. Stat. Mech.: Theory Exp.*, 2014(9):P09023, 2014.

[65] E. Omeya, S. V. Gulcka, and R. Vesilo. Semi-heavy tails. *Lith. Math. J.*, 58:480–499, 2018.

[66] W. Palma. *Long-memory time series: theory and methods*. John Wiley & Sons, 2007.

[67] K. Pearson. Contributions to the mathematical theory of evolution. In *Proc. R. Soc.*, volume 54, page 329–333, 1894.

[68] G. Peters, H. Yan, and J. Chan. Statistical features of persistence and long memory in mortality data, ann. *Actuar. Sci*, 15:291–317, 2021.

[69] S. Pincherle. Una nuova estensione delle funzioni sferiche. *Memorie della accademia R. di Bologna (in Italian)*, I:337–369, 1891.

[70] S. J. Press. Estimation in univariate and multivariate stable distributions. *J. Amer. Statist. Assoc.*, 67:842–846, 1972.

[71] V. Reisen. Estimation of the fractional differencing parameter in the arima(p, d, q) model using the smoothed periodogram. *J. Time Series Anal*, 15:335–350, 1994.

[72] V. Reisen, A. Rodrigues, and W. Palma. Estimation of seasonal fractionally integrated processes. *Comput. Statist. Data Anal.*, 50(2):568–582, 2006.

[73] M. S. Ridout. Generating random numbers from a distribution specified by its laplace transform. *Stat. Comput.*, 19(4):439–450, 2008.

[74] P. Robinson. *Time Series with Long memory, Advanced Text in Econometrics*. Oxford University Press, Oxford, 2003.

[75] J. Rosiński. Tempering stable processes. *Stochastic Process Appl*, 117:677–707, 2007.

[76] F. Sabzikar, A. I. McLeod, and M. M. Meerschaert. Parameter estimation for artfima time series. *J. Statist. Plann. Inference.*, 200:129–145, 2019.

[77] F. Sabzikar and D. Surgailis. Tempered fractional Brownian and stable motions of second kind, statist. *Probab. Lett*, 132:17–27, 2018.

[78] G. Samorodnitsky and M. Taqqu. *Stable Non-Gaussian Random Processes*. Chapman and Hall, Boca Raton, Florida, 1994.

[79] B. Schelter. *Handbook of time series analysis*. Wiley Online Library, 2002.

[80] J. L. Schif. *The Laplace Transform: Theory and Applications*. Springer Science & Business Media, 1999.

[81] M. Shitan and S. Peiris. Generalized autoregressive (gar) model: A comparison of maximum likelihood and whittle estimation procedures using a simulation study. *Comm. Statist.—Simulation Comput.*, 37(3):560–570, 2008.

[82] E. Slutsky. The Sommation of Random Causes as the Source of Cyclic Processes. *Econometrica*, 5:105–146, 1937.

[83] F. Sowell. Maximum Likelihood Estimation of Stationary Univariate Fractionally Integrated Time Series Models. *J. Econometrics*, 53:165–188, 1992.

[84] F. Steutel and K. Harn. *Infinite Divisibility of Probability Distributions on the Real Line*. Marcel Dekker, New York, 2004.

[85] A. M. Sykulski, S. C. Olhede, A. P. Guillaumin, J. M. Lilly, and J. J. Early. The debiased Whittle likelihood. *Biometrika*, 106(2):251–266, 2019.

[86] A. M. Sykulski, S. C. Olhede, A. P. Guillaumin, J. M. Lilly, and J. J. Early. The debiased Whittle likelihood. *Biometrika*, 106(2):251–266, 2019.

[87] M. Taniguchi. Minimum contrast estimation for spectral densities of stationary processes. *J. R. Stat. Soc. Series B Stat. Methodol.*, 49(3):315–325, 1987.

[88] L. Torricelli, C. L., and A. Tempered positive linnik processes and their representations. *Electron. J. Stat.*, 16(2):6313–6347, 2022.

[89] V. Uchaikin and V. Zolotarev. *Chance and Stability*. Utrecht:VSP, 1999.

[90] J. E. Vera-Valdés. Nonfractional Long-Range Dependence: Long Memory, Antipersistence, and Aggregation. *Econometrics*, 39, 2021.

[91] G. T. Walker. Correlation in seasonal variations of weather—a further study of world weather. *Mon. Weather Rev.*, 53(6):252–254, 1925.

[92] P. Wang, X. Zheng, G. Ai, D. Liu, and B. Zhu. Time series prediction for the epidemic trends of covid-19 using the improved lstm deep learning method: Case studies in russia, peru and iran. *Chaos, Solitons & Fractals*, 140:110214, 2020.

[93] P. Whittle. *Hypothesis Testing in Time Series Analysis*. Almqvist & Wiksells boktr., 1951.

[94] P. Whittle. Estimation and information in stationary time series. *Arkiv för matematik.*, 2(5):423–434, 1953.

[95] H. Wold. *A Study in the Analysis of Stationary Time Series*. Almgrist & Wiksell, Stockholm, 1938.

[96] W. Woodward, Q. Cheng, and H. Gray. A k-factor garma long-memory model. *J. Time Ser. Anal*, 19:85–504, 1998.

[97] G. Yule. Why Do We Sometimes Get Nonsense-Correlations between Time Series? A Study in Sampling and the Nature of Time Series,. *J. R. Stat. Soc*, 89:1–64, 1926.

[98] S. Zhang and X. Zhang. On the transition law of tempered stable ornstein-uhlenbeck processes. *J. App. Probab*, 46:721–731, 2009.

[99] M. Zheng and G. Karniadakis. Numerical methods for spdes with tempered stable processes. *SIAM J. Sci. Comput.*, 37(3), 2015.